SOME ADAPTATIONS OF THE ANTHOCEROPHYTE *Megaceros pellucidus* (Colenso) E.A.Hodgs. TO EXTREMELY LOW LIGHT ENVIRONMENTS

A thesis presented in partial fulfilment of the requirements for the degree

Of Master of Science

In

Plant biology

At Massey University, Palmerston North,

New Zealand

Roger Lionel Sloane Watkins

2002

Errata

p2 Mache (1973) should be Marche & Loiseaux (1973); Citations referencing; Aro, should not be underlined.

p5/6 Smith et al = Smith & Griffiths (1996).

p18 Line 3; delete Campbell ; 1984 retain 1995 as the one citation.

p20 Raemaekers (1987) should be Raemakers and Longwith (1987).

p21 3.3.1 line 8 the □ should read ±.

p29 Line 6 .."At the of which"...should read, "At the end of which"..

p37 Table number 4.1 should read 4.0 not 4.1.

p39 Figure 4.4 suffers from heavy pixellation.

p41 Table number 4.2 should read 4.1 not 4.2.

p42 Table number 4.3 should read 4.2 not 4.3.

p43 Table number 4.4 should read 4.3 not 4.4.

p44 Table number 4.5 should read 4.4 not 4.5.

p54 Figure 5.2 caption .."white light or blue light".. should read, .." white light. Blue light > 3 µmoles $m^{-2}s^{-1}$ produces a similar result."

P55 Figure 5.5 the caption should read; "Micrograph (x100) of a transverse section across an *M. pellucidus* thallus "after 24 h in light of ~3 µmoles $m^{-2}s^{-1}$ showed the chloroplasts aligned on the periclinal walls".

p60 Figure 5.11 chloroplast mis-spelt in the second figure, cluster caption.

p61 Figure 5.12 add, □ = 3;..

p78 Line 10/11, Kagawa & Wada1, 2002;.. should read Kagawa & Wada, 2002;

p80 Should be Loomis and Connor (1992).

p84 Citations referencing; Aro, should not be underlined.

p90 Line 10 Tlalka & M.., 1999; should read; Tlalka & Fricker,1999;

p97 Burr, F.M. (1968) should be Burr, F.A. (1968).

ABSTRACT

The New Zealand Anthocerophyte *Megaceros pellucidus* (Colenso) is found in wet, cool temperate rain forest and is associated with extremely low light habitats (0.5-7 μmoles photons m^{-2} s^{-1}). The light available to *M. pellucidus* was found to be only 0.2% of the overhead crown canopy light and was heavily attenuated after passing through many leaf canopies. This thesis shows that the photon flux density in these extremely low light habitats can be augmented by two additional light sources, sunfleck light, especially at midday, and light reflected from adjacent water surfaces, such as rivers or ponds, as the sun's incident ray path angle diminishes late or early in the day.

This thesis looks at some of the strategies *M. pellucidus* uses to survive in its low light habitat and, in adapting to acquire such sensitivity to low light parameters, how *M. pellucidus* protects itself from photoinhibition if exposed to high white light of more than 140 μmoles photons m^{-2} s^{-1} or blue (470 nm) light of more than 3 μmoles photons m^{-2} s^{-1}.

The chloroplast position in *M. pellucidus*, when in its normal habitat, was found to retain an expanded form situated on the periclinal cell wall proximal to the light source (an epistrophe position). When thallus tissue sections of *M. pellucidus* were irradiated with blue light of more than 3 μmoles photons m^{-2} s^{-1} or white light of more than 140 μmoles photons m^{-2} s^{-1} the chloroplast shrank dramatically and assumed a position on anticlinal walls (a parastrophe position). Red (662 nm) light of less than 130 μmoles photons m^{-2} s^{-1} or darkness had no obvious effect on the morphology epistrophe chloroplasts, but this treatment resulted in the chloroplasts expanding and moving back to the epistrophe position after irradiation by blue or high levels of white light.

Based on the rate of volume change occasioned when the chloroplasts were irradiated with blue, white, red light or darkness it was concluded that a water flux was induced across the membranes of the various intracellular organelles that depended on the wavelength of the light and the photon flux density.

Various concentrations of polyethylene glycol-20 (PEG) were used as an osmoticum and induced chloroplast shrinkage to an extent and at a rate similar that induced by blue light. Red (662 nm) light of 130 μmoles photons m^{-2} s^{-1}, was observed to expand the chloroplast volume against the osmotic gradient, while darkness had no effect.

A comparison of transmission electron microscope (TEM) micrographs taken of both blue / high light conditions and dark or red irradiated chloroplasts show differences in thylakoid membrane architecture, the dark-exposed samples having a loose open form with pseudograna and greater areas of stroma compared to the blue and high light samples that showed a tight compression of the thylakoids and very reduced areas of stroma. Large numbers of starch granules were apparent in all but the blue irradiated TEM micrographs. Examination of the micrographs showed there were obvious differences between the size of the starch granules (TEM, x7800, micrographs having starch granules with a dark to light ratio of 2.165) as well as in the texture and density.

ACKNOWLEDGEMENTS

Firstly I wish to extend my gratitude and thanks to my mentor and initial supervisor Dr. Simon Brown not only for his supervision but also for his friendship, personal support under sometimes-trying situations and his unfailing enthusiasm for this project. Also thanks to my co-supervisors; Dr. Heather Outred for her encouragement, hospitality and help, and to Dr. Al Rowland for his advice and the extensive joke entrepôt.

My thanks also to Professor Paula Jameson for her support, Professor Roderick Thomas for his initial advice and to the various staff members and technicians of the Institute of Molecular Biosciences who were always friendly and willing to help.

I count myself in being fortunate in having received the expertise, friendship and help of two very charming ladies; Elizabeth "Liz" Nickless with the Confocal microscope and microphotography and Judy Englebrecht for her help in the preparation of samples and use of the CRI transmission electron microscope .

My thanks also to the Dept. of Plant Health for the loan of both the LI-COR 185 and LI-COR 250 light measuring instruments as well as to the Massey electronics workshop for the modification and supply of the optic pen and light projector source.

My thanks to my wife Barbara who had to put up with my very late nights, absences from home and the piles of books and papers spread throughout the house during the course of this study.

CONTENTS

LIST OF FIGURES

LIST OF TABLES

ABBREVIATIONS USED IN TEXT

2n	diploid
CCM	carbon concentrating mechanism
Ch Thy	channel thylakoid
Chl *a*	chlorophyll *a*
Chl *b*	chlorophyll *b*
Chl E	chloroplast envelope
Cw	cell wall
Cyt	cytoplasm
DMSO	dimethyl sulfoxide
ER	endoplasmic reticulum
Gs	grana stack
H	"honeycomb" effect
L/S	longitudinal section
LCP	light compensation point
LED	light emitting diode
LHCP	light harvesting complex protein
LRW	London Resin Co. Ltd. (white resin)
LSP	light saturation point
m.y.a.	Million years ago
MIP	major intrinsic protein
Ml	middle lamella
n	haploid
nm	nanometer
NMR	nuclear magnetic resonance
PAR	photosynthetically active radiation
PEG	polyethylene glycol-20
PFD	photon flux density
PG	plastoglobuli
Pl	plasmalemma
PSII	photosystem II
PSI	photosystem I
P_s	photosynthesis
Q_{10}	respiratory quotient
Rubisco	ribulose bisphosphate carboxylase / oxygenase
SEM	scanning electron microscope
SG	Silicon Graphics
SOD	super oxide dismutase
Spp	species
St G	starch granule
St	stroma
T/S	transverse section
TEM	transmission electron microscope
Thy O	thylakoid (open ended)
Thy S	thylakoid strands
Thy	thylakoid
TIP	tonoplast intrinsic protein
Ton	tonoplast

Voxel	$pixels^3$
V	query vacuole
X/S	cross section

Chapter 1

Introduction

Ecologically plants can be classified into sun or shade plants depending on the degree of genotypic and/or phenotypic adaptability to a particular light intensity (Bjorkman, 1981; Bjorkman & Holmgren, 1963; Boardman, 1977).

In areas subject to extreme shading only a few specialized plants are able to survive. The plants associated with these sites are mainly Bryophytes, Anthocerophytes and Pteridophytes. Generally all of the extreme shade areas, on which the various varieties grow, are cool and well supplied with water. The dry heavily shaded areas have few plants growing on them. The flora of these extremely shaded positions appear to have adapted to these low light situations by modifying and changing their physiological, anatomical and metabolic functions, to a greater or lesser extent.

Shade plants have their photosynthesis (P_s) saturated by relatively low photon flux densities (PFD) (light saturation rate of CO_2 uptake ranged from 2.1-3.1 mg CO_2 dm^{-2} h^{-1} for shade species compared to high light species which ranged from 21-36 mg CO_2 dm^{-2} h^{-1}) whereas full sun plants have a higher level of P_s since they have higher light saturation rates (Bjorkman, 1968)). The light is utilised within the chloroplasts that are able to function over a very wide range of light environments, (xerophytes in full sun >2500 μmoles photons m^{-2} s^{-1} to shade recesses in rainforest floors < 5 μmoles photons m^{-2} s^{-1}) (Barbour *et al.*, 2000; Bjorkman & Holmgren, 1963; Chazdon *et al.*, 1996; Etherington, 1982; Nobel, 1991; Osmond *et al.*, 1987).

The extreme shade plants are exceptionally efficient in their P_s ability; a ratio between the available PFD and the level of photosynthesis, the P_s efficiency of the shade plants is greater than the full sun plants (Böhning & Burnside, 1956). The extreme shade plant habitats have ample water, cooler temperatures than the sun exposed sites, adequate CO_2 (an average CO_2 concentration of 360 ppm at the forest floor level in a Queensland rainforest) (Bjorkman, 1981), but are limited by light,

thus any survival strategy must be directed towards some form of light enhancement or a more efficient metabolism (Khurana, 1998).

Light, in respect to shade plants, is the major limiting resource and requires an optimal cost benefit strategy (Grime, 1981; Hodgson *et al.*, 1999; Larcher, 1995; Rincon & Grime, 1989).

Shade plants and aquatic plants utilise a combination of strategies such as extended light harvesting antennae and use of alternative light wavelengths, changes in light harvesting chloroplast protein (LHCP) ratios (Grignon, 1999), changes in photosystem I : photosystem II (PSI: PSII) ratios (Boardman, 1977), light magnification and optic path modification (Vogelmann & Bjorn, 1986), changes in cellular ultra-structure (Chow *et al.*, 1982) and a wide range of gross morphological changes to achieve an ultimate light utilisation efficiency (Aro, 1982).

Since deep shade plants are genotypically adapted for survival in low light situations any exposure to high light could seriously compromise their survival (Boardman, 1977). Shade plants have adjusted to low light levels by acquiring low light compensation points (LCP), where respiratory CO_2 production equals P_s CO_2 uptake (Bjorkman, 1981).

In a shade plant the amount of light required to attain a P_s light saturation, where any further increase in PFD will not produce any further increase in P_s, is usually small for example, Mache (1973), estimated a value of 2-3 klux in *Marchantia polymorpha*. In light response curves of CO_2 uptake *vs* time with set PFD the efficiency of P_s can be seen when the slope of the curve is observed, the steeper the slope the more efficient the P_s. In shade plants the initial slope is generally very steep with a clearly defined saturation point and associated plateau in which no further P_s takes place (Bjorkman & Holmgren, 1963; Boardman, 1977) (Figure 1.1).

Photoinhibition occurs when light quanta absorbed exceeds that used for P_s, and if leaves cannot dissipate the extra energy harmlessly, molecular and biochemical damage will eventually occur as a result of excessive levels of free radicals (the oxide anions; O_2^-, HO_2, H_2O_2). Moderate excesses of free radicals are rendered safe by being scavenged and oxidised by such enzymes as superoxide dismutase (SOD) and peroxidases (Ishikawa *et al.*, 1993). Shade plants are more susceptible to

photoinhibition from high PFD levels because of their low light saturation point. So shade plants with adaptations to enhance light capture and optimize P_s, must also include mechanisms to reduce the likelihood of photo-damage (Boardman, 1977).

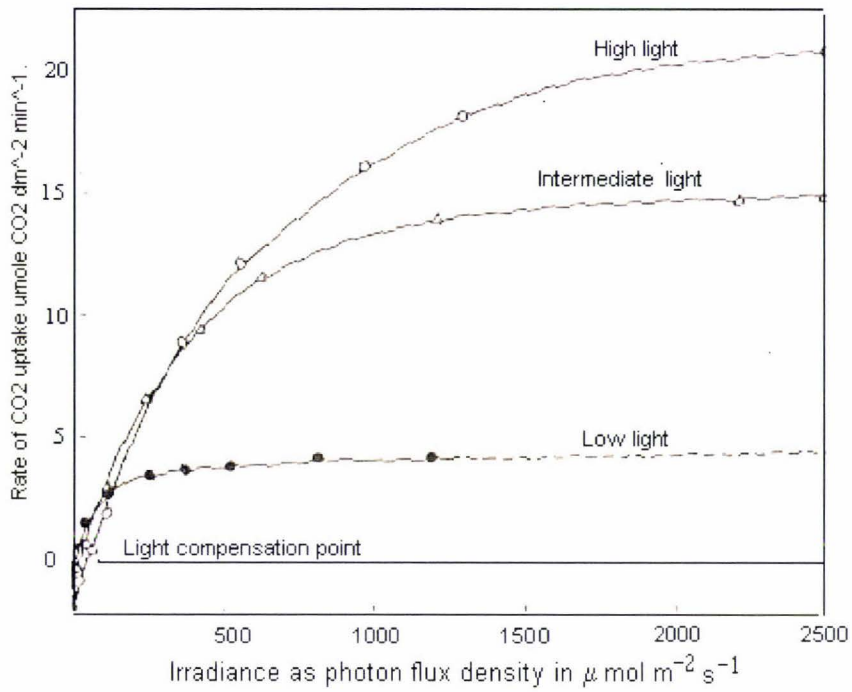

Figure 1.1. An example of light saturation curves, as exhibited by *Atriplex patula* grown at high light (20mW cm^{-2}) intermediate light (6.3mW cm^{-2}) and low light (2mW cm^{-2}) from (Bjorkman *et al.*, 1972).

Some strategies that have evolved in shade plants to minimize photoinhibition and bleaching are largely mechanistic. Changes in chloroplast volume (Ivanchenko *et al.*, 1980; McCain & Markley, 1992; McCain, 1995; McCain, 2000; Nobel, 1968) reducing surface area, and chloroplast movement that creates a minimal surface exposure to the light source (Haupt, 1982; Haupt, 1999; Haupt & Hader, 1994), a compaction of thylakoids reduces the LHCP's and electron chain sensitivity (Anderson & Aro, 1994; Anderson *et al.*, 1988; Bischof *et al.*, 1999; Lichtenthaler *et al.*, 1982; Vaughn *et al.*, 1992), and changes in light ray paths and photon scattering that disperses excess light energy (Vogelmann, 1993; Vogelmann & Bjorn, 1986; Vogelmann *et al.*, 1996).

Generally the majority of shade plants possess leaves that are thinner with greater surface area, with larger chloroplasts and have higher chlorophyll levels than the leaves of sun plants. The ratios of chlorophyll *a* (Chl *a*) to chlorophyll *b* (Chl *b*) drop, shade plants having higher proportions of Chl *b* (Anderson *et al.*, 1973; Chazdon *et al.*, 1996).

Ultrastructure investigations of shade plant chloroplasts show that thylakoid architecture differs from that of sun plant chloroplasts. Thylakoids of shade plant[1] chloroplasts have large irregularly arranged stacks (grana stacks of up to 100 thylakoids per granum) (Anderson *et al.*, 1973). This irregular arrangement would optimize the harvesting of weak diffuse light. In contrast the thylakoid architecture in chloroplasts exposed to high PFD is characterized by an arrangement of very condensed compact stacking with a paucity of visible stroma (Anderson & Aro, 1994). This arrangement suggests a sheltering pattern with the external units creating a shading effect on the more interior platelets.

Any shift in the proportions of stroma lamellae to grana stacks, in comparison between sun and shade plants is not evident but the length of the shade plant stromal lamellae is much shorter (Chow, 1999; Chow *et al.*, 1990). The ratio of appressed thylakoid regions between the stroma lamellae and the grana was 3:2, in the shade plant *Alocasia*, compared to 1:4, in a Spinach sun plant (Anderson *et al.*, 1973). In *Helianthus* it was found that the thylakoids in contact with the stroma surface-to-volume ratio, did not change relative to that of a high-irradiance control but remain significantly lower than that of a low-irradiance control. The change in the ratio of appressed thylakoids to thylakoids in contact with the stroma occurred within a relatively short time (5 min) with low PFD exposure and indicated a broadening and shortening of the appressed thylakoid stack (Wheeler & Fagerberg, 2000).

It appears that the sun/shade acclimatization process of the chloroplast thylakoids is mostly driven by changes in photon flux densities and not by specific spectral band-dependent receptors (Ghoshroy & Fagerberg, 1998). Although changes in the thylakoid distribution can be compacted in *M. pellucidus* by; light of PFDs > 3 μmoles photons m^{-2} s^{-1} in the blue (460-480 nm) waveband and expanded by red light (660-680 nm) of PFDs of up to 130 μmoles photons m^{-2} s^{-1} .

[1] Vascular plants

Anderson proposed that a more efficient collection of light quanta would result with any increase in Chl *b* and its associated LHCP's and it is this increase that is responsible for the expansion in the thylakoid shade orientation (Anderson *et al.*, 1973). A similar thylakoid expansion and similar stroma lamellae can be seen in *M. pellucidus* chloroplasts (section 5.7). However stroma diminishment in shade plants does not occur in *Megaceros*, rather the reverse and the extent of this is shown in Figure 5.21.

The sample plant that was chosen for this thesis, the Anthocerophyte *Megaceros pellucidus* (Colenso) E.A.Hodgs. (Chapter 2) is an extreme shade plant and common to all of the four sample sites (Chapter 4) and is found growing in light ranging from 0.1 up to 7 μmoles photons m^{-2} s^{-1}. The range, 0.1-7 μmoles photons m^{-2} s^{-1}, is referred to, in this text, as the habitat light.

While the chlorophyll content in shade plant chloroplasts is generally higher, relatively, than that found in sun plants, the chloroplast number per unit area of leaf is very much reduced (Chazdon *et al.*, 1996; Chow *et al.*, 1990). This has been explained on a cost / benefit analysis, where there exists a diminishing return for increasing chloroplast concentration.

Measurements made of the PFD at four *M. pellucidus* sites (Chapter 4) show a extremely low level of available light PFD (0.07 moles photons m^{-2} day^{-1}), an attenuation of 99.84 % of a crown canopy PFD irradiance of 42.93 moles photons m^{-2} day^{-1} (Chapter 4). Bjorkman (1981) concluded that in extremely low light situations a further doubling of the chloroplast number will only increase absorption by 3-6%, an energy budget deficit.

The size of the single chloroplast in the cells of *M. pellucidus* was found to be ideal for microscopy and volume measurement and a precedence of using the *M. pellucidus* chloroplast has previously been established: such as chloroplast gross morphology and ultrastructure (Valentine, 1984), the phylogeny and division of chloroplasts (Burr, 1968). Vaughn published a comprehensive review of the Anthocerophyta ultrastructure, incorporating much of his own research (Vaughn *et al.*, 1992). The evidence of carbon concentration in the Anthocerophyta species chloroplast pyrenoid and the associated Rubisco levels was described by Smith

(1996). Molecular genetics, especially RNA editing, was investigated by Yoshinaga (1997).

However, in all of the Anthocerophyte literature surveyed, there were only brief references to light stimulus and no actual quantification of light flux was made. As will be seen in these results any plant cellular ultrastructure experimentation, involving light, should include the light wavelength and PFD used. Earlier work has been done investigating the chloroplast movement in thallose Bryophytes by (Britz, 1979; Hader, 1987; Haupt, 1982; Haupt, 1999; Haupt & Hader, 1994; Kendrick & Kronenberg, 1994) and many others. But apparently little research has been conducted on volume changes to chloroplasts in response to light. (Chapter 2).

This work observes the effects of light at various PFDs, specifically red and blue wavelengths, on the chloroplast and its ultrastructure, of *M. pellucidus*. All previous workers have only briefly commented that the *Megaceros* chloroplast, orientation and size was subject to considerable variation when exposed to light (Burr, 1968; Valentine, 1984; Vaughn *et al.*, 1992) but there were no recorded qualitative or quantitative measurements taken.

During the exposure to high PFDs or blue light the volume of the *M. pellucidus* chloroplast was observed to shrink (Chapter 5). However the total cell volume did not appear to decrease at the same time, although no measurements of total cell volume were taken.

It could be assumed therefore, that the constituents of the cell are retained and simply relocated into other organelles or extended within the cytoplasm as a reconstituted product. This appears very similar to an osmotic reaction and has been commented on and investigated by a number of workers using species other than extreme shade plants (Gupta & Berkowitz, 1988; McCain & Markley, 1992; McCain, 1995; McCain, 2000; Robinson, 1985; Weiss, 1996). In this work the tissue of *M. pellucidus* was immersed in an osmoticum and a similar contraction to high PFD and blue light was seen to occur (section 5.6).

In the low light conditions of its natural habitat, the various species of Anthocerophyta collected, exhibited a maximum of "chloroplast to light exposure" both in surface area and in spatial orientation. This chloroplast characteristic was

first reported by Bohm in 1856 (Kendrick & Kronenberg, 1994) who commented on the change that occurred in chloroplast orientation in response to light conditions.

Chloroplasts respond to high light intensity by diminishing their exposed surface area (the major plane of the chloroplast lying parallel to the path of incident light) whereas in low light intensity their surface area tends to be maximized, (the major plane of the chloroplast at right angles to the path of incident light). This chloroplast phenomena was also investigated by Frank (in 1871) and Stahl (in 1880) (Haupt, 1982; Kendrick & Kronenberg, 1994) who commented that the orientation of these organelles appeared to depend on the direction of the light source and the intensity of this incoming light.

Chloroplast migration, in response to light, is common to the majority of plants (Britz, 1979; Haupt, 1982; Haupt, 1999; Haupt & Hader, 1994). Three species, in particular, *Selaginella, Mougeotia and Lemna,* have been intensively researched and the chloroplast arrangements, in response to light of various intensities, has been described (Britz, 1979) (Figure 1.2).

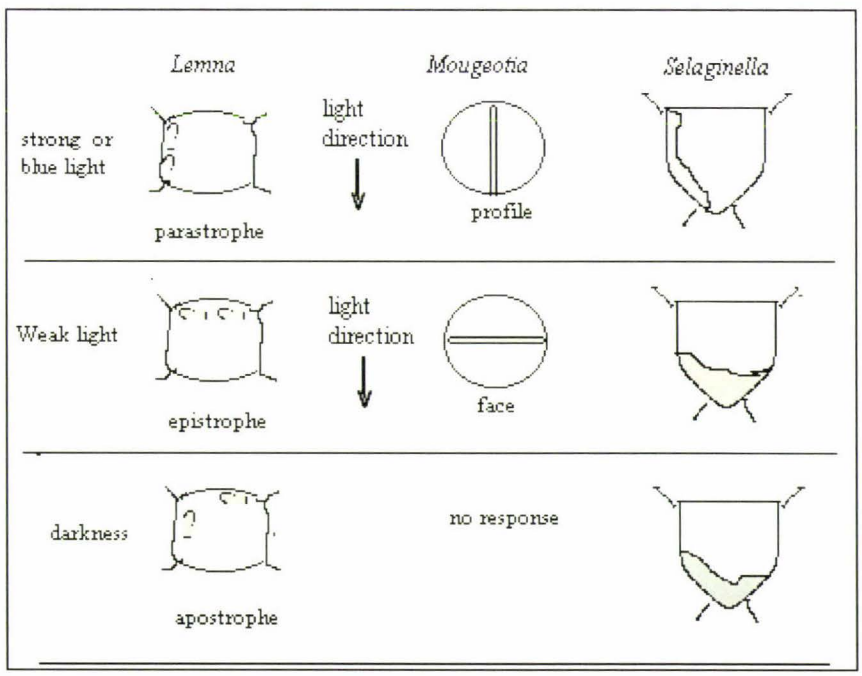

Figure 1.2. Diagrammatic representation of the various chloroplast arrangements in three plant species. The direction of the incident light is indicated by the arrows. The terms parastrophe, epistrophe and apostrophe have been used within this thesis (Adapted from Britz 1979).

The chloroplast arrangement for the species *Lemna*, as illustrated in Figure 1.2, appears analogous to *M. pellucidus,* detailed in this thesis, and the arrangement terminology as used by Britz (1979) will be used in this thesis.

1.1 Hypothesis

That the extreme shade tolerant plant, *Megaceros pellucidus* (Colenso) E. A. Hodges), has a number of co-ordinated, anatomical and physiological characteristics that enable it to survive in the extreme low light situations in which it is found.

Chapter 2

A brief review of the Anthocerotophyta, specifically (*Megaceros pellucidus* (Colenso) E.A.Hodgs.)

2.1 The Anthocerotophyta

Anthocerotophyta, commonly known as "Hornworts" in reference to their horn like sporophyte morphology, are a cosmopolitan group of plants that are generally found in moist shaded areas; in forests, along rivers, on moist banks and in wet shaded pasture. All appear to have adapted as sciophytes (low light tolerant plants).

The greatest diversity of the Anthocerotophyta is found in the wet tropical forests (Schuster, 1984). All known species are small, and prostrate; of waxy, dark-green appearance and thallose in habit (Bold *et al.*, 1987) and are, though controversially (Figures 2.1 to 2.4), represented by six common genera: *Anthoceros, Phaeoceros, Notothylas, Dendroceros, Folioceros*[1] *and Megaceros*. The taxon radiates out to the cool temperate areas where it declines in the number of genera but the species diversity remains high (Richards, 1984; Schuster, 1984).

Previously (pre-1977) the Anthocerophyta were classified as Anthocerotopsida in the division Hepatophyta, but by virtue of many unique distinguishing features (based on plastid, gametophyte and sporophyte differences (Bold *et al.*, 1987; Renzaglia, 1978; Schuster, 1984; Stotler & Crandall-Stotler, 1977)) they were elevated to divisional rank, to distinguish them from the earlier class. These workers suggested that ancestors of the Anthocerotophyta, invaded the land sometime during the late Devonian (350 m.y.a.) and, because of these unique features, the division had a closer phylogeny with an alternative algal ancestor, possibly representing a case of parallel evolution with the Mosses and the Hepatics (Figure 2.1. and 2.2). This ancestral genesis is thought to be closely allied to the aquatic algae *Coleochaete* (Figure 2.3) (Duckett & Renzaglia, 1988) and chloroplast similarities are apparent in many of the homologous structures and physiology of the Anthocerophyta

[1] Hasegawa (1988) considers *Folioceros* to be a subgenus of *Anthoceros*.

chloroplasts, particularly the *Notothylas* (Figures 2.2 and 2.3) (Chapman & Chapman, 1973; Cook *et al.*, 1977; Salisbury & Floyd, 1978; Toyama, 1974).

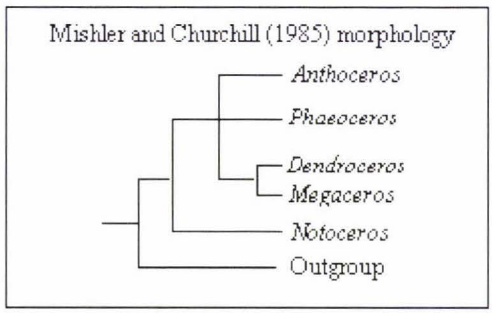

Figure 2.1. Early cladistics that propose a differentiation of the Anthocerophytes as a unique division rather than a class within the division Hepatophyta (Mishler & Churchill, 1985).

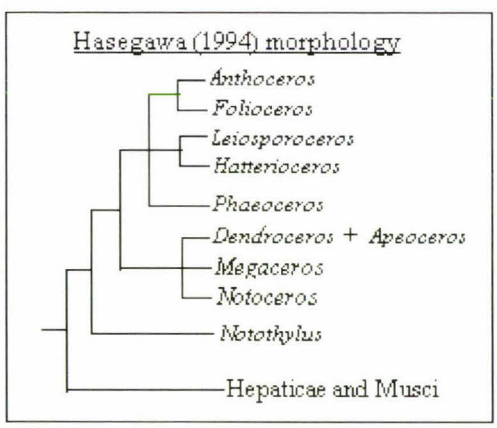

Figure 2.2. Cladistics of Anthocerophyta. A new classification proposed by Hasegawa in 1994, based on anatomical and morphological characteristics (Hasegawa, 1994).

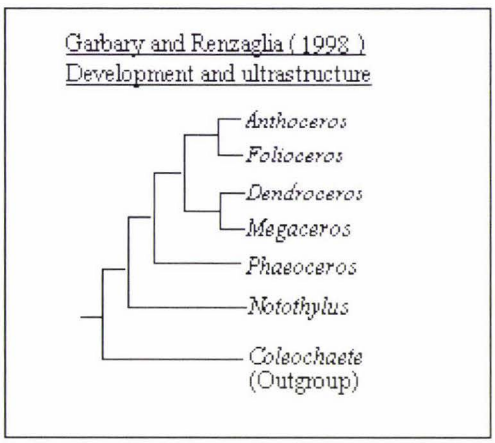

Figure 2.3. Anthocerophyte phylogeny based on ultrastructure and developmental anatomy indicating an ancestral association with the *Coleochaete* (Garbary & Renzaglia, 1998).

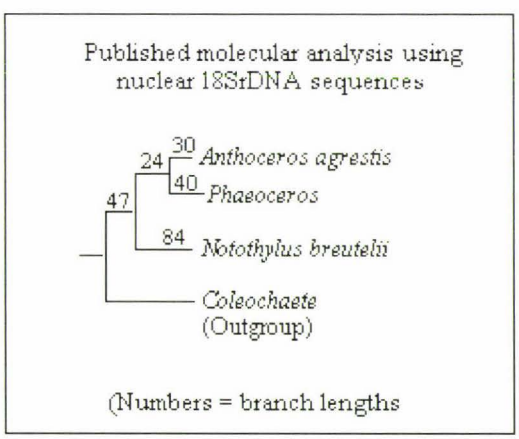

Figure 2. 4. Phylogenetic analysis of Anthocerophyte nuclear 18S rDNA sequences available from GenBank® (Analysis using PAUP v 4.0).

This putative origin and associated outgroups is worthy of consideration when investigating the reactions of the contemporary Anthocerophyta in the extremely low light fluence, moisture levels, temperature and the photosynthetically active radiation (PAR) characteristics of its habitat.

The vegetative gametophyte (n), the dominant phase, is a simple, thin thallus that is composed of parenchymous isodiametric cells of equal size, except for the occurrence of small epidermal cells and large internal cells in *Megaceros*. Schizogenous mucilage cavities develop in the dorsal thallus of *Anthoceros, Notothylas* and *Dendroceros* and ventral mucilage clefts are found in all species (Bold *et al.*, 1987). The clefts are invaded by species of the filamentous cyanobacteria, *Nostoc*, which develops nitrogen producing symbiotic colonies that characterize all hornwort thalli (Dodds *et al.*, 1995). The host cells become modified as the *Nostoc* colony develops (Duckett *et al.*, 1977)

On the ventral thallus some epidermal cells develop into nontuberculate rhizoids which primarily anchor the thallus (Bold *et al.*, 1987; Renzaglia, 1978; Schuster, 1984), there is a possibility of transfer cells above the rhizoid epidermal core; an association that would indicate that the rhizoid is functioning as a nutritive uptake cell (Figure 5.5).

Scattered mucilage idioblasts (cells with very different constituents from other similar cells within the same tissue, they can vary in size, form or structure (Esau, 1953), occur in most species, while slime secretions from epidermal cells serve to protect the apical region and developing gametangia (Schuster, 1984).

The dorsal thallus produces the sexual phase of the reproductive cycle, the sporophyte (2n), and is not of significance in the context of this thesis. Brief mention is made of the specific light requirements for spore germination (Wada *et al.*, 1984). More detailed information on the Anthocerotophyta sporophyte development and anatomy can be obtained from (Bold *et al.*, 1987; Burr, 1968; Renzaglia, 1978; 1986; Schuster, 1984).

Plants, within the division Anthocerotophyta, are generally characterised by a single, or very few (<14) giant chloroplasts, per cell (Figures 5.3 and 5.4), that contain a pyrenoid body (Burr, 1968; Kaja, 1954; Valentine, 1984; Vaughn, 1992). These two

phenomena, except the *Megaceros* which does not have pyrenoid bodies (Burr, 1970; Valentine, 1984; Vaughn *et al.*, 1992), have been a distinguishing feature in the identification of Anthocerotophyta (Bold *et al.*, 1987; Schuster, 1984). There are also major differences in the chloroplast ultrastructure between the Anthocerotophyta and other terrestrial plants (the Anthocerotophyta have open-ended thylakoids (Burr, 1970; Valentine, 1984; 1986; Vaughn *et al.*, 1992).

Unique thylakoid architecture is also characteristic of the Anthocerophyta. The thylakoids are distributed throughout the chloroplast interior and are contained within a stroma matrix. An unusual compression of thylakoids with open ends (see TEM micrographs in Figures 5.19, 5.20, 5.23, 5.25 and 5.26) has been commented on by various workers. This compression of thylakoids has variously been called granal stacking (Vaughn *et al.*, 1992) or pseudograna (Lembi & Lang, 1965; Manton, 1962). The term pseudogranum applies to the distinctive forms the thylakoids assume in the various species of Anthocerophyta. The pseudograna were originally applied to the thylakoid stacks arising from the invagination that is seen in many algal chloroplasts (Toyama, 1974). Much controversy regarding the architecture of thylakoid stacking, granal arrangement and other structural differences, in the various Anthocerophyta chloroplasts, has occurred and has been reviewed and commented on (Burr, 1970; Toyama, 1974; Valentine, 1984; Vaughn *et al.*, 1992).

Connecting the granal stacks, between the top and bottom of adjacent stacks, are thylakoids that run perpendicular to the long axis of the granum. These inter-granal thylakoid channels, termed channel thylakoids (Burr, 1968), are another unique feature in the Anthocerophyta (Figure 5.18). Channel thylakoids are suggested to be analogous to the stroma lamellae that connect grana and likewise have high levels of PSI (Vaughn *et al.*, 1992). The photosynthetic reaction centres, PSI and PSII, in the grana stacks, appear to be distributed similarly to most "higher" plants, appressed grana thylakoids containing high levels of PSII while non-appressed stroma thylakoids contain PSI.

Another identifying characteristic of the Anthocerophyta, with the exception of the *Megaceros* spp., is the inclusion of a pyrenoid body within the chloroplast. These pyrenoid units generally measure 0.5 μm × 1.5 – 2 μm in cross section (Vaughn *et*

al., 1992) and normally occupy a central region of the chloroplast (Valentine & Campbell, 1986).

Transmission electron microscopy (TEM) reveals the presence of thylakoids, both stacked and unstacked, together with areas of normal chloroplast stroma, traversing the pyrenoid region (Burr, 1970; Valentine, 1984; Vaughn *et al.*, 1990). Studies into the biochemistry of the pyrenoid bodies, using immunocytochemical techniques have identified the pyrenoid as the site of ribulose-1,5-bisphosphate carboxylase / oxygenase (Rubisco) concentration (McKay & Gibbs, 1989; McKay *et al.*, 1991; Vaughn *et al.*, 1990) hence a point of carbon concentrating mechanism (CCM) (Hanson *et al.*, 2002).

In algal chloroplasts the pyrenoid thylakoids contain mostly PSI and are deficient, or poor in PSII, the stromal thylakoids contain both PSI and PSII (Murakami, 1992). This suggests that the distribution of the thylakoid photosystems and the associated concentration of Rubisco within the stroma, in higher plants, and pyrenoid bodies, in algae, is further proof of the ancestral origin of the Anthocerophyta.

Variation in PFD on the individual cells of the Chlorophyte *Dunaliella tertiolecta* showed that the levels of Rubisco activity in the pyrenoid bodies was correlated with light intensity with Rubisco redistributing itself between the pyrenoid and the stroma in response to PFD levels, the pyrenoid being the location of Rubisco and CO_2 fixation. The stroma operates as a reservoir of deactivated Rubisco that would be transported to the pyrenoid as the PFD increased (Lin & Carpenter, 1997).

In a recent comparison of the Anthocerophytes (*Phaeoceros* Prosk.; *Notothylas* Sull. and the pyrenoid-lacking *Megaceros* (Campbell) with the Hepatophyta, *Marchantia polymorpha* (which has a similar thalloid growth, habitat requirement and is a $P_s C_3$ plant) it was found that the CO_2 concentrating mechanism (CCM) varied considerably with *Notothylas* having more CCM activity than *Phaeoceros*, and that *Megaceros* had the least (Hanson *et al.*, 2002). Compensation points of *Notothylas* and *Phaeoceros* were 11-13 ppm CO_2 compared to *Megaceros* of 31 ppm CO_2 and *Marchantia* of 64 ppm. The catalytic rate of carboxylation by Rubisco between the species was *Marchantia* 2.6 s^{-1} (8% Rubisco of the total soluble protein), *Megaceros* 3.3 s^{-1} (4% Rubisco of the total soluble protein), and *Phaeoceros* and *Notothyla* 4.2

and 4.3 s^{-1} respectively (both having 3% Rubisco of their total soluble protein). The thalloid *Marchantia polymorpha* can survive exposed to full summer sunshine (PFD of < 2000 μmoles photons m^{-2} s^{-1}) as long as sufficient water is available whereas the Anthocerophytes rapidly expire (Pers. obs.).

Associated with the Anthocerophyte chloroplast envelope are peroxisomes, which appear in both pyrenoid-devoid and pyrenoid-present genera (Vaughn *et al.*, 1990). However both rough and smooth endoplasmic reticulum (ER) have only been found in the chloroplast envelopes within developing and developed sporophyte (2n) cells (Vaughn *et al.*, 1990).

The great majority of Anthocerophyte chloroplasts contain starch granules. Those with pyrenoid bodies have them clustered around the pyrenoid in great numbers, and those without pyrenoids have the starch granules scattered relatively evenly throughout the stroma, with their long axis parallel to the long chloroplast axis (Valentine, 1984; Vaughn *et al.*, 1992) (Figures 5.23 and 5.24).

Little comment, in the literature, has been made specifically on the vacuoles of the Anthocerophyta, and interpretation, in this thesis, of their general characteristics is based on Esau's and Fahn's descriptions (Esau, 1953; Fahn, 1997). A vacuole's content, in solution with the principal component water, is termed the ergasatic content (Esau, 1953) and is of less viscosity than the cytoplasm. The vacuoles are delineated by a single membrane, the tonoplast, which is heavily infiltrated by the major intrinsic proteins (MIP's) (in tonoplasts they are known as tonoplast intrinsic proteins TIP's). Many of these intrinsic proteins have been found to act as bulk water channels, termed aquaporins, which can regulate the tonicity of the vacuole and cytoplasm very rapidly (Eckert *et al.*, 1999; Kjellbom *et al.*, 1999; Maurel, 1997; Tyerman *et al.*, 1999).

There are three methods by which a cell modulates water uptake: (a) reducing wall stress thereby reducing cell turgor pressure (which reduces cytoplasmic water potential), (b) altering the solute concentration of the cytoplasm or organelle or its surroundings (also modifying the water potential), and (c) altering the bulk flux (the hydraulic conductance) of the water uptake pathway (occurs in cells spatially removed from water potential equilibrium) (Cosgrove, 1993).

The two ions, in vacuoles, that have been found to influence the tonoplast and plasmalemma water permeability are K^+, the principal osmoticum which is also thought to be regulated by light (Leigh, 1997), and Ca^{2+} which creates a cascade of reactions and signals effecting the entire metabolism of the cell (Berecki *et al.*, 1999; Brownlee *et al.*, 1999; Pandey *et al.*, 2000; Tazawa *et al.*, 1995).

The influence of induced changes in the osmotic potentials on the volume change in the *M. pellucidus* chloroplast and its correlation to light induced changes is examined in Chapters 5 and 6, and more detailed discussion of the possible effect the vacuole action has on *M. pellucidus* is given in section 6.11.

Many of the chloroplast characteristics; single mega-chloroplasts, thylakoid stacking architecture, pyrenoids; found in the Anthocerophyta are also found in various algae (Chapman & Chapman, 1973) and so any obvious anatomical uniqueness cannot be used as an exclusive Anthocerophyte identifying marker (Valentine, 1984; Vaughn *et al.*, 1992).

Although several hundred species of Anthocerotophyta have been described many of them are synonymous; the taxon is thus more likely to comprise a hundred or less individual species (Hasegawa, 1988; Schuster, 1984), the New Zealand taxa also has many synonymous species (Glenny, 1998). In New Zealand the Anthocerotophyta are represented by four genera, *Anthoceros* (2), *Dendroceros* (2), *Megaceros* (4) and *Phaeoceros* (4). The bracketed numbers refer to the accepted names and include twenty-three various synonyms and basionyms (Glenny, 1998).

2.2 The specimen plant (*Megaceros pellucidus* (Colenso) E.A.Hodgs.)

All of the specimens sourced for this thesis were situated in wet and extreme shade habitats and no Anthocerophyta specimens were seen on any of the more exposed or higher light areas. Since the reproductive system of the Anthocerophyta relies on zoospores for its reproduction, the presence of a water envelope is crucial to their survival. The optimum period for the initiation of a reproductive phase would therefore be at a time in which water conservation is favoured, low temperatures, high water vapour levels, low atmospheric pressure and minimal wind flow. Thus

inducing zoospore formation and a suitable pathway from the antheridia to the archegonia.

The observation of *M.pellucidus* producing sporophytes in low light and cool conditions, plus personal observations in the field of the sporophyte development occurring only in cold winter months producing the green spores, is characteristic of *Megaceros* and *Dendroceros* (Bold *et al.*, 1987). *Megaceros* is differentiated from the *Dendroceros* by not possessing the prominent mid-rib that is typical of the *Dendroceros* gametophyte (Bold *et al.*, 1987; Schuster, 1984).

The location and the number of pyrenoids vary within the Anthocerophyta However, the *M. pellucidus* specimens used in these experiments did not appear to have any pyrenoid, which isolates and is typical of the genus *Megaceros* (Valentine, 1984; Valentine & Campbell, 1986; Vaughn *et al.*, 1992).

The gross morphology and ultrastructure of the Anthocerophyte chloroplast has been established by Valentine (1984), the phylogeny and division was earlier researched by Burr (1968). Vaughn (1992) has published a comprehensive review of the Anthocerophyte chloroplast. The evidence of carbon concentration and Rubisco reactions in the chloroplast pyrenoid was described by (Smith & Griffiths, 1996). Molecular genetics, especially RNA editing, was investigated by (Yoshinaga *et al.*, 1997).

2.3 Identification of specimens

Plants of *Megaceros pellucidus* (Colenso) E.A.Hodgs. (Figure 2.5) were used and were identified by their morphology, location, chloroplast ultrastructure (lack of pyrenoids), and spore colour. In 1998 (Glenny, 1998), synonyms and basionyms of the following (*Anthoceros arachnoideus* Steph, *Anthoceros granulatus Colenso, Anthoceros longispirus* Carrington & Pearson, *Anthoceros pellucidus* Colenso, *Megaceros arachnoideus* Steph, *Megaceros flagellaris* (Mitt.) Steph., *Megaceros grandis* (Asngstr.) Steph., *Megaceros longispirus* (Carrington & Pearson) Steph., *Megaceros membanaceus* (Colenso) E.A.Hodgs., *Megaceros zotovii* Khanna.) were included under the species *Megasceros pellucidus* (Colenso) E.A.Hodgs.

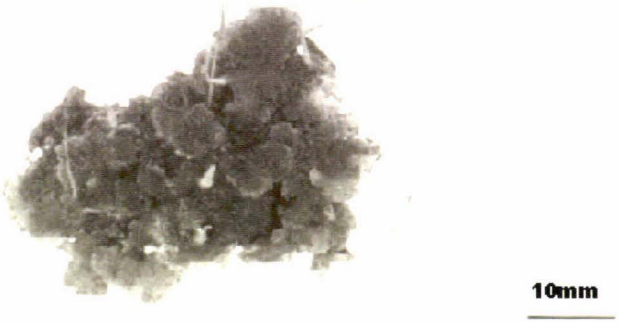

Figure 2. 5. *Megaceros pellucidus* (Colenso) E.A.Hodgs. Synonymous *to Megaceros arachnoideus* (Steph.) Steph. Photograph by Dr E.O.Campbell.

Previous workers that investigated the ultrastructure of various species of the Anthocerophyta have used *Megaceros arachnoideus* (Steph.) Steph. (Campbell, 1995; 1984; Valentine & Campbell, 1986). These specimens were obtained from the Apiti Glow worm caves (Figure 4.0 and section 4.1) and from Tiritea Valley (represented in E. O. Campbell's Hornwort collection, at Massey University). Plants of *M. pellucidus* (Colenso) E.A.Hodgs were also identified by comparison with named specimens in Dr E. O. Campbell's Anthocerophyte collection at Massey and identification by Dame Dr E. O. Campbell.

Chapter 3

Materials and methods

3.0 Plant material and sample preparation

Five specimens of *M. pellucidus* were collected from each of the sites, variously indicated in Chapter 4. Each specimen was washed in the fresh water surrounding the site and then packed in "Plaspak M250®" containers together with 50 mL of water obtained from the collection site. Subsequently all the containers were kept in a refrigerator at 4-6°C. All specimens were washed in mille-Q water prior to being placed on a pre-formed 35° slope composed of 50% mille-Q-soaked vermiculite (1#) and 50% site substrate (crushed limestone) in plastic 1L or 2L containers.

The planted containers were covered in "Gladwrap®" then stored in a cool room at 4°C and a PFD of 2 μmoles photons m^{-2} sec^{-1}. A constantly high humidity was maintained within the container by maintaining a 3 mm deep pool of site water. Samples were kept in an illuminated cold room at 4°C between experiments. Once a month all specimens were irrigated with Hutner's (Hutner *et al.*, 1950) combined solution (Appendix A). When maintained in these conditions, the *M. pellucidus* gametophyte produced sporophytes, but plants grown at ambient temperatures showed no evidence of sporophyte production, irrespective of the season. This cool temperature phenomenon has also been seen in some thallose Hepatophyta, including *Marchantia polymorpha* and *Monoclea forsteri* (Pers. Obs.).

Control samples were either exposed to sunlight filtered with Sarlon® 64% shade-cloth to give a PFD of about 140 μmoles m^{-2} s^{-1} (high white light regime) or to total darkness (dark regime).

3.1 Tissue sectioning

Tissue samples (aa', bb', cc'... in Figure 3.1) were cut across the distal portion of the *M. pellucidus* thallus, by hand sectioning under mille-Q water, in a plastic Petri dish. Tapering sections, with tapers ranging from 0.1mm to zero, were removed from the dissection bath by brush and mounted onto either a microscope slide and covered with a standard glass slip or the appropriate sample stage.

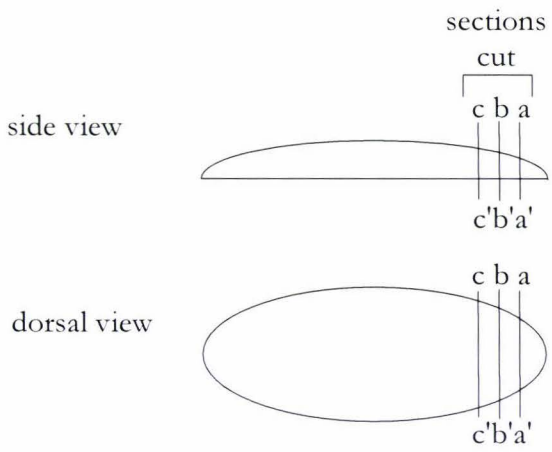

Figure 3.1. Cutting orientation in tissue sample preparation.

3.2 Chlorophyll determination

Chlorophyll (Chl) was extracted from the *M. pellucidus* tissue using dimethyl sulfoxide (DMSO), as described by Raemaekers (1987). Segments of fresh tissue were cut from the youngest sections of the *M. pellucidus* thallus, flash frozen in liquid air and then dried between clean tissues. Weighed samples were placed in glass tubes and 5 mL of DMSO, sufficient to submerge each sample, was added. These were then incubated in a water bath at 65°C for 16 hours, which Raemaekers (1987) recommended as giving optimal Chl extraction with the minimal effect on the Chl *a* : *b* ratio. If necessary, the tubes were stored in a dark refrigerator at 4°C, which prevented any significant deterioration of the Chl *a* : *b* ratio for up to 64 h (Raemaekers & Longwith, 1987).

The tubes were then centrifuged at 4500 rpm in a bench centrifuge and the supernatant drawn off and stored at 4°C until assayed. Chlorophyll was assayed spectrophotometrically (Pye Unicam SP8-400 UV/VIS spectrophotometer), at 645 nm and 663 nm using a 1.0 nm slit width. Total Chl, Chl *a* and Chl *b*, and their ratios, were determined using the absorbances at 663 nm (A_{663}) and 645 nm (A_{645}) from the following expressions (Witham *et al.*, 1986)

Chl *a* (mg g^{-1}) = (12.7 A_{663} - 2.69 A_{645}) × total volume / tissue weight (g)
Chl *b* (mg g^{-1}) = (22.9 A_{645} - 4.68 A_{663}) × total volume / tissue weight (g)
Total Chl (mg g^{-1}) = (20.2 A_{645} – 8.02 A_{663}) × total volume / tissue weight (g)

3.3 Light

Various light responses of the chloroplasts of *M. pellucidus* were observed and quantified over a period of three years. Both environmental light regimes and laboratory light experimentation were undertaken. All the laboratory light related work was either conducted in the photographic dark room at Massey University or in association with a metal shroud that surrounded both the light source and the objective specimen.

3.3.1 Measurement of photon flux density (PFD)

Photon flux density (PFD) both in the field and in the laboratory was measured using a LI-250 quantum-radiometer fitted with a LI-190SA quantum sensor (LI-COR, Lincoln, USA). This sensor is sensitive to photosynthetically active radiation (PAR), and so it does not measure ultraviolet (<400 nm) or infrared (> 700 nm) light. Unfortunately this precluded light measurements in the far-red band (700 - 800 nm). The LI-250 meter had a digital display that reported values in μmoles photons m^{-2} s^{-1} and the manufacturer specified an error of ± 0.4% of reading at 25°C (equivalent to □ 3 counts on the least significant digit displayed). Therefore, the instrument resolution in the 0-199 μmoles photons m^{-2} s^{-1} range was 0.01 μmoles photons m^{-2} s^{-1}. The LI-250 meter reported readings every 15 s and it could average these over a period set by the user, a facility that was used for all measurements made with this meter.

The sensor was held perpendicular to the major light source and reoriented until a maximum reading was achieved (Figure 3.2). This sensor position was then maintained while the meter averaged the PFD over a 5 min period.

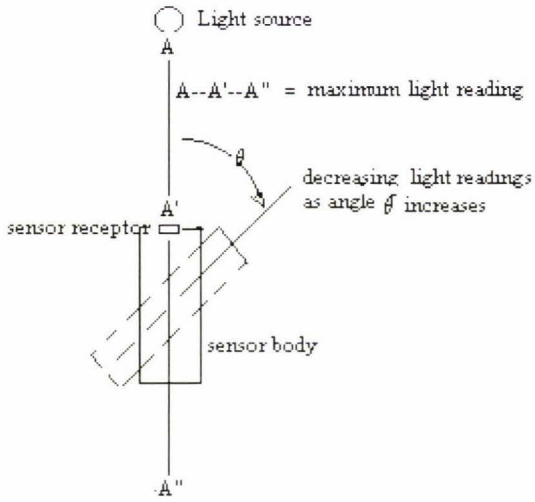

Figure 3.2. Sensor orientation to light source.

3.3.2 Illumination of samples

Two separate systems were employed to illuminate samples, the first involved a source of white light and bandpass filters (section 3.3.2.1), and the second used light-emitting diodes (LEDs, section 3.3.2.2).

3.3.2.1 Filtered light illumination

The light irradiation experiments used a flexible optic fibre cable that was connected to a light source consisting of an enclosed projector bulb with an effective unfiltered PFD of 225 μmoles photons m^{-2} s^{-1}. The enclosure also contained a mount on a sub-stage for an optical filter between the lamp and the fibre optic cable and a baffle to minimise stray light (figure 3.3). Bandpass optical filters (Zeiss), with transmission maxima ranging from 399 nm and 778 nm, could be mounted within the enclosure on the sub-stage. Each of these optical filters had a maximum transmission of 29% and width at half height of 15

nm, which was confirmed spectrophotometrically (figure 3.4). The PFD of the light emitted by this device fitted with different filters is given in table 3.1. Experiments confirmed that the light emitted by this system did not cause any heating of the sample (data not shown).

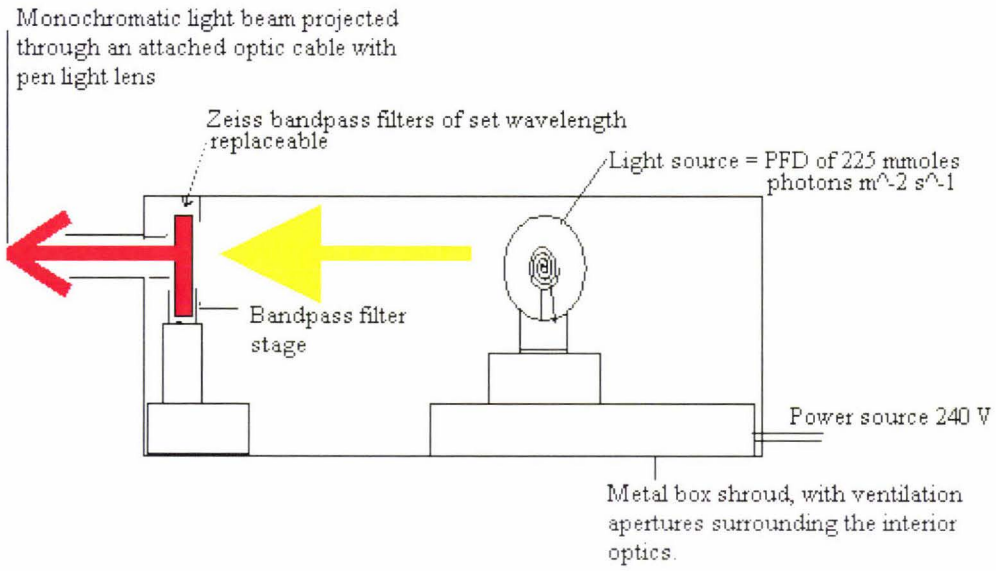

Figure 3.3. Diagram of the modified projector box incorporating a bandpass filter stage.

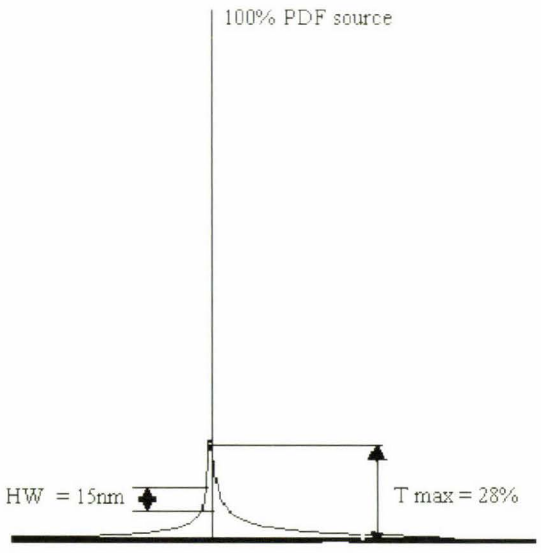

Figure 3.4. Ziese monochromatic bandpass specifications. Range minimum of 399nm to a maximum of 778nm.

Table 3.1. Photon flux density of light after passing through bandpass filters.

Wavelength	Photon flux density PFD (μmoles photons m^{-2} s^{-1})
453	1.6
480	2.5
618	9.1
662	13.8
720	0.2
unfiltered	225

The PFD was measured (Table 3.1) using a LI-250 quantum radiometer fitted with an LI-190SA sensor. Note that the sensor is not sensitive to light of wavelengths longer than 700 nm. The distance between the end of the fibre optic cable tip and the sensor was 10 mm.

Temperature increases induced in the specimen holding media by the proximity of the light was checked and found to be innocuous. The ambient room temperature of 24.5°C was maintained in the samples throughout all of the experiments.

3.3.2.2 Light-emitting diode (LED) illumination

Selected light-emitting diodes (LEDs), emitting at putatively optimal wavelengths for sample irradiation, were incorporated into in a simple circuit (Figure 3.5). The LED was inserted through a bezel into one end of a cylindrical container, forming a shroud (Figure 3.6). This shroud was placed over the concave platform that held the tissue sample and incubation medium. The geometry of the sample platform ensured that the sample was held at a constant distance from the LED (10 mm) and, since the geometry was similar to that of the LI-190SA sensor, the PFD within the shroud could be measured easily by switching between the sample and the sensor.

This apparatus enabled illumination of the sample for prolonged periods without heating; at easily selectable wavelengths (by replacing the LED); with little temporal variation in the PFD, which could be varied simply and reproducibly

using the potentiometer; elimination of any stray light; and ease and reproducibility of sample manipulation.

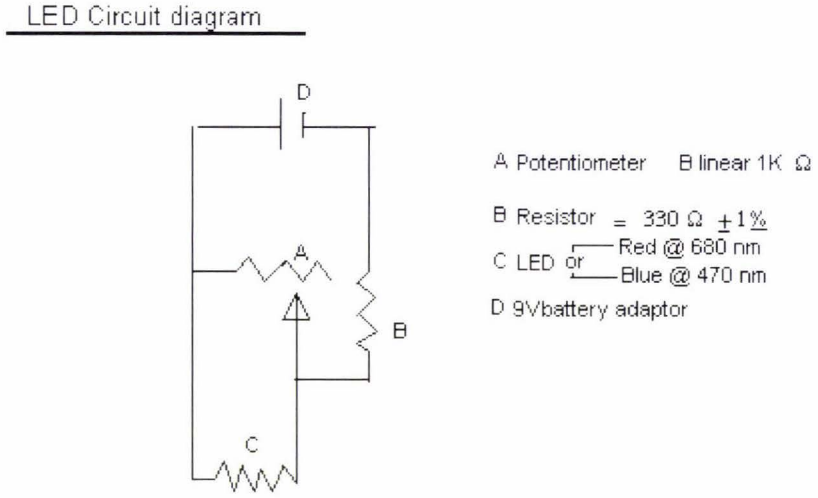

Figure 3.5. The simple circuit used to drive the LED illumination system

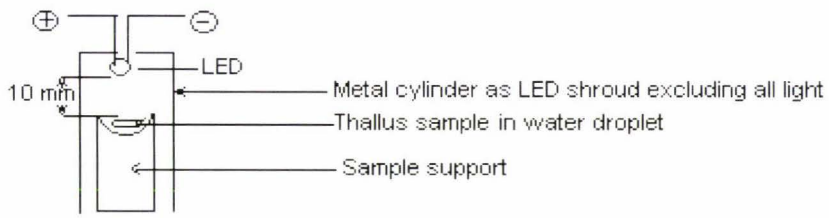

Figure 3.6. The cross section of the shroud surrounding the LED at C in Figure 3.5.

3.4 Microscopy

Three different microscopical techniques were employed: light microscopy was used for transverse section measurements of chloroplasts and general observation of chloroplast location or orientation within cells and tissues. Confocal microscopy was used to image chloroplasts in three dimensions; and transmission electron microscopy was used to obtain ultrastructural details of *M. pellucidus* chloroplasts.

3.4.0 Light microscopy

Observations of chloroplast morphology and measurement of chloroplast cross section were carried at ×400 magnification using an Olympus 370646 microscope fitted with a graticule. The graticule, also known as an eyepiece micrometer, is a small glass disk etched with a scale for linear measurement, which was fitted within the microscope eyepiece (Figure 3.7).

Tissue samples were prepared as described in section 3.1. and chloroplasts were selected as those touching a hair transect placed across the slide cover. Only those chloroplasts, "touching", the transect were observed and measured.

The transverse section (T/S) area of both high light, blue, red and dark adapted chloroplasts was calculated by measuring the two axis, x and y, each at right angles to the other. To obtain the alternative axis the eyepiece was rotated by 90° and a new measurement taken. Each of the axes would always measure the greatest T/S distance (see Figure 3.7).

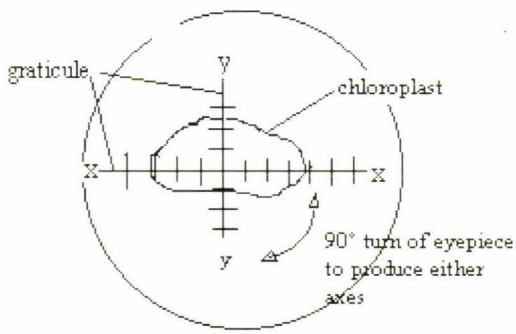

Figure 3.7. Diagram of axes used in measuring the T/S area of chloroplasts. The x and the y measure the widest portion of the chloroplast.

3.4.1 Confocal microscopy

A confocal laser scanning microscope (Leica TCS 4D) was used to image chloroplasts in a three dimensional perspective using their intrinsic chlorophyll fluorescence and to determine chloroplast volume relativity to cross sectional

measurements (section 3.4.3). Tissue samples were prepared as described in section 3.1 and then covered with a cover slip (Escol # 122 × 22 mm) and sealed with amyl acetate. The sections were then scanned by the confocal microscope, using an objective of (100 × 1.4 oil) × 10, with a dwell light of 512 nm on the dark to light sequences (A) and 662 nm on the light to dark sequences (B) to retain the chloroplast volume integrity during microscopy. The set operational protocols on the confocal were observed.

Following confocal microscopy, scanned sections representing the target chloroplasts were electronically transferred to the Silicon Graphics (SG) computer for volume measurement. Individual chloroplast volumes were calculated in voxels (pixel^3) and converted to μm^3 using the Data Manager software provided. Since the confocal SG programme aggregates the number of voxels with a specific tone density greater than that of the transparent cell portions into selected clusters, care must be taken that the chloroplast retains its integrity and is not encumbered with artifacts, other organelles, plasmalemma or cell wall. To eliminate this potential error use was made of the SG cutting facility in which voxels not involved with the target chloroplast could be deleted by reducing their opaque density, thus eliminating them from the total to be summed.

3.4.2 Transmission electron microscopy

Tissue sections were cut as described in section 3.1 and subsequent preparation for transmission electron microscopy (TEM) was based essentially on the techniques recommended by Bozzola (1992).

Sections of tissue were placed in watch glasses and immersed in mille-Q water before treatment with various light regimes. Tissue samples were then removed with curved tip forceps and placed in 10 mL watch glasses, and about 2 mL of a modified Karnovsky's fixative solution (3 mL 25% glutaraldehyde (EM grade), 6.25 mL 8% formaldehyde, 3.25 mL mille-Q water, 12.5 mL 0.2 M phosphate buffer pH 7.2, then made up to 30 mL with mille-Q water (Roland & Vian, 1991; J. Engelbrecht, pers. comm.)) was added. The ratio of fixative to tissue volume

was at least 5-10 fold (Bozzola & Russell, 1992) and each sample batch remained in the fixative for a period of 30 min after which they were irrigated (3 × 10 min) in 0.1 M phosphate buffer pH 7.2.

Thorough washing is imperative to prevent free aldehydes, both surface and outward diffusing, being oxidized by the osmium fixative and creating "pepper background" artifacts during the processing (Bozzola & Russell, 1992).

After the third wash the sections were immersed in a post-fixative of osmium tetroxide solution (1.5 mL OsO_4 in 1.5 mL of 0.2 M phosphate buffer pH 7.2) for 60 min. After removal from the OsO_4 post-fixative solution, all sections were washed (3 × 10 min) in mille-Q water.

Residual water was removed from the samples in a series of EM grade absolute ethanol dehydration immersions (10 min plunges into 35%, 50%, 90%, 95% and 100% (×3)). Ethanol was used rather than the usual lipophyllic 80% acetone to maintain the integrity of the chloroplast envelope and since ethanol is the solvent of the LR White embedding resin.

Infiltration was carried out with L.R.White (LRW) resin (London Resin Co., UK) in ethanol. The low viscosity and hydrophilic nature of LRW resin allowed for a shorter period of tissue infiltration than could be achieved with the hydrophobic Epon© 812, epoxy, Spurr's or Araldite resins. The sample was immersed in 35% LRW in ethanol for 2 h, after which the LRW was carefully extracted. A similar procedure was followed for a further four infiltration baths: in 60% LRW for 16 h; two baths of 100% LRW each of 2 h; and a final immersion in fresh 100% LRW for a further 3 h (Lao, 1998).

The main problem encounted with LRW resin is its reaction to oxygen during polymerisation (Bozzola & Russell, 1992; Lao, 1998), but this can be circumvented by the use of "Beem" or other capped gelatine capsules. Embedding of samples in this case was done by using gelatine capsules finally filled with 100% LRW which, after labeling, were capped making sure that minimal air was entrapped. This exclusion of air bubbles and complete

dehydration of the sample prevented any clouding of the resin during polymerisation.

Before the capsule was filled, care was taken to orient the sample in the bottom of the capsule in such a way as to optimally facilitate microtoming. The prepared capsules were baked in the lab oven at 60°C for 16 h to effect adequate polymerisation. At the of which, each capsule was checked for cloudiness and strength using a pin and the ultramicrotome binocular. Post-fixative investigations, prior to embedding, were carried out using an Olympus at 400× incorporating an ocular micrometer.

All sectioning was performed on a Reichert-Tung Ultracut-E automatic ultramicrotome using handmade glass knives prepared from ethanol washed, Leica Feldspar plate glass strips using a L. K. Knifemaker (Bozzola & Russell, 1992). Each knife was edge evaluated under the microtome stereomicroscope. After checking, each capsule was placed in the ultramicrotome chuck and manually shaped ("rough shaping") using a single blade safety razor. Until an appropriately formed trapezoid block, of 1 mm maximum width was obtained that was suitable for fine sectioning. These were then mounted in the chuck of the Reichert-Tung Ultracut-E automatic ultramicrotome and positioned to ensure an appropriate cutting face. Thick sections of approximately 1 μm were cut and then placed on an ethanol cleaned microscope slide and stained with a drop of 1% Toluidine blue stain, which facilitates rapid identification of organelles and ultrastructure (Roland & Vian, 1991). The slide was placed on a wax warming plate (45°C) to dry. After about 5 min, the stain was drained off and the slide gently rinsed in two separate immersions in distilled water. The slides were then checked using a light microscope, for suitable domains, clarity and orientation that would justify further processing.

As soon as the specimen was providing satisfactory sections, the microtome was set to cut fine, even sections and a fresh glass knife was mounted. Sections of 50

nm ("silver standard"[1]) were then cut from the polymerized resin capsules using glass knives. After cutting, selected sections were removed from the water boat using a platinum disk and placed on copper 200 # grids where they were dried by placing them on the warm plate of the waxing machine. After drying, the grid and specimen were placed in a disk holder ready for staining.

All sections were stained with two separate "radio-opaque" stains. The grids were placed in droplets of 2% uranyl acetate in 50% ethanol that had previously been placed on a strip of Parafilm©. The Parafilm© rested on moistened filter paper at the bottom of a standard plastic Petri dish. The moistened filter paper provided a high water vapour pressure within the Petri dish to prevent the 2% uranyl acetate stain from evaporating.

The grids were kept in the stain droplet for 30 min and then the Petri dish and its lid were covered separately with aluminum foil to exclude light. The grids were then gently washed in 50% ethanol, followed by two further washes of H_2O, and then air-dried prior to final staining.

The final stain consisted of Reynolds lead citrate stain which was prepared in a 50 mL volumetric flask from 1.33 g lead nitrate, 1.76 g sodium citrate and 30 mL of mille-Q water. The resultant cloudy solution was shaken vigorously for one minute and then allowed to stand with intermittent shaking in order to ensure complete conversion to lead citrate. The pH was adjusted to 11.9-12 by addition of 8 mL of 1N NaOH[2] and finally the solution was made up to 50 mL with mille-Q water (Reynolds, 1963).

Drops of the Reynold's stain were placed on Parafilm© in a similar manner to the uranyl staining procedure. A pellet of NaOH was placed in the Petri dish

---

[1] The thickness of thin sections, after being cut on an ultramicrotome, is generally determined by the reflection from the water bath surface when a fluorescent light, mounted in the microtome, is shone onto the water/knife specimen area. The colour is produced as a result of interference arising from the passage of white light through the cut section. The colour observed is indicative of the thickness of the specimen: colourless to gray - 30-60 nm; silver gray to silver - 50-70 nm; gold - 70-90 nm; purple - 100-190 nm; and blue - ≥ 200 nm (Bozzola & Russel, 1992).

[2] The pH is critical. If the pH of the solution varies by ±0.1, poor staining or precipitation will occur. Equally important is the exclusion, as far as practical, of CO_2 (Reynolds, 1963).

alongside the stain droplets as a CO_2 absorbent while the sections were being stained.

Sections were stained by immersing the grid in a drop of the Reynolds stain for a period of 15 min after which the grid and sample were carefully washed (×3) in H_2O and then air dried. After staining had been completed, the grids with their specimens were air dried and individually inserted into a marked dial safe storage box.

The prepared chloroplast grids from the *Megaceros* samples were photographed on a Philips 201C TEM (Crown Research Institute) at magnifications ranging from 5 200 to 72 100 times. All of the films were developed by the Crown Research Institute TEM facility.

3.4.3 Chloroplast volume

While a volume capacity in μm^3 would be ideal, the error involved to produce accurate values is great and the time taken to acquire a meaningful statistical sample of chloroplasts with such a defined volume would be impractical for this programme. So, confocal microscopy was used to correlate the chloroplast volume (Figure 5.10) with the more practical cross section measurement that could be done by light microscopy, which has previously been used to measure chloroplasts in the study of *Nannochloropsis* (Fisher *et al.*, 1998). Chloroplast volume has also been estimated using flow cytometry (Paau *et al.*, 1978), a packed volume technique (Robinson, 1985), and nuclear magnetic resonance (McCain & Markley, 1992; McCain, 1995; McCain, 2000), but these techniques were impracticable in this instance.

In the light microscope measurements chloroplasts were selected that had a long axis (y) parallel to the line of sight and a measurement across the x and z-axes was taken (Figures 3.7 and 3.8). The two dimensional plane (x × y) has been previously used as a representative measure of chloroplast volume (Fisher *et al.*, 1998).

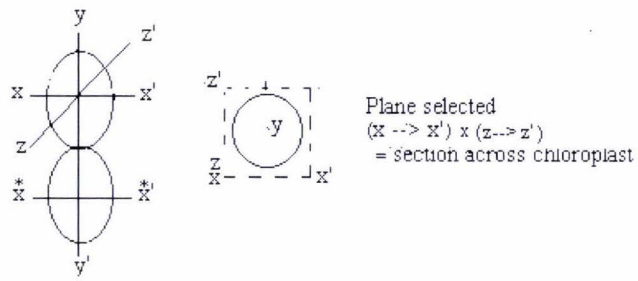

Figure 3.8. Diagrams of planes used in measurement of chloroplast volume.

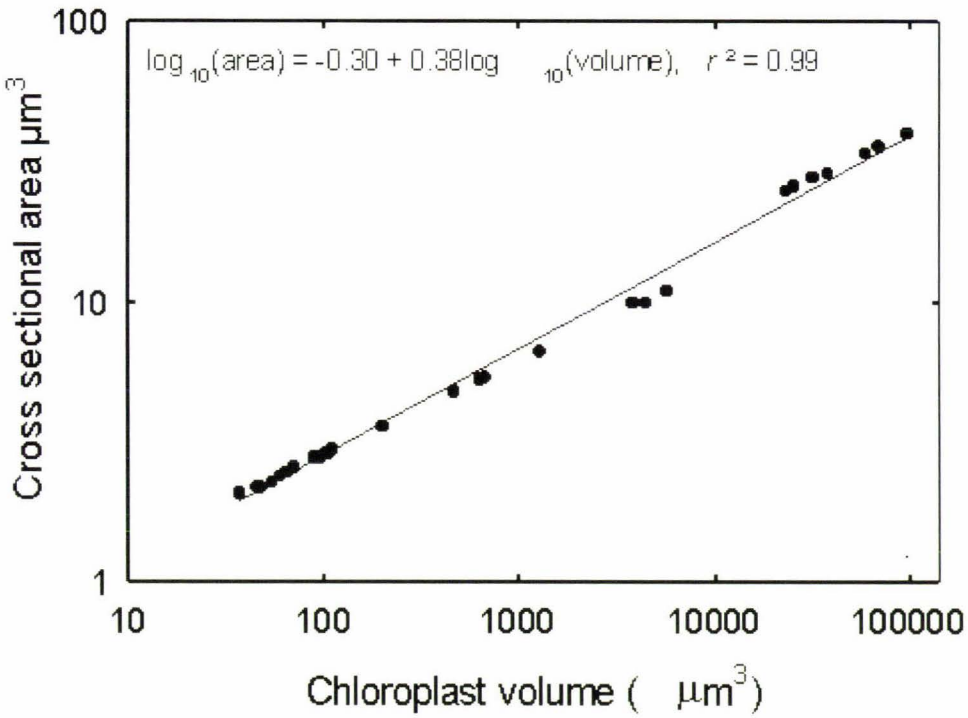

Figure 3.9. Relationship between chloroplast volumes measured by confocal microscopy and cross sectional areas measured by light microscopy.

Using the SG analysis software, measurements similar to that used at the light microscopy graticule section (Figures 3.7 and 3.8) were made in both light adapted and dark-adapted chloroplasts. These measurements were then used to obtain a ratio of (T/S area) μm^2/ (vol) μm^3.

The product x × y measured by light microscopy has been taken as an arbitrary standard with which to ascertain changes in chloroplast size, rather than as an accurate volume measurement. These two-dimensional measurements correlate well with the volume measurements taken with the confocal microscope on other samples (Figure 3.7). Therefore, measurements of the dynamics of chloroplast volume changes were carried out using light microscopy.

Micrograph images of one of the chloroplasts showing the section build up for a chloroplast volume analysis is included as Figure 5.9.

Chapter 4

Results A: Field measurements and site descriptions.

The results in this thesis have been separated into two chapters. Chapter 4 includes the field descriptions and light measurements existing at the respective sampling sites, and Chapter 5 contains the laboratory results and measurements.

4.0 Site locations

Five specimens of *M. pellucidus* were collected from each of four widely separated areas, within the central North Island (Figure 4.1), from sites that were selected to be representative of a range of light environments.

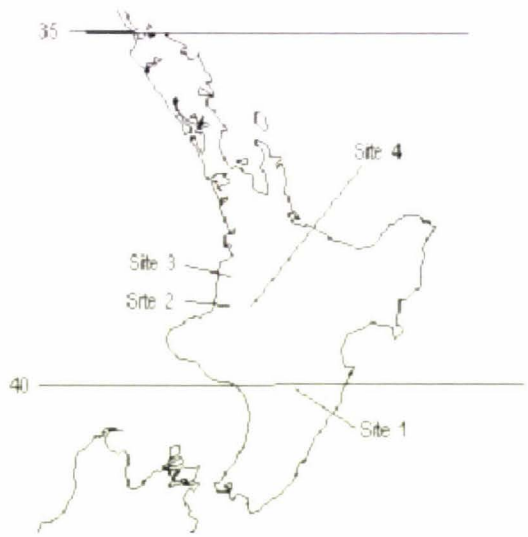

Figure 4.1. North Island, New Zealand, showing the locations of the four sites from which *M. pellucidus* were collected. The sites were Apiti Cave (site 1), Rerekino (site 2), Taumatamaire (site 3) and Tangarakau (site 4).

Each of the sites is similar in having high surface water levels and heavy shading from natural land contours, forest top canopies and sub-canopies of ferns and other plants. The early-to-mid-Tertiary foraminiferal limestone substrate was found at all the sites (Hay, 1967; Miller, 1968) and is also associated with a range of bryophytes growing in the vicinity. Specimens were selected from random regions at each site

and the photon flux density (PFD) was recorded (see this chapter under specific site sections). Water irrigating the *M. pellucidus* at all sites was found to have an average pH of 7.3 ± 0.1. The Apiti and Rerekino sites were investigated in more detail.

4.0.1 Site 1: Apiti Cave

Apiti Cave is situated off Limestone Road (39° 58' 30" S, 176° 0' E) and is known locally as the Apiti Glow Worm Cave. It consists of a cleft in a Tertiary limestone (Hay, 1967) fault fracture. Water runoff flows down the sides of the cave and its surroundings, and a small river (Limestone Creek) runs through the cleft. While the site is referred to as a cave, it is actually an open-ended fault with a high arch (Figure 4.2, 1). Similar smaller caves are situated upstream on the same fault line. Samples of *M. pellucidus* were taken by and inside the mouth of the caves at sites indicated in Figures 4.2 and 4.3. The PFD was recorded at each sampling site, the centre of the river pond immediately in front of the cave (Figures 4.2 and 4.3) and at an unshaded location on the road immediately above the cave. The unshaded, much higher PDF, was equivalent to that of the canopy top and was taken immediately above foliage, on the side of the road adjacent to the cave gully.

All the areas in which *M. pellucidus* specimens were found (Figure 4.1) are subjected to a constantly wet environment from water dripping from the upper canopy, ground water run off, mist, water spring flow and on the external sites, rain. The PFD at each sampling site was low, however, after 4.00 pm, summer and winter[1], sunlight reflected off the river surface is projected some considerable distance[2] inside the cave (Figure 4.3) onto exposed areas of limestone outcrops (Figure 4.2, 3 and 4). There is normally minimal light at this point and only bryophyte, algal and growths of cyanobacteria can occasionally be seen.

---

[1] Autumn measurements not recorded, the sampling day was very overcast and raining, with measurements taken summer and winter it could be assumed that autumn would also have measurable reflections.

[2] The distances varied because the incident angle of the light onto and the reflected light off the river water surface was constantly changing (Tang, 1997).

Figure 4.2. A montage of four photos of the Apiti Cave site: 1= the limestone cleft through which the Limestone River runs, showing the far end of the Apiti Cave; 2 = the cave entrance of limestone, access into the cave is through the river, the entrance collection site is close to the river surface see arrows; 3 = the interior of the cave showing *M. pellucidus* growth on limestone outcrops, each with optimal light in this area.; 4 = cleft showing *M. pellucidus* growth.

Table 4.1. PFD for Apiti Caves.

Site	Location	Season	Conditions	Time of day (h)	PFD (μmoles photons $m^{-2} s^{-1}$) ($\pm$ SEM, n = 10)
Apiti 1	Canopy	Winter	Heavy mist	1530-1545	923.0 ± 23
Apiti 2	Canopy	Autumn	Light rain	1400-1430	924.4 ± 4.1
Apiti 3	Canopy	Summer	Cloudy	1300-1315	1081 ± 1.8
Apiti 1	River ext. pool	Winter	Cloudy	1445-1515	273. 0 ± 21.0
Apiti 2	River ext. pool	Autumn	Light rain	1230-1300	7.4 ± 0.2
Apiti 3	River ext. pool	Summer	Cloudy	1345-1400	426 ± 8.1
Apiti 1	Reflection 1	Winter	Sun gap	1330-1345	7.4 ± 0.8
Apiti 2	Reflection 1	Autumn	Light rain	1300-1315	0 readings
Apiti 3	Reflection 1	Summer	Cloudy	1730-1830	6.56 ± 0.1
Apiti 1	Cave interior 2	Winter	Sun gap	1300-1315	2.6 ± 0.3
Apiti 2	Cave interior 2	Autumn	Light rain	1300-1315	0 readings
Apiti 3	Cave interior 2	Summer	Cloudy	1415-1430	0.25 ± 0.01
Apiti 1	Cave interior 3	Winter	Sun gap	1240-1255	2.4 ± 0.4
Apiti 2	Cave interior 3	Autumn	Light rain	1315-1330	0.2 ± 0.03
Apiti 3	Cave interior 3	Summer	Cloudy	1430-1445	0.7 ± 0.02
Apiti 1	Cave mouth 4	Winter	Sun gap	1400-1430	5.1 ± 0.4
Apiti 2	Cave mouth 4	Autumn	Light rain	1330-1345	2.76 ± 0.1
Apiti 3	Cave mouth 4	Summer	Cloudy	1500-1515	3.03 ± 0.2

The PFD at each of the Apiti sampling points was low (<10 μmoles photons $m^{-2} s^{-1}$) irrespective of the season (Table 4.1). During gaps in the cloud cover, continuously moving reflections of sunlight from the river surface were observed on the cave roof and sides. This additional light source was not measured during the initial recordings. The change in the suns position over the recording period (1200 – 1830 h) showed that two different reflective light phases were taking place (Figure 4.3).

The first light phase, 1200h to approximately 1400h was very oscillatory, reflections, arising from the rapidly varying reflective planes of the river surface

produced large numbers of small transient patches of light within the cave, and these were not measured.

The second phase, from 1400-1845 h, occurred as the suns rays were at an angle that gave a reflection of more permanence, that reached onto the cave interior roof. The *M. pellucidus* colonies, site 4 the cave entrance, received the highest light incidence from both 1st and 2nd phase reflections (Figure 4.3, 2 foreground) while the deepest site (1) only received late phase 2 reflections.

Five field trips were made to Apiti Cave and each time the weather was cloudy or misty, at the site, with intermittent sun gaps even though the weather was optimal at the start of the trip.

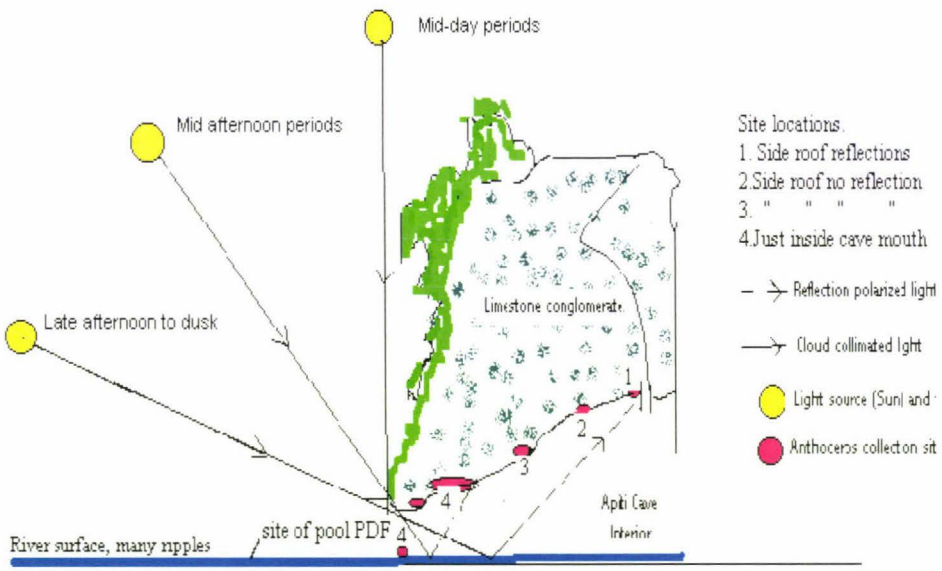

Figure 4.3. Drawing showing sunlight paths at various periods (see Table 4.1 for seasonal times) and their resultant reflections onto the interior cave walls at Apiti. The roof colonies of *M.pellucidus* proximal to the mouth have reflections covering the period 1400 – 1700 h while those colonies in distal areas receive appropriately less light and of a different quality (see 4.2).

4.0.2 Site 2: Rerekino

Site 2 is the most isolated of the sites. It is situated on the southern side of the Rerekino spur approximately 200 m up on the right hand side from the end of the Rerekino Road (39° 01' 30" S, 174° 39' E).

Specimens of *M. pellucidus* were found growing in deep, heavily shaded recesses in foliage covered, water scoured channels situated in an old roadside cutting. In all cases the sampling sites had a constant water flow and were in deep shade (Figure 4.4) provided by overhanging ferns and tree canopy. The area in which the samples were growing was subjected to late afternoon (4.00 pm) sun reflected off surrounding water and leaf surfaces (Figure 4.5).

Figure 4.4. The Rerekino site with arrows showing the location of the *M. pellucidus* sites. In the foreground is an embankment composed of road work spoil and covered by *Tradescantia fluminensis*, an exotic weed. The sites arrowed are overhung with a dense fern canopy. The natural bank has continuous water seepage and associated pools are present at the base of the fern covered bank.

Site PFD measurements (Table 4.2) were taken in August, on a sunny day between 1330 and 1630 h, over two *M. pellucidus* locations. The "canopy" readings were taken on top of a ridge that was level and adjacent to the tree canopy that shaded the cave. The sensor was held approximately 6 cm above the foliage crown of a bushy

Melicytus ramiflorus (Mahoe) in an endeavour to simulate foliage reflection. Forest floor sub-canopy readings were taken 6 cm above the ferns, which overhung the *Megaceros* sample site.

The sample site was situated in very heavy overhead shade but the South Western side was exposed to late afternoon sunlight reflections off the small stream and pools of water that were at the base of the bank. Reflection from the very shiny leaves of *Tradescantia fluminensis*, established on the road tailings were thought to be a significant reflective light source but recordings of photosynthetically active radiation (PAR) showed no significant variation from the ambient levels. However the light meter used, a LI-250 (Section 3.3.1) was unable to record wavelengths beyond 700 nm and below 400 nm and since leaf reflections are high in far red and infrared wavelengths (Myneni & Ross, 1991; Neinhuis *et al.*, 2001; Tang, 1997; Vogelmann & Bjorn, 1986), no true quantitative record of the reflection level was possible.

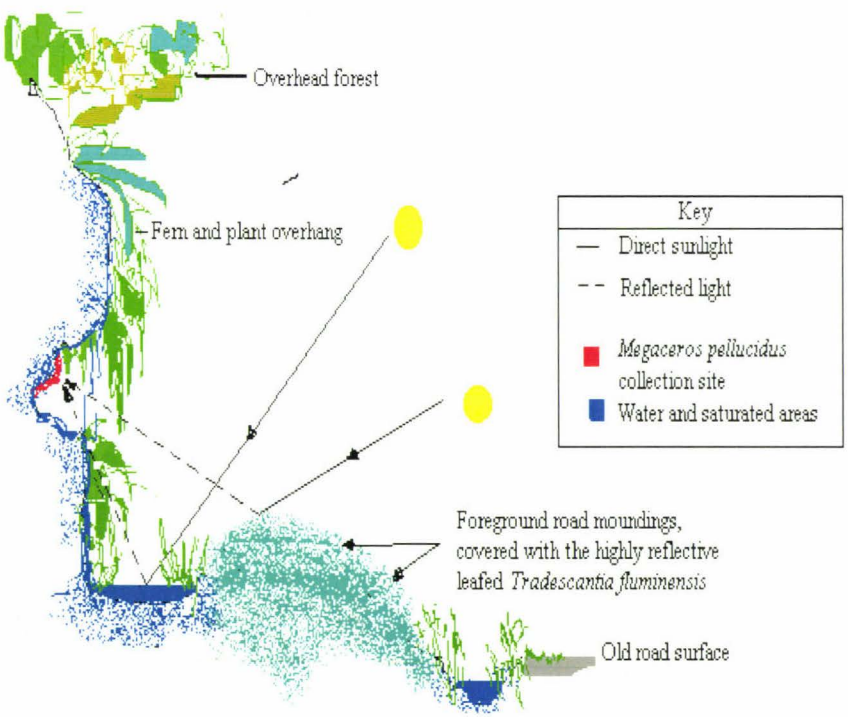

Figure 4.5. Cross section diagram of the Rerekino *M. pellucidus* collection site. The site, in red, was continually immersed in water run off from seepages arising from higher up the bank.

The overhanging foliage in Figure 4.5 consists of dead and living fern fronds plus other plants that exclude all direct sunlight. The area under the foliage, between the inside of the foliage canopy and the bank allowed access to light reflected from the surface of both water pools and the highly reflective leaf surfaces of the *Tradescantia*. The highest PFD of the reflection occurred late in the afternoon when the suns declination created appropriate angles of incidence and reflection.

Table 4.2. Showing average PFD readings of Rerekino sampling sites.

Rerekino	Location	Season	Conditions	Time of day (h)	PFD (μmoles photons m^{-2} s^{-1}) ($\pm$ SEM, n = 10)
	Canopy	Winter	Sunny	1330	1707 $\pm$ 5
	Canopy	Winter	Sunny	1600	1404 $\pm$ 3
	F/floor	Winter	Sunny	1430	18 $\pm$ 6
	Spp site	Winter	Sunny	1445	2.2 $\pm$ 0.4
	Reflections	Winter	Sunny	1615	6.1 $\pm$ 0.1

4.0.3 Site 3: Awakino–Mahoenui caves (Mokau River - Pio Pio)

Site 3 is situated off North Taumatamaire Road (38° 36' S, 174° 46' E) where there are three caves, including Black's Cave from which samples were collected. The geology of this area is composed of mudstone diversified with two up-thrusts of thin sections of early to mid-Tertiary foraminiferal limestone (Hay, 1967). Black's Cave (Figure 4.6) is well known to locals and the other adjacent two caves have no specific names. All of the limestone caves have a gravel and sandstone conglomerate floor. Water seepage from various parts of the wall forms pools in wall cavities and on the floor.

The caves are shaded by overhead ferns and trees with the cave entrances being further shaded by plants of Parataniwha and *Elastostema rugosum* that cover the actual entrances (Figure 4.6). This canopy aggregated screening column severely reduces light to the cave interior (Table 4.3). Aprons of bryophytes cascaded from the ceiling at the entrance, but were severely dehydrated forming a light brown

indistinguishable mass. Water, from roof, wall and ground seepage formed puddles on the ground in front of the cave entrances.

Figure 4.6. The entrance to Black's Cave, the actual entrance (see arrow) is concealed behind the undergrowth. The site is also shaded from the direct sunlight by an overhanging tree canopy.

Table 4.3. Showing average PDF readings of environmental sampling sites at the Awakino–Mahoenui (Blacks) caves.

Mahoenui cave	Location	Season	Conditions	Time of day (h)	PFD (μmoles photons m^{-2} s^{-1}) ($\pm$ SEM, n = 10)
	Canopy	Autumn	Sunny	1230	1874 $\pm$ 40
	Fern top	Autumn	Sunny	1300	39 $\pm$ 4.0
	Site	Autumn	Sunny	1330	2.1 $\pm$ 0.4

4.0.4 Site 4: Tangarakau

The collection site (38° 59' 00" S, 174° 50' E) was situated next to the northern abutments of the Tangarakau Gorge Road. High waterfalls cascade down from these abutments to fall onto heavily shaded sheet greywacke with limestone inclusions. All of the *Megaceros* specimens were collected in the wet spray areas at the base of

these falls. The sampling sites are heavily shaded by overhanging vegetation and, being on the southern side of the abutments, receive light early in the morning, during the summer (Table 4.4), and late in the evening during late spring to early autumn. During the winter the papa rock buttresses shelter the site completely from the sun, which lights the area at approx. 1030-1100 h and retreats from direct lighting at approx 1400-1430 h (Pers. Obs.).

Table 4.4. Showing average PDF readings of environmental sampling sites at the Tangarakau site.

Tangarakau	Location	Season	Conditions	Time of day (h)	PFD (μmoles photons m^{-2} s^{-1}) ($\pm$ SEM, n = 10)
	Canopy	Summer	Cloud/mist	1300	1076 $\pm$ 30
	Over cover	Summer	"	1430	32 $\pm$ 4
	Spp site	Summer	"	1340	3 $\pm$ 1

4.1 Light environments

The widely separated sample sites, while providing a diversity of plant samples, presented a problem of practicality. The time involved in travelling to and from the various sites was prohibitive and so only two sites, Apiti and Rerekino, were used for further study. Both sites presented very similar PFD profiles to the other two sites general averages and both the sites excluded, Blacks Cave and the Tangarakau, were subjected to extreme fluctuations in rainfall (flooding) that often created difficulties in access.

There was significant seasonal variation in the PFD measured at canopy levels (Table 4.1, for example), but relatively little in that measured at the sampling sites.

At the canopy level, of the Apiti site, the PFD reached a maximum of about 1000 μmoles photons m^{-2} s^{-1}, irrespective of the season, but the day length was longer during summer and a PFD of at least 800 μmoles photons m^{-2} s^{-1} was maintained for about 12.5 h in the summer compared with about 3 and 5.5 h in winter and autumn, respectively. The PFD at the sampling site was $\leq$ 3 μmoles photons m^{-2} s^{-1} for most

of the day, although light reflected from the surface of the water flowing through the bottom of Apiti Cave (Figures 4.2, 1,2 and 3) increased the PFD at the sampling site for a short period late in summer and winter late afternoons (Table 4.1).

Table 4.5. The total daily flux of photons (PFD) at the canopy level and at the sampling site for each of three seasons.

Season (month)	Photon flux (moles photons m^{-2} day^{-1})	
	Canopy light	Habitat light
Summer (February)	43	0.1
Autumn (April)	27	0.04
Winter (June)	23	0.03

The data shown in Figures 4.7, A and B, for the canopy and sampling sites, respectively, were numerically integrated and the error indicated is that estimated to arise from this procedure.

The total energy available at the canopy level varied considerably with season (the energy available at the canopy in winter was about 50% of that available in summer), but that at the sampling site varied much less (the energy available to the colony in winter was 80% of that available to it in summer (Table 4.5)). The total energy available to the colony was less than 0.2% of that available at the canopy.

4.2 Light quality

Measurements of light quality (carried out using the bandpass filters described in section 3.3) were made at canopy level and at the sampling site at 1000 and 1600 h during summer (February). These data showed little variation in the light quality at the canopy level between these times, but there was some indication of a difference in the light quality at the sampling site (Figure 4.7B). As the PFDs measured at the sampling site were extremely low (<0.2 μmoles photons m^{-2} s^{-1}), although larger than the specified instrumental error (Section 3.3.1), considerable caution must be

applied in the interpretation of these data. However, they imply that there was a decline in the green region of the spectrum (500-580 nm) and increases in the red (600-700 nm) and blue (420–500 nm) regions in the late afternoon compared with the morning (Figure 4.8).

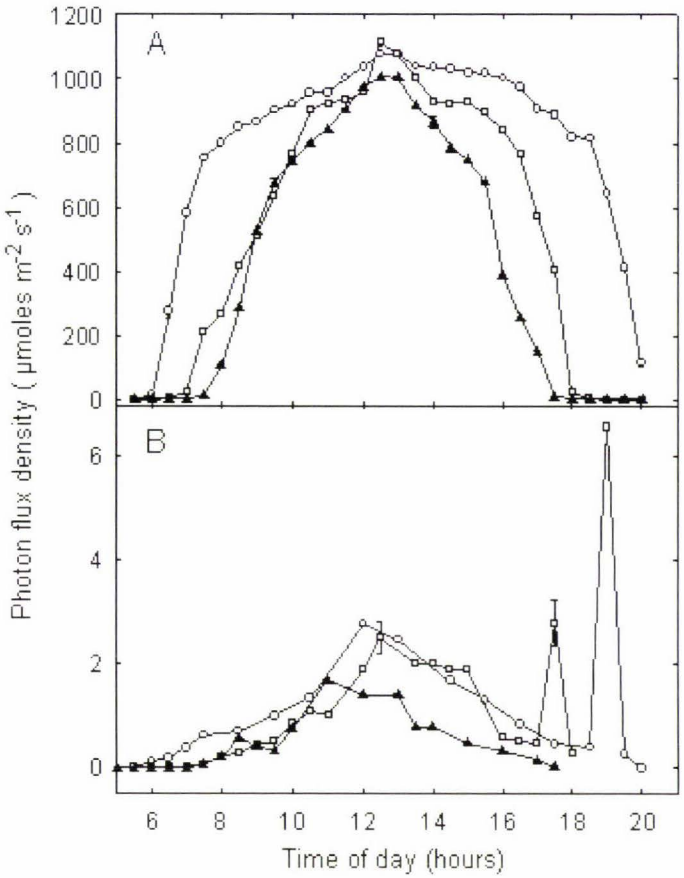

Figure 4.7. The PFD at canopy level (A) and at the sampling sites (B) within Apiti Cave (site 1) at three times in the year (□ =autumn (April); ▲= winter (June);○ = summer (February). The points indicate the average (± SEM) of readings at four different locations as described in section 4.1.

Additional variation in PFD arose from sunflecks associated with movement of the overhanging vegetation. Measurements of the PFD were made over 155 min (between 1000 and 1225 h) during summer (February) at a site that had a PFD of 3 µmoles photons m^{-2} s^{-1} in the absence of additional light (sunflecks and reflected light). The PFD (averaged over 5 min intervals) varied between 3 µmoles photons m^{-2} s^{-1} and 170 µmoles photons m^{-2} s^{-1} (Figure 4.9). The peaks in the graph (Figure 4.10) show the influence of both the sunfleck and the water reflection on the total day PFD.

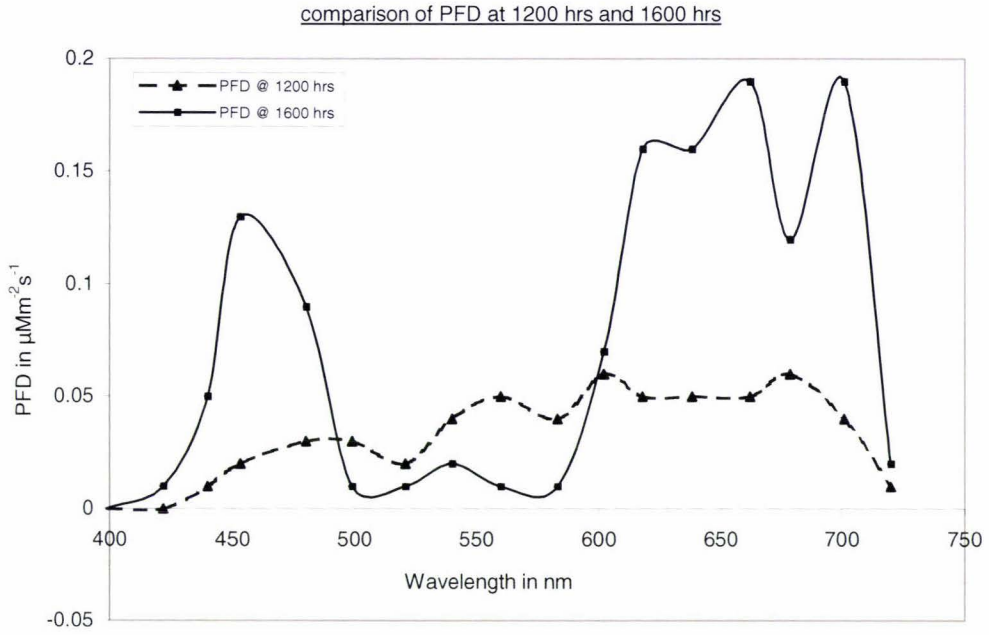

Figure 4.8. Differences in the quality of PAR during a sunny day showing the increase in µmoles photons m^{-2} s^{-1} at 1200 h and 1600 h.

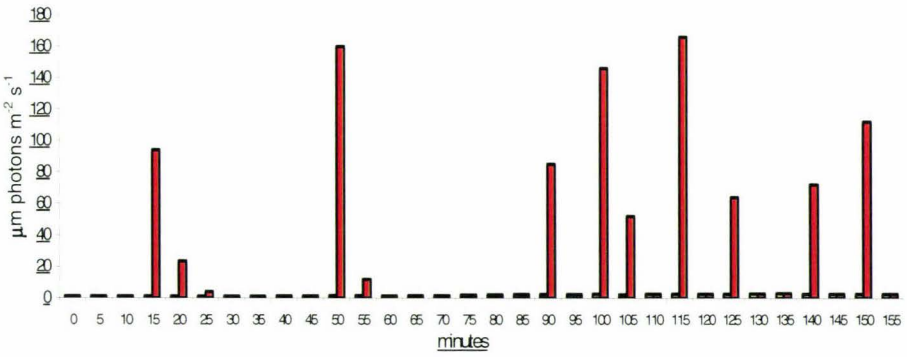

Figure 4.9. Variation in PFD (averaged over 5 min periods) due to sunflecks in a shady site at Rerekino (3 µmoles photons m^{-2} s^{-1} in the absence of additional light) over 155 min during a bright summer day (1000-1225 h).

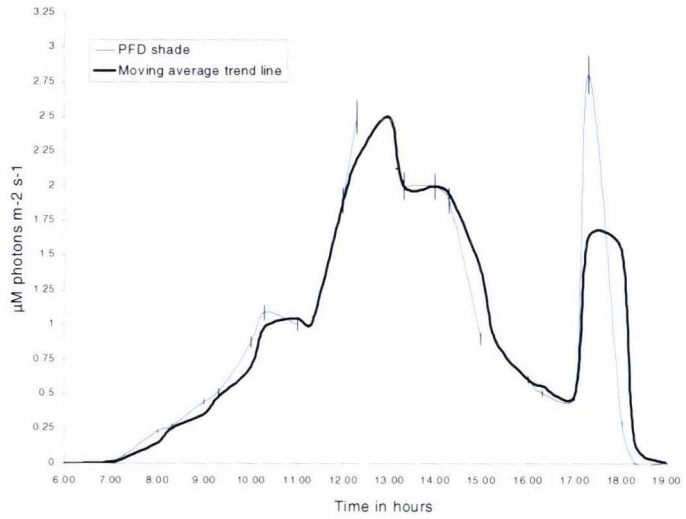

Figure 4.10. Graph of the PFD for a sunny day, 22/04/99, at the *M. pellucidus* site at Rerekino. Two major peaks are shown, peak 1(mid-day) = weight of additional sunfleck illumination and peak 2 (late afternoon) = weight of reflected light. Bars = ± SEM.

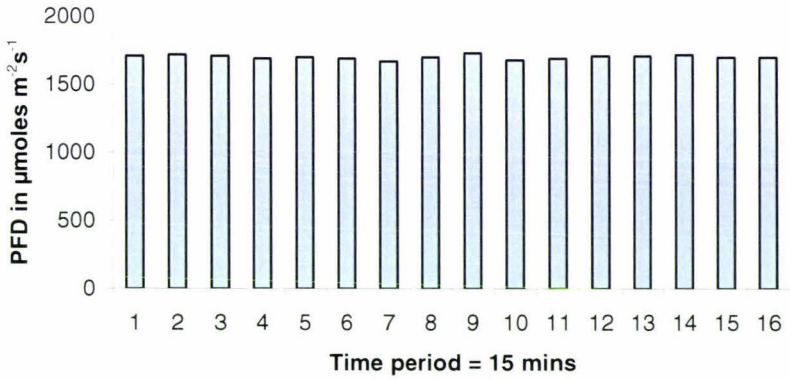

Figure 4.11. Variation in PFD (averaged over 5 min periods) taken at canopy level covering on a summer day showing a very small variation in PFD.

The intermittent nature of the PFD at sub canopy levels (Figure 4.12) was high compared to the small variation in PFD at the canopy (Figure 4.11). The light quality at the canopy (Figure 4.13) was quite different from that at the *M. pellucidus* habitat (Figure 4.14).

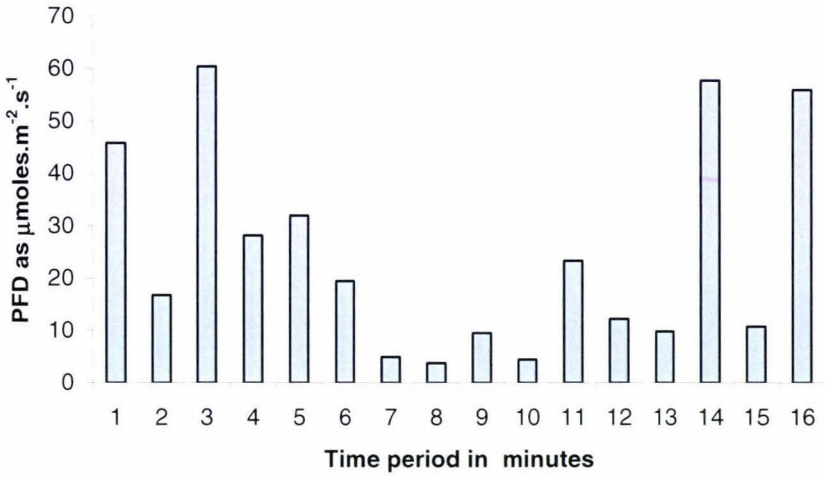

Figure 4.12. Variation in PFD (averaged over 5 min periods) due to sunflecks in a habitat site (3 µmoles photons m^{-2} s^{-1} in the absence of additional light) over 155 min during a bright summer day (1000-1225 h).

Any variation in the available PFD, at extremely low light sites, is a critical factor in many cases only just exceeding the plants light compensation point (LCP). This was not ascertained for *M. pellucidus* but in other bryophytes growing in cool conditions this can vary from 20-400 lux (Valanne, 1984). All of the sites were located in very cool positions, with the winter sampling sites showing frost ice on roadside grasses. The LCP is dependant on the environmental temperatures, increasing with temperature increase and decreasing with temperature fall (Valanne, 1984). All of the four sites were well ventilated and in all cases had cool water running over the thallus surfaces.

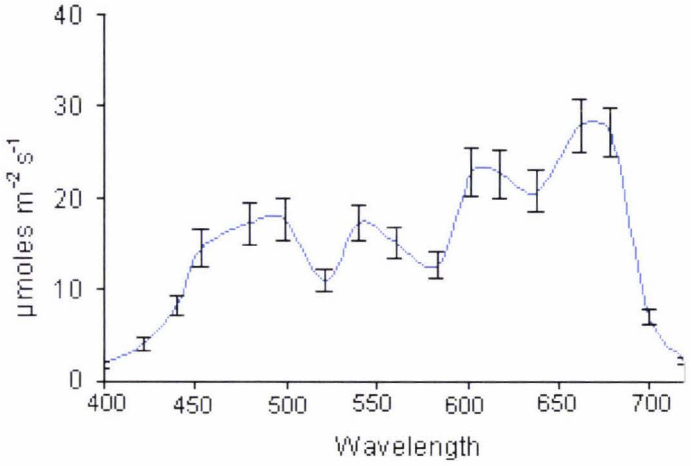

Figure 4.13. The wavelength-dependence of PFD available at the crown canopy over the Rerekino (Site 3) *M. pellucidus* habitats (average PFD = 1707 ± 5 µmoles photons m^{-2} s^{-1}).

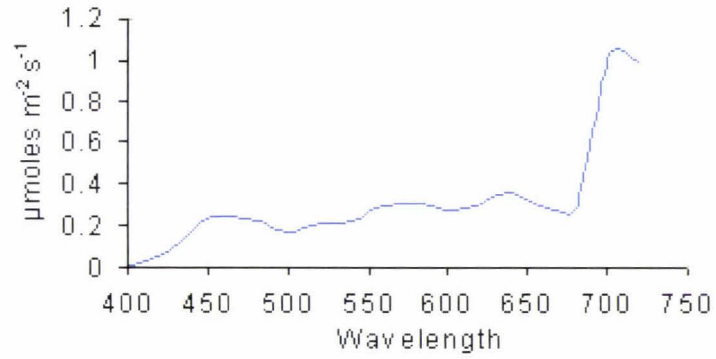

Figure 4.14. The wavelength-dependence of PFD available to *M. pellucidus* habitat after attenuation by the various overhead leaf canopies (average PFD = 2.2 ± 0.4 µmoles photons m^{-2} s^{-1}).

Chapter 5

Results B. Laboratory measurements

5.0 Light environment of the *M. pellucidus* sampling sites

Measurements of the specific light environment at each of the sites have been previously presented (Chapter 4). This chapter covers the observed effects on the chloroplast of *M. pellucidus*, its pigmentation, light effects on chloroplast movement, morphology and volume; osmotic change, the ultrastructural architecture using transmission electron microscopy (TEM) and the association of the chloroplast with the plasmalemma. A generalization of the PFD, covering the various sites, is presented here (Table 5.1) to represent the environment with which these results should be interrelated.

While there is variation in the canopy PFD it should be realized that both the Rerekino and Mahoenui average PFDs were taken on sunny days whereas the Apiti and Tangarakau average PFDs were recorded on cloudy days. All of the measurements should be interpreted in conjunction with the instrument error, (section 3.3.1), especially the very low PFD readings.

Table 5.1. Showing a summary of the four sampling sites, showing the PFD averages of the respective canopies, sample sites and the percentage of initial canopy PFD that finally reaches the *M. pellucidus* thallii.

Site	Average PFD (μmoles photons m^{-2} s^{-1}, ± SEM)		Habitat PFD (% of canopy PFD)
	canopy	habitat	
Apiti (mist + cloud)	923 ± 23	4.4 ± 0.5	0.48
Rerekino (sunny)	1706 ± 5	2.2 ± 0.4	0.13
Tangarakau (cloud)	1076 ± 30	3.2 ± 1.5	0.30
Mahoenui (sunny)	1874 ± 40	2.1 ± 0.4	0.11

5.1 Pigmentation of *M. pellucidus*

The light harvesting pigments are conventionally extracted in a suitable solvent such as 80% (*v/v*) acetone or dimethyl sulfoxide (DMSO). However the pigment spectra are not significantly different in the two solvents ($P < 0.005$) (Raemaekers & Longwith, 1987). Chlorophylls *a* and *b* absorb in the red (at about 660 nm) and in the blue (between about 400 and 460 nm), but do not absorb appreciably in the green (Figure 5.1, high).

It was found that *M. pellucidus*, grown in low light sites, exhibited an absorbance band with an apparent maximum at about 340 nm which was not apparent in pigment extracts from plants grown in higher light conditions (Figure 5.1).

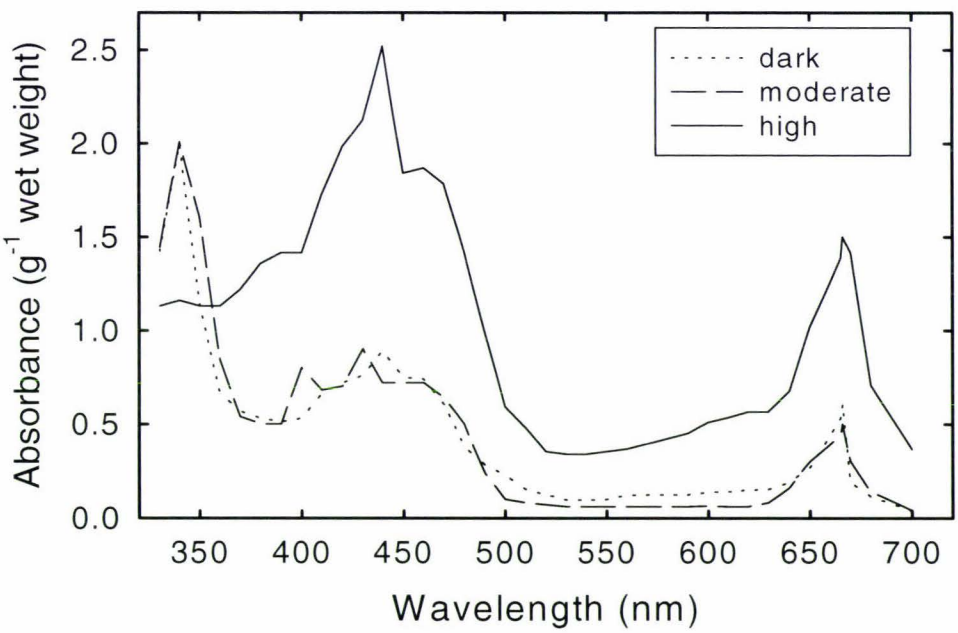

Figure 5.1. Absorbance spectra of 80% (*v/v*) acetone extracts of *M. pellucidus* grown Apiti Cave (site 1) in high (6.9 ± 0.3 µmoles photons m^{-2} s^{-1}), moderate (2.8 ± 0.1 µmoles photons m^{-2} s^{-1}) or dark (0.2 ± 0.1 µmoles photons m^{-2} s^{-1}) light. The PFD were measured at the Apiti site at 1400 h during April and absorbance have been corrected for differences in the wet weight of the tissue used.

5.1.1 Chlorophyll analysis of *M. pellucidus*

Pigment extracts of *M. pellucidus*, grown in moderate or low light levels appeared to have very similar absorbance spectra (Figure 5.1), but they both differed substantially from those of extracts from *M. pellucidus* grown in higher light sites (Figure 5.1 , high). Samples from the highest PFD conditions had significantly more chlorophyll (0.189 mg g^{-1}) than those from lower PFD situations (0.119 mg g^{-1}) (Table 5.2). The chlorophyll content of shade plants tends to be higher than in those receiving full sunlight (Anderson *et al.*, 1973; Barbour *et al.*, 2000; Böhning & Burnside, 1956; Tanaka & Melis, 1997). But given the extremely low light circumstances in which *M. pellucidus* grows the pigmentation could be expected to be unusual.

Table 5.2. Chlorophyll content of *M. pellucidus* grown in two low light environments.

	Low light habitat (0.2 ± 0.1 µmoles photons m^{-2} s^{-1})	**High light habitat** (6.9 ± 0.3 µmoles photons m^{-2} s^{-1})
Weight (g)	0.98 ± 0.0	0.49 ± 0.08
A_{645}	0.8 ± 0.1	0.6 ± 0.1
A_{663}	1.0 ± 0.4	0.8 ± 0.4
Chl *a* (mg g^{-1})	0.054	0.084
Chl *b* (mg g^{-1})	0.065	0.105
total chl (mg g^{-1})	0.119	0.189
Chl *a*:*b* ratio	0.822	0.801

5.2 Movement of the chloroplast within the cell

M. pellucidus chloroplasts change both their morphology and spatial orientation in response to light. The extent of the positional response was related to the location of the cell across the thallus (Figures 5.5 and 5.7).

In dorsal and ventral 'epidermal' cells the chloroplast moved relatively little, whereas in the mid-thallus cells the chloroplast moved significantly in response to

changes in the light environment (Figure 5.7). In high, white light conditions (>140 μmoles m^{-2} s^{-1}) the chloroplast adhered to anticlinal cell walls, a parastrophe position (Figures 1.2, 5.2 and 5.7). In light conditions simulating the natural habitat (~3 μmoles photons m^{-2} s^{-1}), the chloroplast was in an epistrophe position (Figures 1.2, 5.3 and 5.7). In complete darkness, the chloroplasts were randomly distributed, an apostrophe position (Figures 1.2, 5.4 and 5.7).

Light micrographs of representative samples of thallus cross sectional tissue exposed to different PFDs are shown in Figures 5.2 to 5.5. Dorsal 'epidermal' cells exposed to high PFD (>140 μmoles photons m^{-2} s^{-1}) had small (a cross-sectional area of 300 ± 20 μm^2), spherical chloroplasts located on anticlinal walls (Figure 5.2). Chloroplasts exposed to light equating to the average incident light found in the natural habitat of *M. pellucidus* (~3 μmoles photons m^{-2} s^{-1}) had 'hanging drop' chloroplasts on the periclinal wall proximal to the light source (Figure 5.3). Ventral 'epidermal' cells kept in complete darkness for 24 h exhibited large (a cross-sectional area of 1600 ± 200 μm^2), randomly oriented chloroplasts (Figure 5.4).

The position of the chloroplast also varied in response to light quality (using the LED illumination system described in section 3.3.2.2). In blue light (470 nm, > 2 μmoles photons m^{-2} s^{-1}), the chloroplasts responded in fashion similar to those in high white light (data not shown). In red light (660 nm), irrespective of the PFD, the chloroplasts retained the habitat light location (data not shown).

Figure 5.5 shows the dorsal epidermis and the bottom ventral epidermis of *M. pellucidus*, both single cell layers are richly endowed with chloroplasts. Each chloroplast is located in a position nearest to the light source within its host cell. The double chloroplast shapes seen in the large centre cells, are in fact single; being connected by a thin strand of chloroplast tissue (Figure 5.6). The cells adjacent to the dorsal epidermis are parenchymous and smaller than the large central cells while similar cells adjacent to the ventral epidermis have a cylindrical shape. Central cells, in the lumen of the thallus, comprise of < 3 layers of large, parenchymous, tetrakaidecahedral[1] (Lloyd, 1991) and loosely arranged.

---

[1] Tetrakaidecahedron = a geometrical form of a "truncated octahedron," it is an optimal space filler model and can be applied to packed parenchyma cells since they simulate a foam from which the tetrakaidecahedral model has derived its mathematical genesis (Lloyd, 1991).

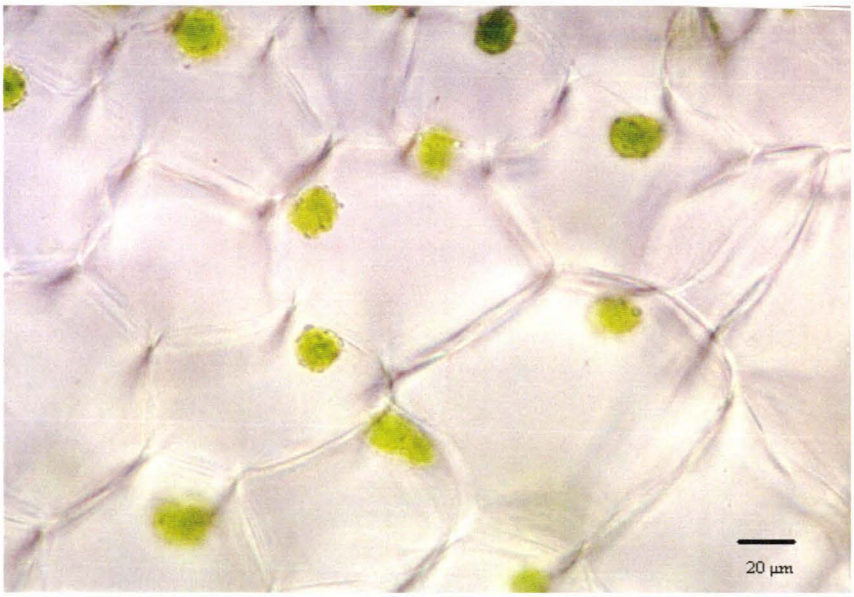

Figure 5.2. Chloroplasts of *M. pellucidus* (×400) exposed to 140 µmoles photons m^{-2} s^{-1} of white light or blue light > 3µmoles m^{-2} s^{-1}. The chloroplasts are situated on the anticlinal cell walls, in the 'parastrophe' position (Britz, 1979).

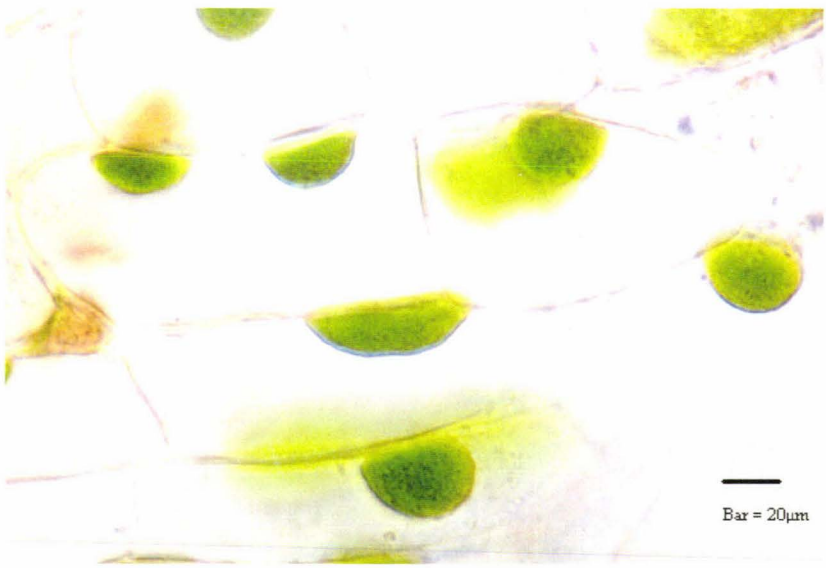

Figure 5.3. Chloroplasts of *M. pellucidus*, epidermal cells (×400). Exposed to white light equivalent to the average habitat PFD level (~ 3 µmoles photons m^{-2} s^{-1}). This illustrates the "hanging drop" or epistrophe position (Britz, 1979).

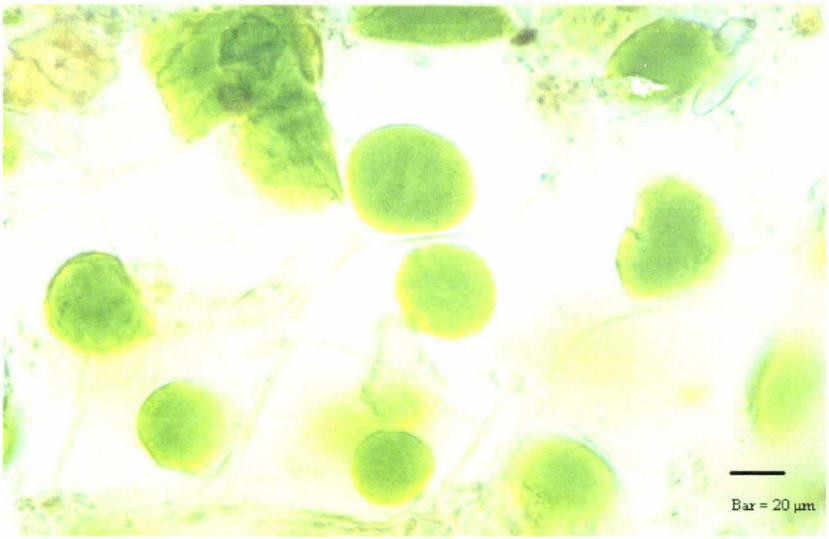

Figure 5.4. Chloroplasts of *M. pellucidus* (×400) after 24 h total darkness showing the maximum chloroplast size and randomness of wall contact position or "apostrophe" position (Britz, 1979).

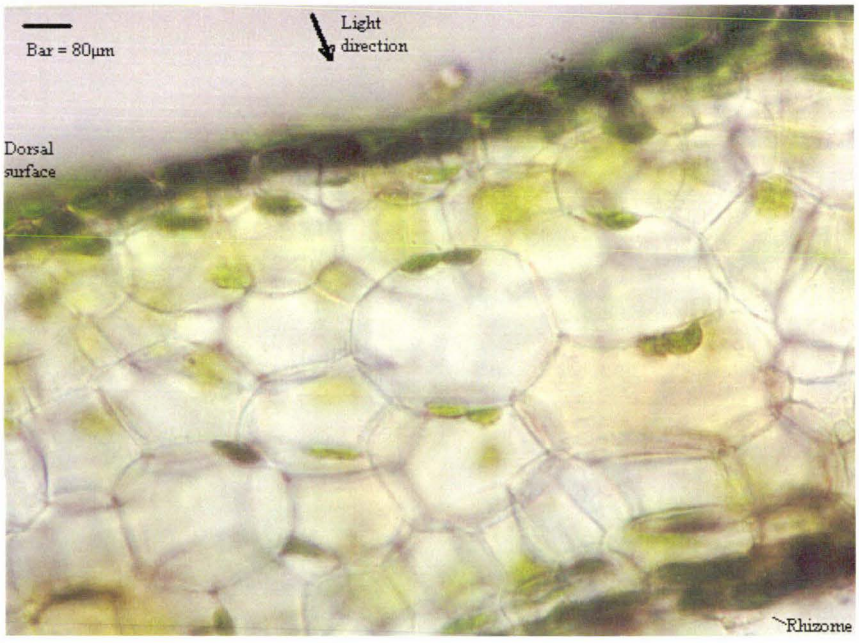

Figure 5.5 Micrograph (×100) of a transverse section across a *M. pellucidus* thallus, after 24 h of darkness the chloroplasts were aligned on the periclinal walls.

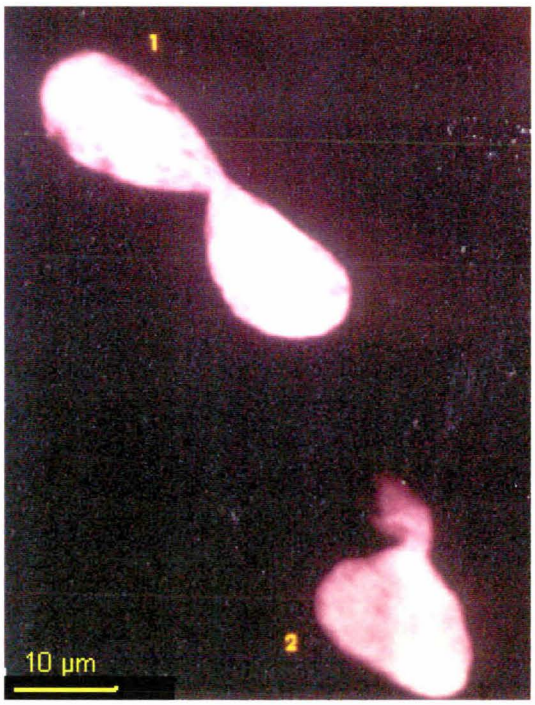

Figure 5.6. A confocal micrograph of two *M. pellucidus* chloroplasts after 33 minutes irradiation of 512 nm. Both chloroplasts show clearly the "hourglass" stem configuration; chloroplast two is oriented along a virtual z-axis.

In all of the *M. pellucidus* thalli examined the thickness of the thallus was ~0.96 mm (taken as a transverse section of the thallus, 4-6 mm from the tip). This 0.96 mm thickness, comprising of seven layers of cells, is similar to the thallus thickness measurements of other *Megaceros* spp, which range from 0.2-1.2 mm (Valentine, 1984). The chloroplasts appear to be concentrated in the dorsal epidermis, providing a mosaic like layer along a periclinal plane situated immediately below the thallus surface. However, while the mid-section cell chloroplasts are far less concentrated per cubic area than the epidermal cell chloroplasts, the actual chloroplast size is similar to both. The dorsal and ventral cell layers appear to have a much higher density of chloroplasts than those cells in the mid section of the thallus (Figure 5.5).

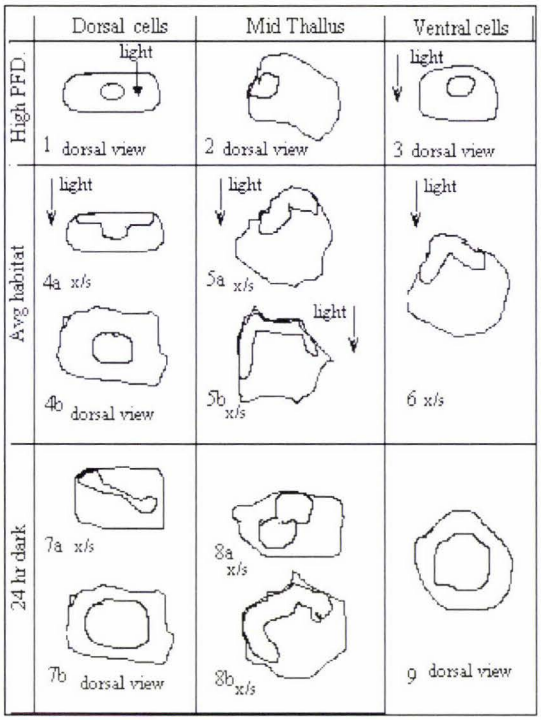

Figure 5.7. Chloroplast position and morphology in cells across the *M. pellucidus* thallus exposed to high (either sun or blue) light, average habitat (3 μmoles photons m^{-2} s^{-1}) light, or complete darkness for 24 h. The light originates from the top of the page (arrows). Cross section (x/s) and top views (dorsal) are differentiated by a and b, respectively. In mid-thallus the cell diagrams that represent the habitat light (5 and 8), describe only two forms of the diversity of morphologies seen.

5.3 Changes in chloroplast volume

The light micrographs shown in Figure 5.2, 5.4 and 5.5 clearly demonstrate the light-induced changes in chloroplast volume from the condensed form in high light (Figure 5.2) to the various structures in the low light conditions in which *M. pellucidus* grows (Figure 5.3) or the enlarged form in complete darkness (Figure 5.4). In high light (>140 μmoles photons m^{-2} s^{-1}) the chloroplasts shrank over a period of about 75 minutes and they expanded over a similar period on subsequent dark incubation.

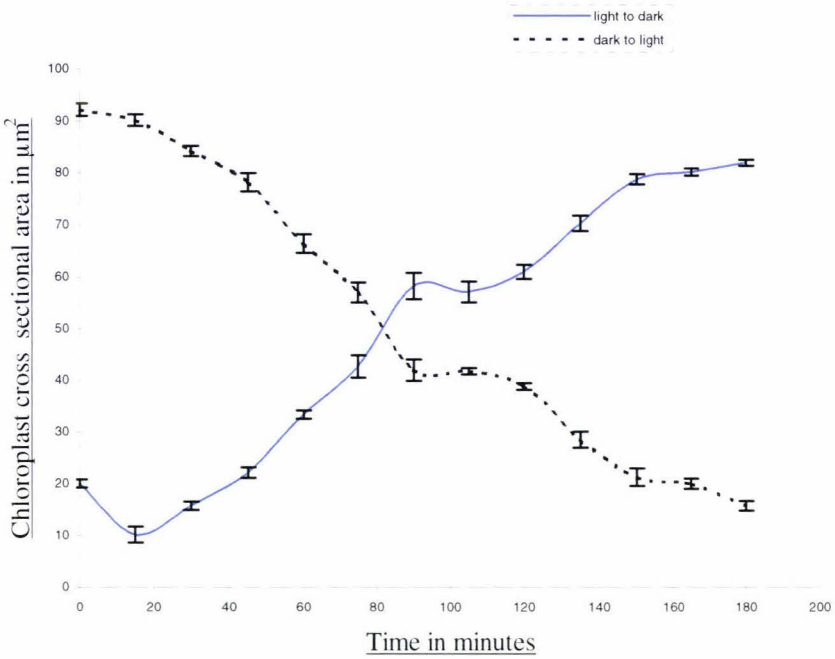

Figure 5.8. Change in the proportions of shrunken chloroplasts on exposure to high PFD (556 µmoles photons m^{-2} s^{-1}) or to complete darkness, after prior exposure to high light (556 µmoles photons m^{-2} s^{-1}). At each time point the cross-sectional area of each of between 7 and 20 chloroplasts was measured. (The error bars represent ± SEM.)

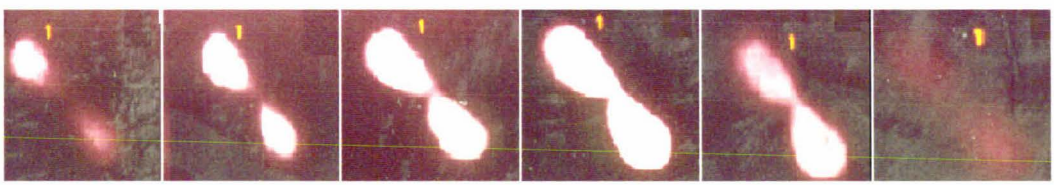

Figure 5.9. Shows a series of confocal micrographs recording the diminishment of a chloroplast volume during the laser illumination, at 512 nm, over a period of 66 min. The sections were taken at 6 µm depth intervals giving a total field depth of more than 30 µm.

The confocal micrographs in Figure 5.9 show section scans at relative depths through the chloroplast enabling a volume calculation to be obtained, however summing errors can be introduced if the scanning sections, individual depth focus, is not sufficiently contiguous (Corle & Kino, 1996; Gray *et al.*, 1999; Pawley, 1995; Stevens *et al.*, 1994) (sections 3.4.1 and 3.4.3).

5.4 Dependence on light quality

Since incubation in white light induced a shrinkage of *M. pellucidus* chloroplasts (Figure 5.8), experiments were carried out to investigate whether this was specifically related to any particular wavelength, as has been observed with green algae (Britz, 1979; Gabrys-Mizera *et al.*, 1997; Haupt, 1982; Ramus, 1978) and Ferns (Augustynowicz & Gabrys, 1999; Kadota & Wada, 1999; Kagawa & Wada, 1996; Kagawa & Wada, 1999) Incubation in complete darkness, average habitat light (2.5 μmoles photons m^{-2} s^{-1}) or red (660 nm) light (up to 130 μmoles photons m^{-2} s^{-1}) for at least 60 min caused no obvious change in chloroplast cross-sectional area. However, incubation with 3 μmoles photons m^{-2} s^{-1} of blue (470 nm) light caused a rapid decline in the cross-sectional area of the chloroplasts (Figure 5.2 and 5.11).

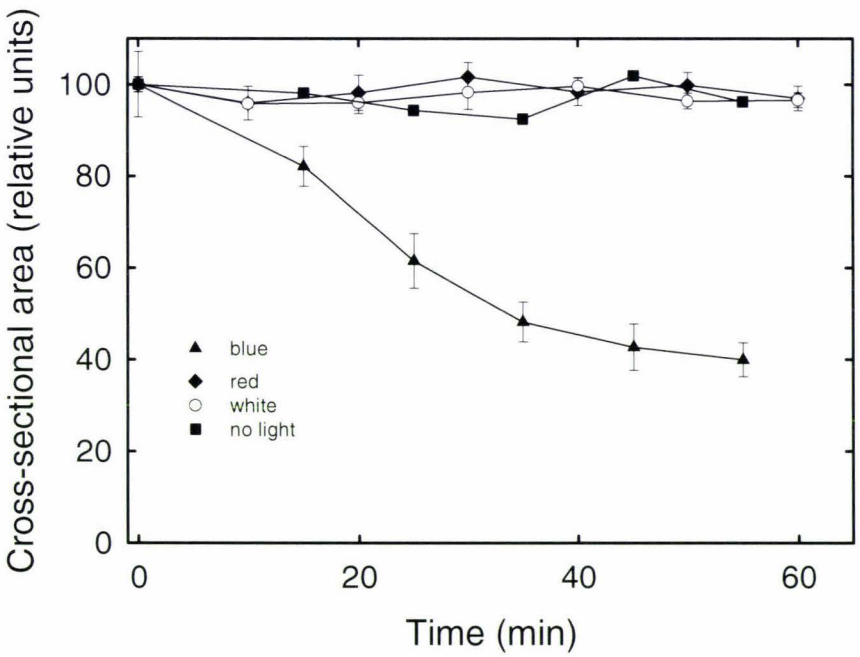

Figure 5.10. Effect of illumination of different light quality on the cross-sectional area of *M. pellucidus* chloroplasts. The *M. pellucidus* tissue was incubated in water in complete darkness (■), white light (2.5 μmoles photons m-2 s-1; ○), blue light (3 μmoles photons m-2 s-1; ▲) or red light (130 μmoles photons m-2 s-1; ♦) as described in section 3.3.2.2. The initial average cross-sectional areas varied between 45 μm2 and 56 μm2 and the error bars represent ± SEM (n = 10 chloroplasts).

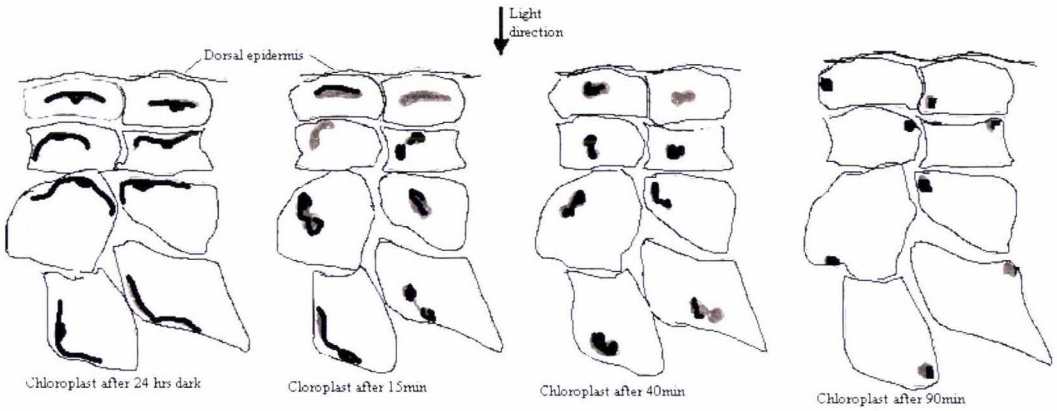

Figure 5.11. This illustration shows the change in *M. pellucidus* chloroplast orientation and morphology in response to blue light (470 nm) at >3 µmoles photons m^{-2} s^{-1} for a period of 90 min. (Graphics representative of ~ ×400)

Varying the PFD (0-10 µmoles photons m^{-2} s^{-1}) of blue light (470 nm) affected the rate at which chloroplast volume decreased (Figure 5.12). Below 1 µmole photons m^{-2} s^{-1} no significant response was observed, but at 2 µmoles photons m^{-2} s^{-1} a slow decline in volume could be ascertained. At PFDs of 3 µmoles photons m^{-2} s^{-1} and above the rate of shrinkage did not appear to increase (Figure 5.12). The rate constant for the process was approximately 0.02 min^{-1} (Figure 5.13), which compares well with the value of 0.005 - 0.009 min^{-1} obtained *in vivo* by McCain (1992; McCain, 2000).

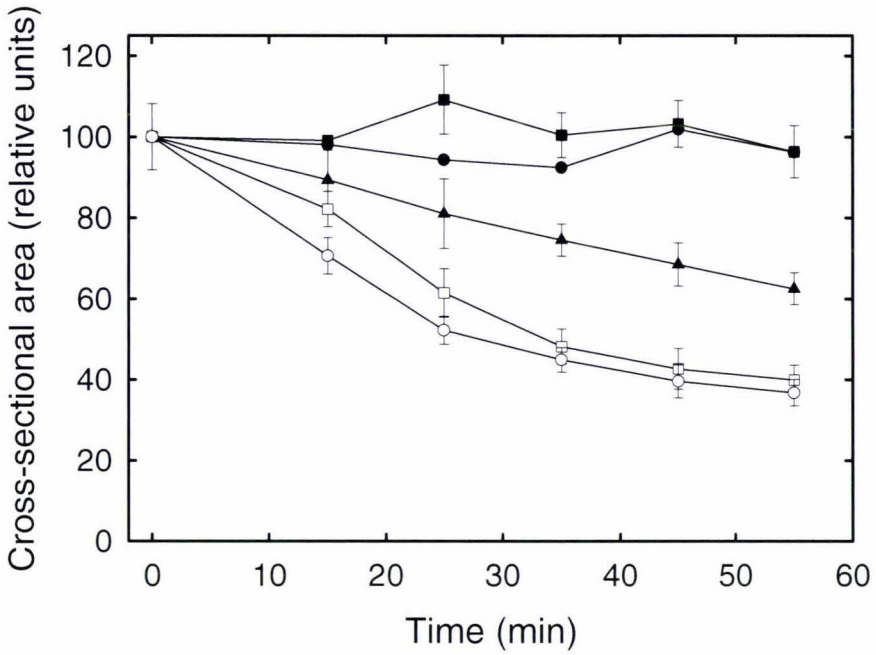

Figure 5.12. Effect of different photon flux densities of blue (470 nm) light on *M. pellucidus* chloroplasts. (Taken as chloroplast X/S area differences) Tissue was incubated in water in complete darkness (•) or various PFDs (■ = 0.1; ▲ = 2; = 3; ○ = 5 μmoles photons m^{-2} s^{-1}) as described in section 3.3.2.2. The initial average cross-sectional areas varied between 45 μm^2 and 56 μm^2 and the error bars represent ± SEM (n = 10 chloroplasts).

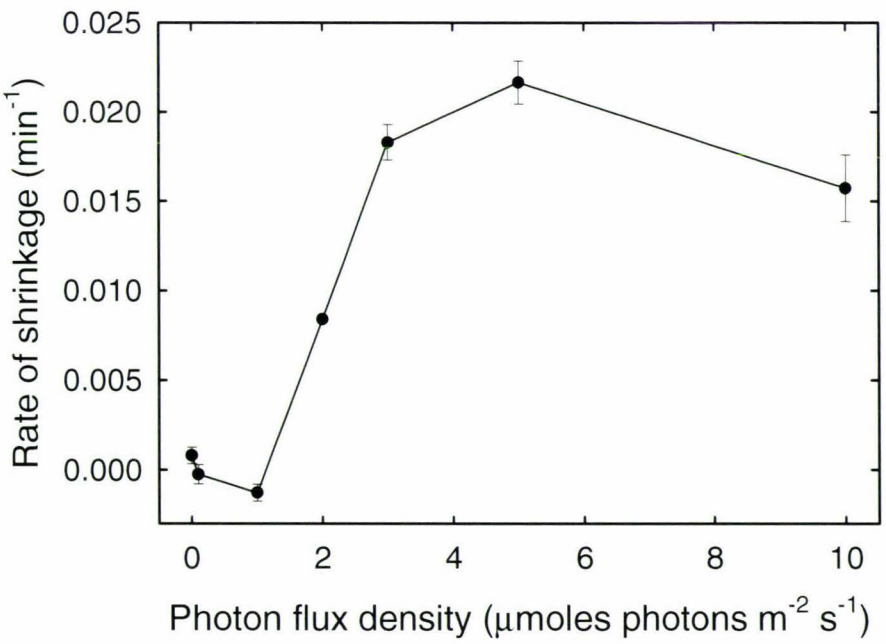

Figure 5.13. Rate of change in cross-sectional area in response to changes in PFD of blue (470 nm) light. The values were obtained by fitting a single exponential decay to the data shown in Figure 5.12. The values plotted are the rate constant ± its estimated standard error.

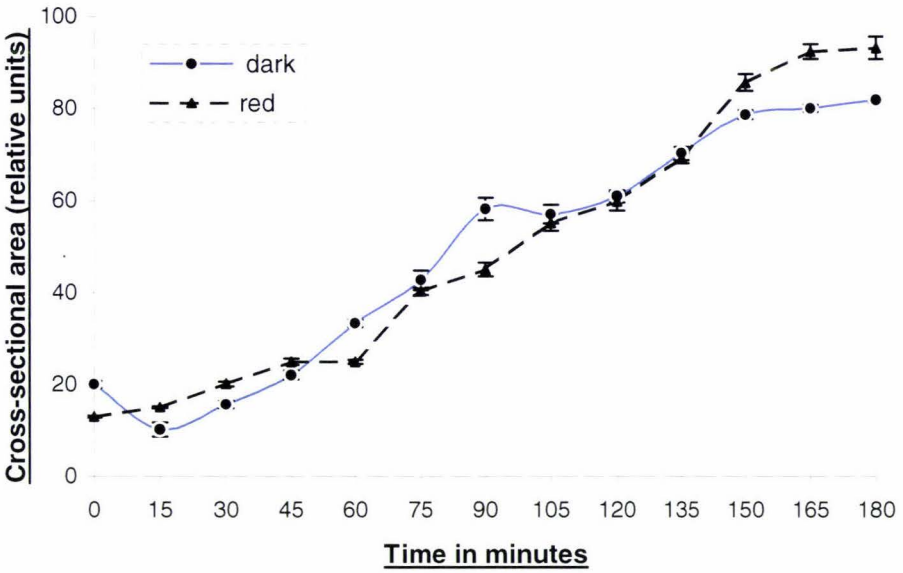

Figure 5.14. Change in the proportions of shrunken chloroplasts on exposure to red light (662 nm, 130 μmoles photons m^{-2} s^{-1}(▲) or complete darkness (▪) after 24 h of illumination in white light (556 μmoles photons m^{-2} s^{-1}). At each time point the cross-sectional area (of each of between 10 and 25 chloroplasts) was measured. (The error bars represent ± SEM.)

Incubating tissue samples in high light (556 μmoles photons m^{-2} s^{-1}) induced chloroplast shrinkage. Once the samples were transferred to darkness or to red light (662 nm, 130 μmoles photons m^{-2} s^{-1}), the chloroplasts in the sample returned to the low light volume shape (Figure 5.14). The rate at which the chloroplasts increased in volume was not altered by illumination with red light of any PFD up to 130 μmoles photons m^{-2} s^{-1} (data not shown).

5.5 Effect of osmotic potential

The rapid changes in chloroplast volume observed (sections 5.3 and 5.4) presumably involved fluxes of water into and out of the organelle (Gupta & Berkowitz, 1988; Long & Iino, 2001; McCain & Markley, 1992; McCain, 2000; Nobel, 1968). Water fluxes can also be induced by osmotic potential gradients between the chloroplast stroma and the surrounding medium, which can be generated in tissue samples (McCain & Markley, 1992; McCain, 1995; Nobel, 1968; Robinson, 1985) or in isolated chloroplasts (Gupta & Berkowitz, 1988; Ivanchenko *et al.*, 1980) by incubating them in osmotica.

When dark-adapted *M. pellucidus* tissue samples were incubated in polyethylene glycol-20 (PEG) chloroplast volume diminished (Figure 5.15). The rate at which the volume decreased was greater than that observed in response to blue light (Figure 5.13). In 1.5% (*w/v*) or 2.9% (*w/v*) PEG (Figure 5.15), the rate constants were 0.032 ± 0.002 min^{-1} and 0.040 ± 0.003 min^{-1}, respectively, compared with approximately 0.02 min^{-1} in blue light.

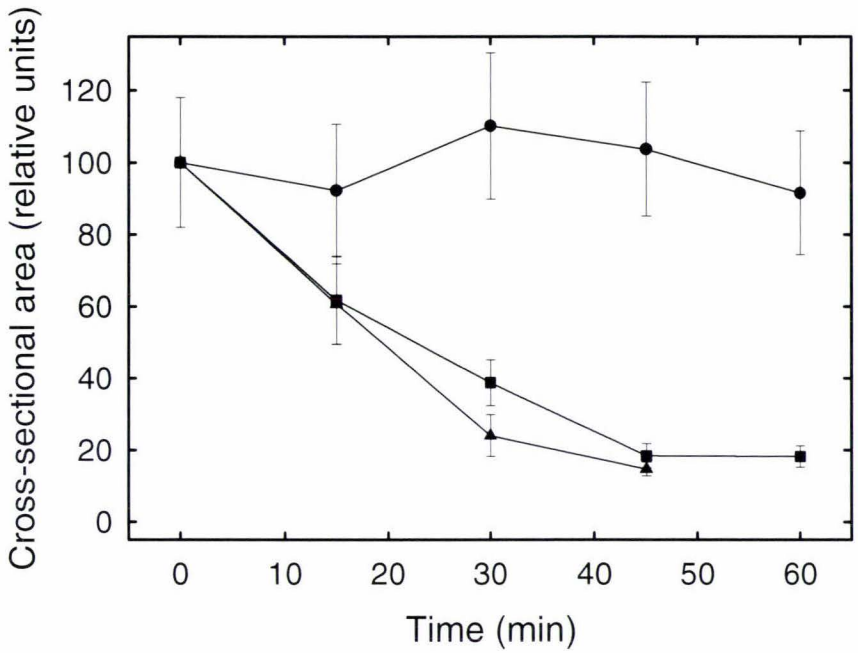

Figure 5.15. Effect of polyethylene glycol-20 (PEG) on chloroplast volume. Plants were kept in the dark. Tissue samples were taken and incubated in water (•), 1.5% (*w/v*) PEG (■) or 2.9% (*w/v*) PEG (▲), respectively. Each point represents the average cross-sectional area of five chloroplasts (± SEM). After 50 minutes in 2.9% (*w/v*) PEG the tissue plasmolysed.

The extent to which the volume decreased was also related to the PEG concentration, which is related to the osmotic potential of the solution (Parsegian *et al.*, 1986). At low PEG concentrations the volume was not affected, but above 0.2% (*w/v*) PEG reduction of the cross-sectional area was observed (Figure 5.16). Above 2.9% (*w/v*) PEG plasmolysis occurred after about 50 min. At 3.6% (*w/v*) PEG, 60% plasmolysis was observed after 15 min.

Incubating tissue samples in PEG solutions in the dark quickly resulted in stable chloroplast volumes (Figures 5.15 and 5.16) that did not change significantly during further dark incubation. However, illumination with red light (662 nm) at a PFD of

130 μmoles photons m^{-2} s^{-1} caused the chloroplasts to increase in volume (Figure 5.17) in spite of the osmotic potential of the medium in which the tissue samples were suspended.

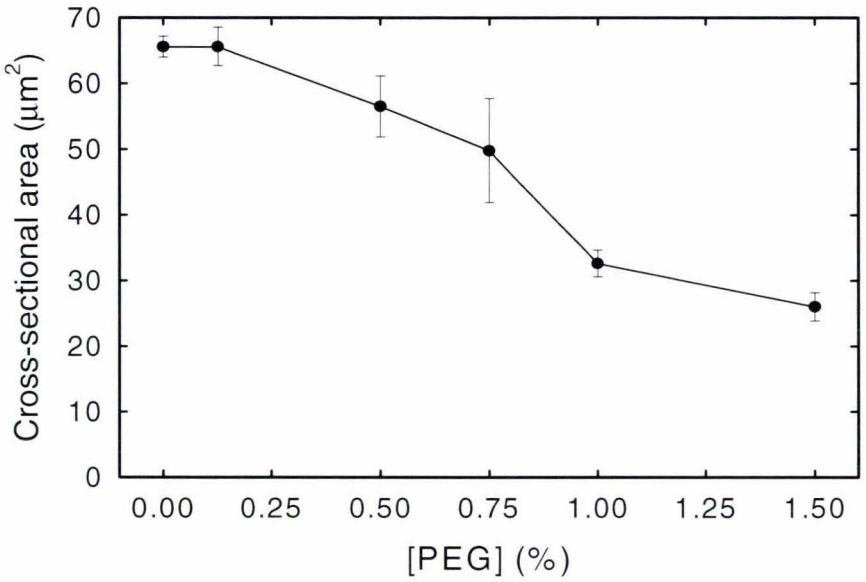

Figure 5.16. Chloroplast cross-sectional area after 2 h incubation in different polyethylene glycol-20 (PEG) concentrations. Tissue samples were incubated in the dark for 2 h in the appropriate PEG solution before measurement of the chloroplast cross-sectional area. The points represent the average (± SEM) of 5 chloroplasts. A 1.5% PEG solution has an osmotic potential of 0.37 MPa (Parsegian *et al.*, 1986).

Illumination with blue light of tissue samples incubated in PEG solutions had less effect on the rate of chloroplast shrinkage as the PEG concentration was increased (data not shown).

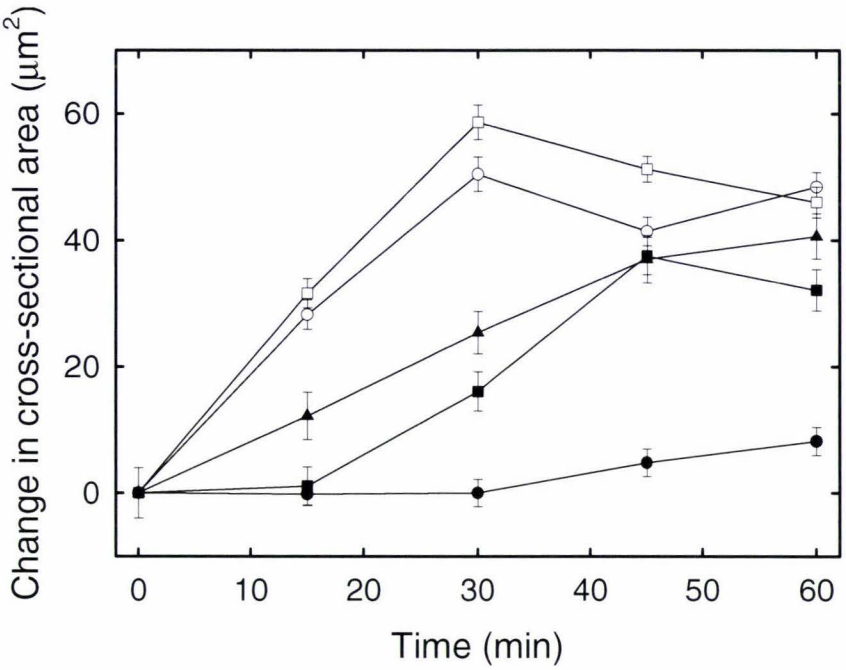

Figure 5.17. Change in the cross-sectional area of chloroplasts in PEG-incubated tissue samples during illumination with red (662 nm) light (130 μmoles photons m^{-2} s^{-1}). Tissues samples were incubated in the PEG solutions for 2 h prior to start of measurement and were maintained in the same solutions throughout the illumination period. The initial cross-sectional areas were those shown in Figure 5.16 and the points represent the average change (± SEM) in the cross-sectional areas of 5 chloroplasts. PEG concentrations: • – 0%; ■ – 0.5%; ▲ – 0.75%; ○ – 1%; □ – 1.5% (*w/v*) PEG.

5.6 The ultrastructural character of the *M. pellucidus* chloroplast in response to light

In the work described above the chloroplast responses to various stimuli were monitored by light microscopy. However, any investigation of changes in chloroplast ultrastructure requires the enhanced magnification available using transmission electron microscopy (TEM).

The pyrenoid body, that is present in nearly all Anthocerotes (Burr, 1968; Valentine, 1984; Vaughn *et al.*, 1992), is known to be the localization centre of ribulose-1,5-bisphosphate carboxylase/oxygenase (Rubisco) and its activase in the green algae *Chlamydomonas reinhardtii* and *Coleochaete scutata*. (McKay & Gibbs, 1989). This same relationship has been shown to be homologous to the Anthocerophyta (Vaughn *et al.*, 1992). The *M. pellucidus* used in these experiments did not display any obvious pyrenoid body that concurs with the observations of Valentine (1984;

Valentine & Campbell, 1986). It was found that all species of *Megaceros*, that have no pyrenoid, have Rubisco evenly distributed through the stroma (Vaughn *et al.*, 1990).

Many thylakoid membranes are found throughout the chloroplast interior in stacks and as stroma lamellae, which in all Anthocerophyte species, except *Megaceros,* can be seen to differentiate the large pyrenoid bodies into smaller irregularly shaped ones (Vaughn *et al.*, 1992). Another Anthocerote characteristic is the unique channel thylakoids (Burr, 1970) (Figure. 5.18) which connect the grana stacks perpendicularly to their long axis. This creates the "spongy, honeycomb texture" of the thylakoid system (Vaughn *et al.*, 1992). Other characteristic features include the atypical grana end membranes that lack the usual sharply curved nature that typifies chloroplasts of other embryophytes (Burr, 1968; Manton, 1962; Vaughn *et al.*, 1992).

Using TEM the *M. pellucidus* chloroplast envelope and the thylakoid membranes, in both contracted (high and blue light) and the expanded (dark and red light) forms, were examined. The objective was to characterise the ultrastructural features of the organelles in different conditions.

Both high intensity white and blue light cause the *M. pellucidus* chloroplast to contract (section 5.3). Figures 5.18. and 5.21 show transmission electron micrographs of chloroplasts from tissue samples exposed to darkness while Figures 5.19 show high light effects (556 μmoles photons m^{-2} s^{-1}, for 24 h prior to fixation). The dark-adapted tissue had elongated chloroplasts (Figure 5.11), which could not be imaged in their entirety at this magnification (Figure 5.18), whereas the light-adapted tissue had contracted chloroplasts (Figure 5.7, 1 - 3) all of which could be imaged (Figures 5.19 and 5.24). Images of chloroplasts from tissue incubated in the same way were obtained by confocal microscopy (Figures 5.6 and 5.9) to confirm that any variation in the orientation of the organelle did not explain the apparent differences in chloroplast volume. Tissue exposed to blue light (3 μmoles photons m^{-2} s^{-1}) also exhibited contracted chloroplasts (data not shown).

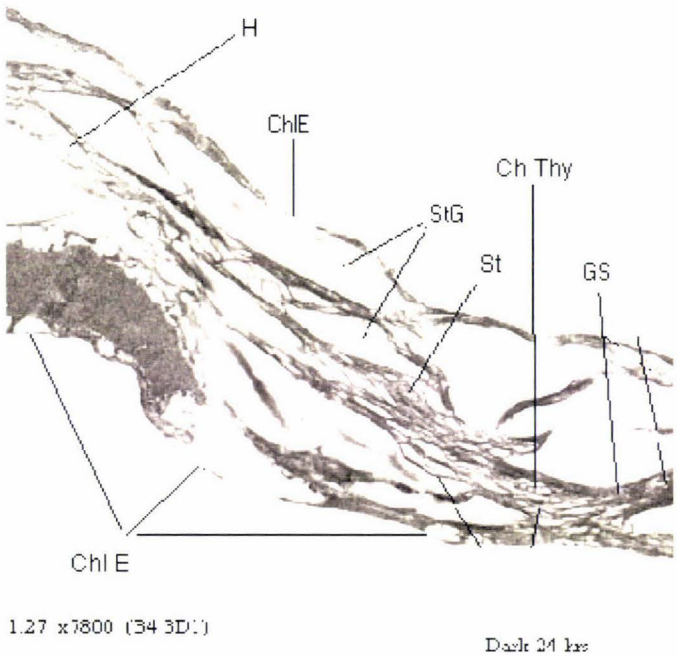

Figure 5.18. TEM (×7800) micrograph of the mid-section of a M. pellucidus chloroplast from tissue held in darkness for 24 h. Note the very open texture and the large number of starch granules. Key H = honeycomb effect, Chl E = chloroplast envelope, StG = starch granules, St = stroma, Ch Thy = channel thylakoids, GS = grana stacking. The large dark mass at the mid left of the microphotograph is thought to be an artefact rather than a pyrenoid body.

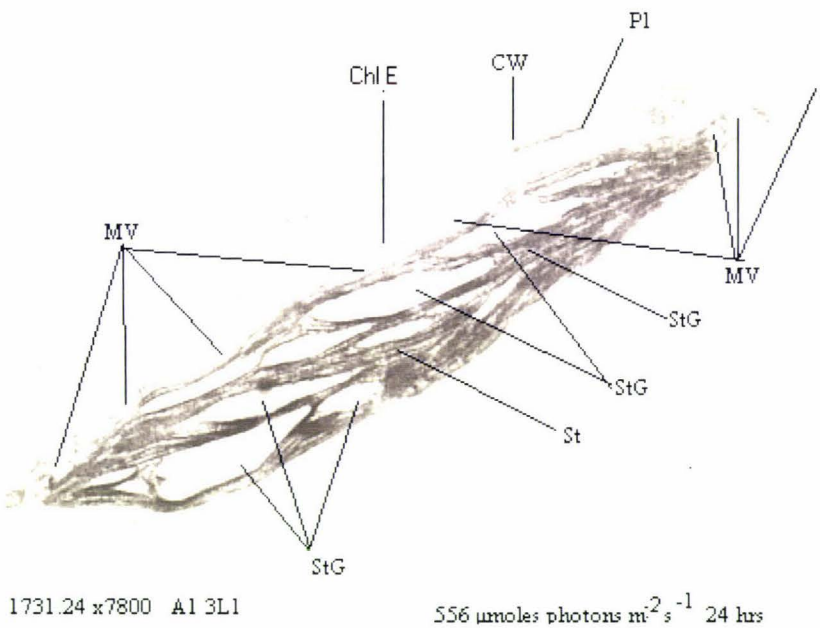

Figure 5.19. TEM (×7800) Micrograph of a *M. pellucidus* chloroplast from tissue sections held in natural light of 556 µmoles photons m^{-2} s^{-1} for 24 h. Note the compacted texture and the diminished size of the starch granules. Key = Chl E = chloroplast envelope, StG = starch granule, St = stroma, CW = cell wall, Pl = plasmalemma, MV = possible envelope membrane vesicles.

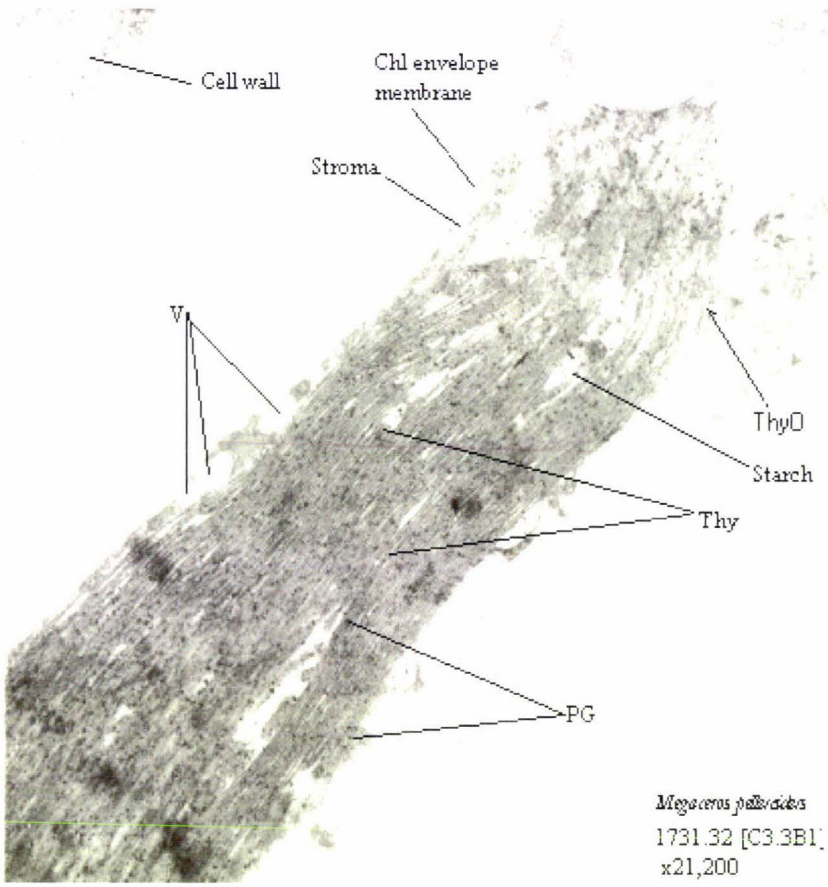

Figure 5.20. TEM (×21200) micrograph of a portion of the tissue section showing chloroplasts of a *M. pellucidus* section after 2 h illumination by blue light (458 nm at a PFD of 10 μmoles photons m^{-2} s^{-1}). Note the tight compression of thylakoids (Thy). Starch granules were very reduced. The stroma was generally reduced and confined to very small areas. Note the open ended thylakoid = (ThyO) a characteristic of algae and the Anthocerophyta (Valentine, 1984; 1986; Vaughn *et al.*, 1992). Spherical shapes (V) indicated just inside the chloroplast envelope, are possibly starch granules but lack the characteristic shape. Note the high concentrations of plastoglobuli (PG), thought to be possible sites of carotenoid accumulation (Vaughn *et al.*, 1992).

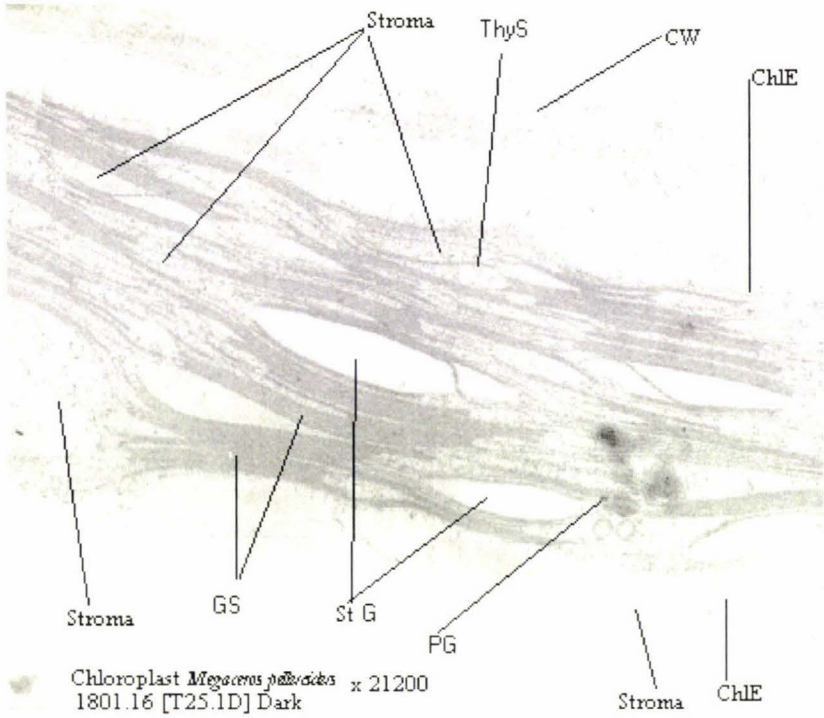

Figure 5.21. TEM (×21200) micrograph of a portion of the chloroplast from *M. pellucidus* after 24h of darkness. Showing expansion of stroma, separation of thylakoid strands (ThyS) and groups of grana stacking (GS), also termed pseudograna (Manton, 1962). Starch granules (StG) are also proportionally larger than in chloroplasts subject to higher PFD or blue light of 458 nm (Figure 5.21.). There are fewer plastoglobuli (PG) compared to Figure 5.21. The chloroplast envelope (ChlE) shows no sign of associated vacuoles.

Chloroplasts from dark-adapted tissue sometimes had large numbers of starch granules around which the thylakoid membranes were wound (Figure 5.18 and 5.21) and these granules were sometimes rather larger than those observed in light-adapted tissue (Figure 5.19 and 5.20). Very little stroma was apparent in either of the chloroplasts shown (Figure 5.19 and 5.20), although other regions of chloroplasts from dark-adapted tissue had more stroma (Figure 5.21). In the Figure 5.22 there are channel thylakoids (labelled TC) (Burr, 1968) that connect the top and bottom of adjacent grana.

At higher magnification the compaction of the light-exposed chloroplast becomes more apparent. Chloroplasts from dark-incubated tissue exhibited obvious grana and appreciable regions of stroma (Figure 5.21), whereas those from high or blue light-incubated tissue were very compressed and showed no obvious stroma or

grana, although there was considerable membrane appression (Figures 5.19 and 5.20).

There was no obvious invagination of the chloroplast envelope in chloroplasts from high-light adapted tissue (Figure 5.20) although there were some vesicles (V) that could be worthy of further investigation. In either case, the thylakoids were 'open ended' (Figure 5.20 (T)), which is typical of Anthocerotes (Burr, 1968; Valentine, 1984; Vaughn *et al.*, 1992), rather than having the highly curved closed granal margins that are usually observed in higher plants.

5.7 Starch granules

The possibility that starch granules and their associated hydration characteristics could account for the volume changes of the *M. pellucidus* chloroplast, when subjected to various light stimuli was questioned.

In all of the TEM micrographs the change in the starch granule outline is apparent. Those in dark environments (Figures 5.18 and 5.21), show an apparent loose boundary while those starch granules exposed to white or blue light (Figures 5.19 and 5.20) exhibit boundaries that are more constrained. Measurements were taken of the largest granules by measuring the length of two axes, x = the length and y = the breadth.

Table 5.3. Table of *M. pellucidus* (×21200 and ×7800) comparing chloroplast starch granule cross-sectional area measurements between light / blue irradiated and dark environment.

Magnification	Cross-sectional area (μm^2)		Ratio of size
	Dark	Light	
×21000	0.059 ± 0.004 μm^2	0.04 ± 0.01 μm^2	Dark: light = 1.454
×7800	0.01 ± 0.002 μm^2	0.006 ± 0.001 μm^2	Dark: light = 2.165

Table (5.3.) shows a significant variation ($P < 0.005$) in size ratios, between the dark and high light areas of both micrographs (TEM of ×21000 ratio of dark: light size = 1.454; TEM of ×7800 ratio of dark: light size = 2.165).

Micrographs (Figures 5.22, light, and 5.23, dark) show a distinct variation in the density and size of the respective grains. In the high PFD sample (556 µmoles photons m^{-2} s^{-1} for 24 h, Figure 5.22), the starch granules have a series of concentric patterns with a central core, whereas in the sample that was held for 24 h in darkness (Figure 5.23) the starch grains appear to have more uniform texture and show no concentric patterns.

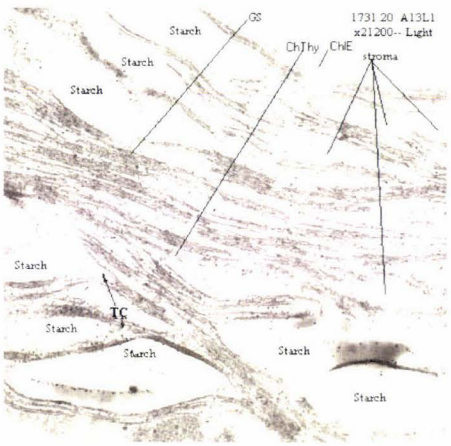

Figure 5.22. TEM (×21200) of a *M. pellucidus* chloroplast exposed to light (556 µmoles photons $m^{-2}s^{-1}$) for 24 h. Note the starch granule borders and compacted shape. ChlE = chloroplast envelope, ChThy = channel thylakoid, GS = grana stacking "pseudograna".

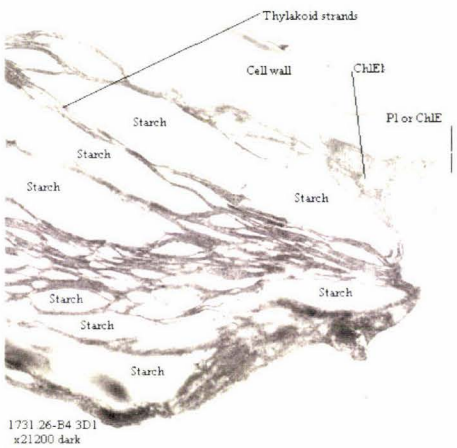

Figure 5.23. TEM (×21200) of a *M. pellucidus* chloroplast section previously exposed to 24 h dark. Note the starch granule borders, open shape, and the intimate contact between the chloroplast envelope and plasmalemma. CEM = chloroplast envelope, Pl = plasmalemma.

5.8 Chloroplast plasmalemma apoplast association

The degree of association between the chloroplast and potential bulk water reservoirs was examined by TEM since on all observations, both confocal, light and TEM, the chloroplast appeared always to be in intimate contact with the plasmalemma, tonoplast and cytoplasm.

In the TEM micrographs (Figures 5.19, 5.21, 5.23, 5.24, 5.25 and 5.26) and in the light micrographs (Figures 5.2, 5.3, 5.4 and 5.5) the *M. pellucidus* chloroplast shows that an amalgamation between the chloroplast and the plasmalemma and cell wall does occur although the contact in some cases (Figure 5.20) appears to be localised rather than uniform. While the contact between the chloroplast and the cell wall was observed on all the confocal observations it was not technically possible to obtain microphotographs because of the difficulty in a definitive interpretation and a manual trimming separation of the various densities.

A further series of TEM micrographs (Figures 5.24, 5.25 and 5.26) shows very clearly the high level of contact that exists between the chloroplast and the cell wall.

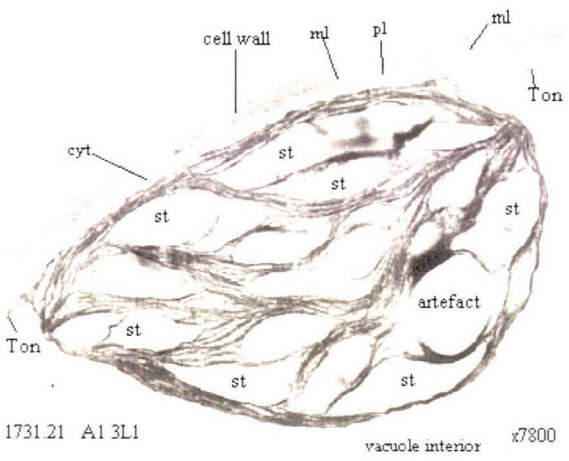

Figure 5.24. TEM ×7800 micrograph of a *M. pellucidus* chloroplast after exposure to natural light of 556 µmoles photons m^{-2} s^{-1} for 24 h. Note the close association between the cell wall and the chloroplast envelope. Key: Ton = Tonoplast, ml = middle lamella of cell wall, st = starch, pl = plasmalemma, cyt = cytoplasm

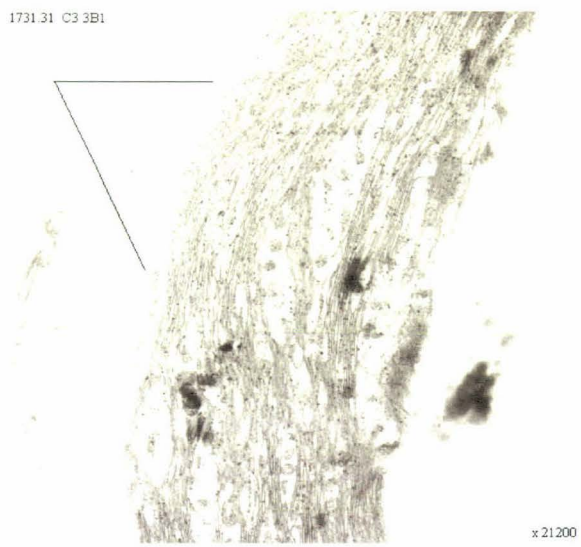

Figure 5.25. TEM × 21200 micrograph of a *M. pellucidus* chloroplast after exposure to blue light (458 nm at a PFD of 10 µmoles photons m^{-2} s^{-1}). The area indicated (between the base of the lines) shows one of a number of extrusions from the chloroplast towards the cell wall.

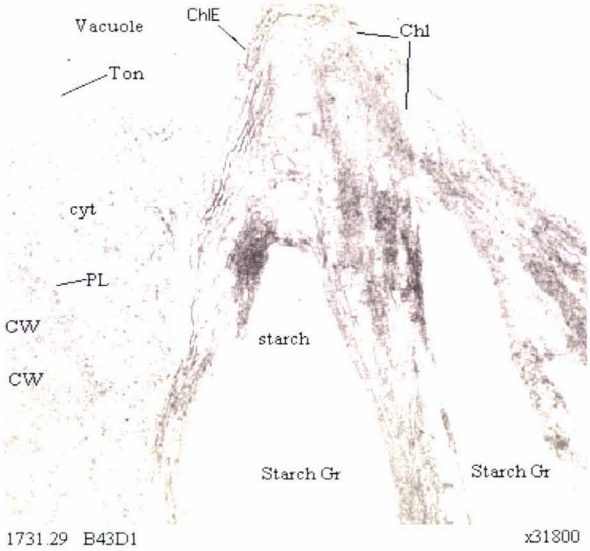

Figure 5.26. TEM ×31800 micrograph of a *M. pellucidus* chloroplast after being in a dark environment for 24 h. This micrograph shows the chloroplast (Chl) compressing the cytoplasm (cyt) against the plasmalemma (Pl) lining the cell wall (cw). Chloroplast envelope (ChlE) The vacuole tonoplast (Ton) surrounds the chloroplast and cytoplasm edges. Both high bulk water resources are in contact.

Chapter 6

Discussion

6.1 Light

Light from solar radiation becomes dramatically altered, in both quality and quantity; by the time it reaches the forest floor (Bjorn, 1994; Boardman, 1977; Gates, 1980; Kendrick & Kronenberg, 1994; Koller, 2000; Niinemets *et al.*, 1999; Nobel, 1999; Pearcy, 1989; Richards, 1984). At the *M. pellucidus* sites the summer difference between the canopy PFD (43 moles photons m^{-2} day^{-1}) and the collection site PFD (0.07 moles photons m^{-2} day^{-1}), was 42.93 moles photons m^{-2} day^{-1} an attenuation of 99.84 %. The winter, 23 to 0.03 moles photons m^{-2} day^{-1} (99.87% attenuation) and autumn readings 27 to 0.04 moles photons m^{-2} day^{-1} (99.85% attenuation) showed a seasonal diminishment in PFD quantity coupled with very similar attenuation percentages (Table 4.5). The seasonal canopy light PFD showed that the duration of PFD rather than a difference in peak amplitude was the prevailing factor (Figure 3.6A). As an example of universality, these summer PFD values were similar to the crown canopy (40 moles photons m^{-2} day^{-1}) and leaf top of the sub-canopy (5 moles photons m^{-2} day^{-1}) in a tropical Australian rainforest (Chazdon *et al.*, 1996).

All of the *M. pellucidus* plants were found in extreme low light conditions (section 4.0) in rain forest situations, the Apiti site ranging up to 5.1 ± 0.4 μmoles photons m^{-2} s^{-1} (Table 4.1). The potential light energy, as quanta, available each day at these sites, was calculated and found to possess a summer maximum of 0.07 moles of photons m^{-2} day^{-1} which diminished to 0.04 photons m^{-2} day^{-1} and, during the winter, fell to 0.03 photons m^{-2} day^{-1}.

It is of interest to note, that although the *M. pellucidus* sites received almost double the PFD during the summer months, compared to the autumn and winter periods, the sporophyte production, a major energy expenditure, occurred during the period of apparent minimal energy availability. This phenomenon is also a characteristic, in

Britain, of *Anthoceros laevis*, which becomes fertile in short days (8 h), and remains sterile in long (18 h) days (Benson-Evans, 1963).

As to be expected, in a sub-canopy light environment (Smith, 1986; Smith & Morgan, 1981; Tang, 1997), the quality of the light (Figure 5.1) that was available to the *M. pellucidus* colonies showed that attenuation by the various canopy layers above the site had reduced the available PAR to an average PFD of 0.3 ± 0.07% of the direct canopy light, and changed the quality of this available PAR by reducing the PFD of blue and red wavelengths and elevating the PFD of the far red (>680 nm) fraction (Figures 4.7, 4.10 , 4.13 and 4.14).

The colouration of *M. pellucidus* was also typical of bryophytes growing in extremely low light situations (Richards, 1932) these plants appear very dark green, almost black until viewed from perpendicularly above the plant when the colour shows as an intense jade green. Vogelmann (1993) has attributed this light difference to the convex shape of the epidermal cells which focus light on the chloroplasts below and the light that is not absorbed is reflected or transmitted. Since light at the forest floor is generally diffuse (Yoda, 1974) a convex surfaced cell would minimise the amount of specular reflection when light, at low angles, is incident on the cell surface (Vogelmann *et al.*, 1996).

The habitat light available to *M. pellucidus* was found to be supplemented on sunny days, particularly over the summer months, by sunflecks during the period between 1000 – 1200 h (Figures 4.8 and 4.9), and by light reflections off nearby water after 1600 h by light reflections off nearby water (Figure 4.9).

6.2 Sunfleck

As the sun's declination changes it causes considerable change in the PFD levels within the foliage. Any gaps in the canopies, caused by wind motion or reflection, can allow some direct light penetration to the forest floor as sunflecks (Anderson & Aro, 1994; Larcher, 1995; Ross, 1981; Tang, 1997; Vogelmann *et al.*, 1996). The continuously changing gaps, occasioned by wind motion, create short time length PFD dwell periods while gaps created by foliage architectural change or canopy damage allow light to reach the forest floor for longer periods. All of these forest

floor sunfleck PFDs and their dwell times are dependent on the surrounding biome type and degree of maturity (Brown & Parker, 1994), the season and altitude (Larcher, 1995), the topographical and the latitudinal factors (Chazdon *et al.*, 1996). Sunfleck activity is generally highest at mid-day and lowest at dusk. (Ross, 1981; Tang, 1997). These results appear to confirm this (Section 4.6).

The sunfleck periods were measured over 5 min periods (Figure 4.8) and the PFD taken as an average with occasional maximum single readings being as high as a canopy value (individual point observation during the Li-Cor reading, no record taken). Brief sunflecks, lasting for only a few seconds, can be utilized by heavy shade plants and the sum of the individual sunflecks over the day can provide up to 60% of the daily carbon gain in seedlings of *Claoxylon sandwicense* (Chazdon *et al.*, 1996; Pearcy & Calkin, 1983). Sunflecks, of less than one-minute duration, are often much less than full sun PFD because of interference by penumbral effects (Chazdon *et al.*, 1996; Pearcy, 1989; Smith, 1986). Sunflecks that last longer than 1 min do not become attenuated and provide a spectral range virtually identical in quality to that recorded at the canopy.

6.3 Reflections

The results (Table 4.1 and Figure 4.10) suggest that reflections from water surfaces can also be considered as a supplement to the PFD received by plants located in positions that would otherwise receive no or minimal light. These reflections occur, at the sites investigated, mainly in the late afternoon when the sun is at a very acute angle in respect to the plane of a water surface.

Light reflections were observed to reach into areas that would normally be heavily shaded from any direct light. Water reflections were also constantly changing with incident light being reflected off the ever changing surface planes of ripples, especially in flowing water situations, this produced reflections analogous to the wind motion sunfleck light source that changes in both quality and quantity during the day (pers. obs.).

It is known (first discovered by Malus in 1809), that light reflected off water surfaces (pools, rivers, wet leaves, wet rocks, water droplets) is partially or

completely polarized (Kraml, 1994; Resnick & Halliday, 1966) and that this reflected light, in the late afternoon, is higher in far red and red wavelengths as a result of Rayleigh and Mie scattering (Olesen, 1992). Thus PAR received at the *M. pellucidus* habitats, from canopy transmission plus sunflecks and reflection late in the day, would have relatively high levels of red and far-red wavelengths.

Very little work appears to have been done on the value of light reflection, off freshwater surfaces, as a source of PAR, although reflection and polarization values have been investigated as to their relevance in aiding insect vision (Horvath, 1995). The importance of polarized light as a signal to induce chloroplast movement is well documented (Dong *et al.*, 1998; Haupt, 1999; Haupt & Hader, 1994; Kagawa & Wadal, 2002; Kagawa & Wada, 1996; Können, 1985; Senger, 1984; Yatsuhashi, 1996).

6.4 Water

In all of the sites investigated, water was abundant irrespective of the season or year. Photosynthesis in bryophytes is universally connected to the water content of the tissues, with optimum photosynthesis occurring at maximum saturation levels and diminishing to zero as the level of saturation falls to the equivalent low air vapour pressure levels (Dilks & Procter, 1979; Lee & Stewart, 1971).

The natural habitat of *M. pellucidus* sites is found in extremely low light situations (<5.1 $\pm$ 0.4 µmoles photons m^{-2} s^{-1}) and where water is constantly falling onto and around the thallus. In other bryophytes it has been established that droplets or films of water resting on the dorsal surface or trapped in trichomes can act as a lens, concentrating light up to 20 times (Brewer *et al.*, 1991). Conversely, CO_2 diffuses through 20°C water at approximately 10,000 times slower than through air and slower still at lower temperature (Lawlor, 1993), which might be expected to limit photosynthesis in higher light conditions.

In plants adapted to extremely wet environments cuticles provide efficient water repellant qualities (Neinhuis & Barthlott, 1997), this factor plus the morphology of the leaf and epidermal trichomes creates droplets rather than all enveloping films (Cook & Graham, 1998; Karabourniotis *et al.*, 1999; Neinhuis *et al.*, 2001;

Schreiber *et al.*, 2001). Since droplets of water do not cover the entire surface of the thallus, whereas a thin film would, the impact of water droplets on CO_2 flux might be expected to be less than that of a film (Brewer *et al.*, 1991).

The Anthocerophyta have been found to exhibit poikilohydrism (the ability of an organism to dehydrate and regain normal metabolism on rehydration) (Bold *et al.*, 1987; Bopp, 2000; Black & Pritchard, 2002; Renzaglia, 1978; Schuster, 1984). The blue light response could possibly be a preparatory phase prior to desiccation, since relatively high blue light might indicate high light exposure and the possibility of water loss. The blue light-induced chloroplast shrinkage might represent an early step in the dehydration process.

6.5 Temperature

Temperature in all of the *M. pellucidus* sites were lower than that of the surrounding air, though not recorded, the plant thallus were significantly colder to the touch. Higher temperatures (>30°C) severely limit the photosynthesis of the majority of bryophytes that generally have optimal temperatures similar to the mean daytime temperature of their environment (Gabrys-Mizera *et al.*, 1997; Valanne, 1984). The margin of successful tolerance is skewed towards negative temperature (activation of arctic species, after being subjected to temperatures of -30°C, takes place within a few hours (Valanne, 1984)) rather than increases in temperature. Mid-day temperatures, at any season, are generally above the optimal temperature for bryophyte photosynthesis, and so the photosynthetic rate of bryophytes is reduced in the middle of the day (Hicklenton & Oechel, 1976).

At the time these experiments were conducted the ambient temperature in the laboratory was 19-25°C. Unfortunately environmental temperatures at the collection sites were not recorded, however the annual average soil temperature at 100mm depth (at Stratford, altitude 311 m, for the period 1971-1980) was 12 ± 1°C, and ranged from 6.1°C in July to 17.3°C in January (Thompson, 1981). The soil temperatures of the *M. pellucidus* habitats would be significantly lower than this since they remain in permanent shade with constantly running water.

Chloroplast movement can also be affected by temperature. Cooling *Elodea canadensis* specimens to 5°C inhibited chloroplast movement in detached and incised leaves, but when these leaves were transferred to room temperature chloroplast movement was detected within 20 min (Gamalei *et al.*, 1994). Gamalei *et al.* (1994) found that maximal chloroplast velocity was 36.8 $\mu m\ s^{-1}$ which occurred after several warm-cold-warm cycles. Chloroplast movement was minimal in young leaves and maximal in older tissue and varied diurnally. After further investigating changes in the membrane electrical potential, Gamalei *et al.* (1994) concluded that chloroplast movement in *Elodea canadensis* is initiated and enhanced by wound reactions, possibly transmitted from cell to cell via plasmodesmata.

Temperatures under plants are usually much lower and stable than temperatures at and above the plant canopy (Larcher, 1995; Loomis, 1992). Soil water content is important in maintaining an additional coolness since heat is removed by the evaporation of the water. The water irrigating the *M. pellucidus* sites arises from rain, mist, overhead water run off and droplets, enabling the *M. pellucidus* thallus to remain uniformly cool and moist throughout the year.

A decrease in the sensitivity to photoinhibition has been observed in cold-tolerant plants when in low temperature environments (Huner *et al.*, 1993). Since the temperature of the *M. pellucidus* habitat is relatively low, it might be that the plant is relatively tolerant of the brief periods of higher PFD it experiences. Conversely, warm temperatures can affect bryophyte protonemata grown at 21°C. These protonema showed no photoinhibition after freezing at night, but was readily photoinhibited after one night at 40°C (Valanne, 1984).

One relationship that correlates temperature with chloroplast movement is that of the energy required to actually move the chloroplast to the optimal light position. Inhibition of respiration or photosynthetic gas exchange produced a corresponding inhibition in chloroplast movement, implying that the energy from oxidative phosphorylation or photophosphorylation is used in the chloroplast reorientation in *Mougeotia* and *Lemna* (Britz, 1979). Any variation in temperature (T) affects the Q_{10} (the biological temperature coefficient)

$$Q_{10} = \sqrt{\frac{T+10}{T}} \frac{\exp(10U_{min})}{RT(T+10)}$$

and since enzymatic reaction is generally dependent on the level of kinetic energy any change in temperature has a considerable effect on the energy available from metabolism (Nobel, 1999).

6.6 The anatomy of *Megaceros pellucidus*

The cuticle of *M. pellucidus* was not obvious in any of the microscopical investigations, but would be the first structure to receive light arriving at the thallus. The cuticle of the Anthocerophyte *Notothylas orbicularis*, when examined by both TEM and SEM, has a nodular or sheet-like osmiophilic layer (Cook & Graham, 1998), which would diffuse light and could have a significant effect on water and CO_2 flux (Neinhuis *et al.*, 2001). Very little information regarding the cuticles of the Anthocerophyta is available and presents a field for investigation.

Shade-adapted bryophytes possess rows of chlorechymatous cells on the light proximal surfaces. This arrangement is thought to increase the photosynthetic capacity of the plant in low light conditions (Krupa, 1978; Valanne, 1984). Similar anatomical characteristics prevail in *M. pellucidus* (Figure 5.5). The dorsal epidermal cells of *M. pellucidus*, closest to the light source, have chloroplasts centered on the periclinal wall in a wide spread droplet formation (section 5.2). In low light conditions the chloroplasts expand across the cell plasmalemma surface proximal to the light source (Figures 5.3, 5.4 and 5.7, 4a and b), exposing a maximum area of the chloroplast to the incoming light. In high (140 µmoles photons m^{-2} s^{-1}) or blue light (>3 µmoles photons m^{-2} s^{-1}) conditions the *M. pellucidus* chloroplasts diminish their surface area and relocate to the lower side walls (Figures 5.2 and 5.7, 1-3) thus reducing the area exposed to the light. This change in chloroplast volume would be expected to affect the extent of light absorbance (A), which can be written (Gilbert & Baggott, 1991) for a suspension of particles as

$$A = \ln \frac{I_0}{I} = \sigma \rho L$$

where σ is the cross-sectional area of the average particle (m^{-2} $particle^{-1}$), ρ is the number density of the particles (particles m^{-3}) and L is the path length through the suspension (m). The other parameters are the incident intensity of the measuring beam (I_0) and the transmitted intensity (I). Therefore, the denser the suspension (the more chloroplasts per unit volume) and/or the larger the particles (the greater the cross sectional area of the chloroplasts), the greater the absorbance.

Each cell layer of a leaf or thallus that has a curved transparent surface (Figure 5.5), with a refractive index greater than air, could focus light (Gabrys-Mizera, 1976; Knapp & Carter, 1998; Vogelmann, 1993; Vogelmann & Bjorn, 1986). Light incident on a surface at an angle to the normal greater than the critical angle will be reflected, which is a phenomenon known as total internal reflection. The critical angle is determined by the ratio of the refractive indices of the media on either side of the interface. Changing the solute concentration or water content of a medium will change its refractive index (Resnick & Halliday, 1966). Since illumination of the thallus can change the chloroplast volume, which implies a water flux across the envelope, a change in solute concentration will also occur in both the chloroplast and the cytosol. Such adjustments will occur across every membrane and will extend to the apoplast throughout the thallus. The refractive index of each of these media will also change simply because of the changing solute environment.

The changing refractive index of the apoplast will alter the balance between refraction and total internal reflection within it and therefore to the distribution of light throughout the thallus (Gabrys-Mizera, 1976; Vogelmann, 1993; Vogelmann & Bjorn, 1986).

Generally elongating cells in a column divide in a manner that retains the proportions of the mother cell and its relationships with its neighbours. Epidermal cells divide transversely whereas isodiametric cells, such as central parenchymal packing cells (Figure 5.5), divide in other planes that produce a tetrakaidecahedron geometry (Lewis, 1943). However, all cells divide in such a manner so as to produce three edges at any point on a plane (Lloyd, 1991). Chloroplasts in total darkness appear to be non specific as to a wall contact position (Figure 5.4). However, chloroplasts in a light available situation, appear to be located in the vicinity of these points (Figures 5.2, 5.3 and 6.1).

Most of the light passing through the apoplast would be transmitted into the underlying cell at this point because the angle of incidence is low. In a shaded environment a chloroplast can maximise the amount of light received, but it shades any chloroplasts below it. In most shade species there are fewer chloroplasts per cell than in high light plants (Bjorkman, 1981), which might help to minimise this effect. In high light conditions, the chloroplasts are shrunken and located in the parastrophe position (Figures 1.1 and 6.1). Light entering the cell in these conditions is distributed around the interior of the cell by reflection and its intensity is reduced by refraction and absorbance by other intracellular inclusions (Bjorn, 1994; Vogelmann, 1993; Vogelmann, 1994; Vogelmann & Bjorn, 1986). In high light conditions, light could pass through the thallus and only a small proportion of it would be absorbed by the chloroplast. Light would reach the ventral epidermal / external cell wall / soil interface and be lost to the thallus.

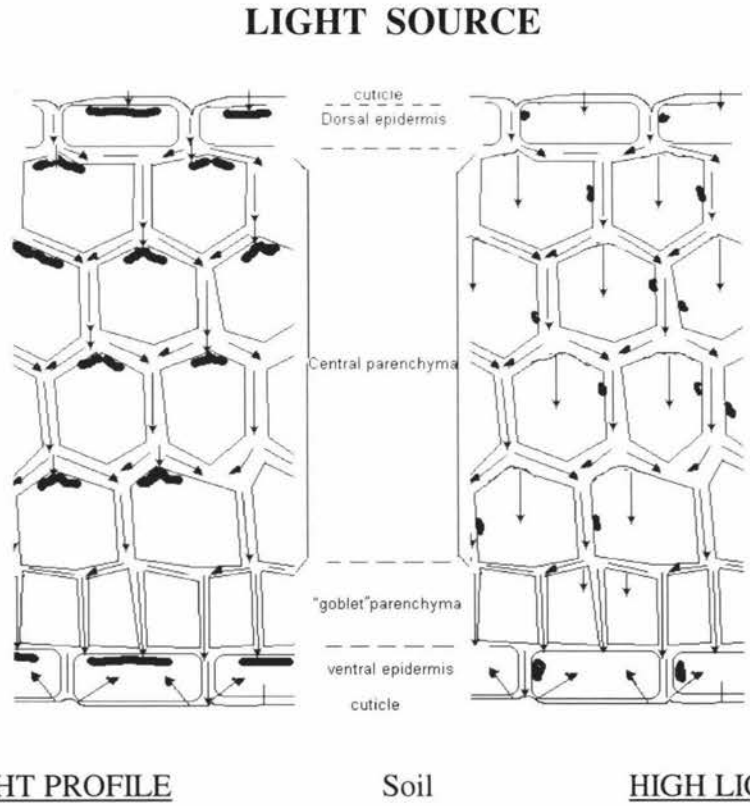

Figure 6.1. Schematic diagram of a *M. pellucidus* thallus column profile showing chloroplast morphology and orientation (dark black areas). The left hand illustration represents a low light environment and the right hand illustration represents the high light situation. Arrows indicate hypothetical light paths (via internal reflection) through the apoplast, perpendicular angle light penetration through the plasmalemma into the cell interior and reflection back into the system by the ventral epidermal / cuticle / soil interface as described by (Bjorn, 1994; Vogelmann, 1993; Vogelmann, 1994; Vogelmann & Bjorn, 1986). Note the orientation of the chloroplasts in relation to the light rays

6.7 Pigmentation of *M. pellucidus*

The chlorophyll content of low light adapted *M. pellucidus* was about 63% that of high light adapted plants (Table 5.2). The absorbance spectra shown in Figure 5.1 are consistent with this, in that plants from high light sites had more chlorophyll than those from moderate and dark sites. Furthermore, the spectra of pigment extracts of plants from the two low light conditions have an absorbance band at about 340 nm which is not apparent in the pigment extract from high light grown plants (Figure 5.1). It is not clear whether this was a novel pigment or whether it was present in all the tissue samples and simply became more apparent as the chlorophyll content decreased. It is conceivable that this represents modified chlorophyll, although more work would have to be carried out to establish this definitively. For example, bacteriochlorophyll *a* has an absorbance band with a peak at about 357 nm (70 nm lower than the 428 nm band of chlorophyll *a*), but it has another at about 768 nm (Sauer, 1975), which was outside the range of the data collected here. The Anthocerophyta lack anthocyanins (Schuster, 1984), but phenylpropanoids, a precursor to pterins and flavonoides, are abundant within the taxa (Becker, 1994) and might contribute to this unidentified absorbance band. Given the mutualistic association between *Nostoc* sp. and *M. pellucidus*, the polysaccharide-linked mycosporine E335, which has an absorbance maximum at 337 nm and is found in *N. commune* (Cockell & Knowland, 1999), is also a possible candidate.

The chlorophyll *a* : *b* ratio was about 0.8 for both shade and high-light adapted plants (Table 5.2). This extremely low value is consistent with the general reduction in the ratio in shade plants compared to canopy plants (Bjorn, 1994; Boardman, 1977; Chazdon *et al.*, 1996; Kendrick & Kronenberg, 1994; Lichtenthaler *et al.*, 1982), but even the high light regime was less than 5 μmoles photons m^{-2} s^{-1} (Table 5.1), which is considerably lower than the PFD in which most understory plants are found (Chazdon *et al.*, 1996). Both the protonema of *Ceratodon purpureus* and the thallus of *Marchantia polymorpha*, have been reported to have a chlorophyll *a* : *b* ratio of only slightly greater than 2 (Aro, 1982). However, unlike *M. pellucidus*, *M. polymorpha* is a shade plant, but is high light tolerant as long as adequate moisture is available (pers. obs.), and *C. purpureus* is essentially a high light plant. Therefore,

the extremely low chlorophyll *a* : *b* ratio reported here (table 5.2) is perhaps related to the extreme low light habitat (Chapters 2 and 4) in which *M. pellucidus* grows.

Higher plants are able to adapt their photosynthetic apparatus to the incident PFD. High light-adapted plants contain less antenna chlorophyll and, at light saturation, are more efficient at photosynthesis than the chloroplasts of low light-adapted plants with their greater range of light harvesting complexes, relatively higher chlorophyll *b* content and high grana stacks (Lichtenthaler *et al.*, 1982). The apparent appression of the *M. pellucidus* thylakoid membranes varied with the light conditions (section 5.7) as did those of *C. pupurea* (Aro, 1982), albeit at much higher PFDs. Those in high PFD were compacted (Figures 5.19 and 5.20), whereas those in lower PFD, the natural habitat flux, red light or darkness tended to be more separate (Figures 5.18 and 5.21). *Megaceros pellucidus* thylakoids do not form true grana (Manton, 1962) and the thylakoids are open ended (Valentine, 1984; Valentine & Campbell, 1986; Vaughn *et al.*, 1992). For this reason, it is not clear whether the models of thylakoid appression can be applied to *M. pellucidus*, but the reduction in the chlorophyll *a* : *b* ratio, which is associated with reduced light harvesting complex II content in higher plants (Lichtenthaler *et al.*, 1982), might be consistent with those models.

6.8 Movement of the chloroplast within the cell

Changes to the cellular orientations of chloroplasts, in response to light, has long been known and has been well reviewed (Augustynowicz & Gabrys, 1999; Britz, 1979; Dong *et al.*, 1998; Gamalei *et al.*, 1994; Garjeanne, 1932; Gorton *et al.*, 1999; Haupt, 1982; Haupt, 1999; Kagawa & Wada, 1996; Kagawa & Wada, 1999; Senger, 1984; Tlalka & Gabrys, 1993; Yatsuhashi, 1996). Changes in chloroplast distribution were reported by Bohm in 1856 and the orientation of chloroplasts to the direction of the light source and the intensity of this light was observed by Stahl in 1880 (Senger, 1984). In 1908, Senn produced an important monograph on chloroplast movement. In general, changes in chloroplast orientation have always been interpreted as either maximising exposure to light, in conditions of low light intensity, or minimising exposure, in situations of high light intensity (Haupt, 1982).

Senn found that the quality of light was a critical factor in the orientation of the chloroplast (Haupt, 1982; Haupt, 1999). Blue light in particular appeared to initiate chloroplast movement while, in *Mougeotia*, red light appeared to reverse the response. In a series of experiments Senn showed that *Mougeotia* maximised the exposure of the chloroplast to red light, a typical low light intensity response, whereas blue light minimised chloroplast exposure, a typical high light response (Haupt, 1982; Haupt, 1999).

The results obtained show that in the low light situations inhabited by *M. pellucidus* the chloroplasts maintained an epistrophe position (Figure 5.3). Exposure to light with a blue content of over 2 μmoles photons m^{-2} s^{-1} initiated chloroplast contraction and movement to the parastrophe position (Figure 5.2), reducing exposure to the incoming irradiation. Exposure of dark-adapted tissue, where the chloroplasts were in the apostrophe position (Figure 5.4), to red light of up to 130 μmoles photons m^{-2} s^{-1} elicited no change in chloroplast volume, but the chloroplasts assumed the epistrophe position (Figure 5.3).

In the habitat, the chloroplasts of *M. pellucidus* probably are maintained in the epistrophe position, since the PFD is low (< 6 μmoles photons m^{-2} s^{-1} for most of the time) and has a high degree of attenuation in the blue band (Figure 4.14). At night, the chloroplasts probably assume the apostrophe position, changing to the epistrophe position at first light. The parastrophe position (Figure 5.2) probably occurs only when the plant is exposed to prolonged periods of relatively high light, such as 'gapping'[1] in which case it presumably represents a protective response.

6.9 Chloroplast morphology of *M. pellucidus* in response to light

In habitat light, the dorsal chloroplasts of *M. pellucidus* adopted a hanging-drop configuration (Figure 5.3) which, on exposure to blue (~3 μmoles photons m^{-2} s^{-1}) or white light (>140 μmoles photons m^{-2} s^{-1}) contracted into a tight, 'granulated' sphere (Figure 5.2) and in complete darkness they became discoid (Figure 5.4). In darkness or habitat light, the chloroplasts in the large parenchymous cells of the central thallus were polymorphous, sometimes adopting the 'dumbbell' shape

[1] Destruction of overhead canopy through either natural causes (wind damage) or forestry, allowing access of sun light to the forest floor.

(Figures 5.5, 5.6 and 5.9). These might have been interpreted as multiple chloroplasts, but confocal microscopy made it apparent that these were not two isolated organelles. The significance of this particular conformation is unclear, but some other Anthocerophyta have chloroplasts of this shape (Vaughn *et al.*, 1992). In high light, the central thallus chloroplasts were contracted into a 'granulated' sphere that was slightly less condensed than the dorsal chloroplasts in this condition. The morphology of the ventral chloroplasts did not change significantly in response to light.

6.10 Volume changes of *M. pellucidus* in response to light

The first reports of Anthocerophyte chloroplast contraction, in response to light, were made by Burr (1968; 1970) who observed that chloroplasts of various *Megaceros* spp. assumed a very contracted form when subjected to high light intensities. When placed in low light intensity, the chloroplasts of various *Megaceros* spp. assumed a laminate shape and appeared to expand across the periclinal plane proximal to the light source (Burr, 1970; 1968). Subsequently, Valentine (1984) made similar observations. In neither case were measurements of either the light quality or the PFD reported.

All of the results obtained here indicate that a change in the *M. pellucidus* chloroplast volume is associated with changes in both wavelength and PFD. High white light (>140 μmoles photons m^{-2} s^{-1}), blue light of 470 nm (~3 μmoles photons m^{-2} s^{-1}) and the blue (512 nm) laser light from the confocal microscope induced chloroplast shrinkage from 45-56 μm^2 to 12-18 μm^2 over a period of 180 minutes (Figure 5.7). In subsequent experiments the maximum chloroplast shrinkage or inflation was accomplished within 60 min (Figures 5.10 and 5.12). The volume changed approximately exponentially with a minimum half time of about 35 min (Figures 5.12 and 5.13).

The light micrographs shown in section 5.2 (Figures 5.2, 5.3, 5.4 and 5.5) clearly demonstrate the light-induced changes in chloroplast volume from the condensed form in high light (Figure 5.2) to the various structures in the low light conditions of the *M. pellucidus* habitat (Figure 5.3) or the enlarged form in complete darkness (Figure 5.4). In high light (>140 μmoles photons m^{-2} s^{-1}) the chloroplasts shrank

over a period of about 75 minutes and swelled over a similar period on subsequent dark incubation (Figure 5.8).

While white light had significant effects on chloroplast volume ($P < 0.001$, Figure 5.8), blue light and red light were also effective (section 5.4). It should be noted that other wavelengths of light were not tested. Below about 2 μmoles photons m^{-2} s^{-1} of blue (470 nm) light no change in chloroplast volume was apparent (Figures 5.10 and 5.12). Above this PFD the rate of chloroplast shrinkage increased to a maximum at about 5 μmoles photons m^{-2} s^{-1}, which was not accelerated by increasing the PFD to about 10 μmoles photons m^{-2} s^{-1} (Figure 5.12). Red light (662 nm, of up to 130 μmoles photons m^{-2} s^{-1}, which was the upper limit of the LED used) had no effect on the volume of expanded chloroplasts (Figure 5.10). However, when condensed chloroplasts were exposed to red light they expanded to the dark-adapted volume, but placing the tissue in complete darkness had the same effect (Figure 5.14).

6.11 Effect of osmotic potential

Chloroplast volume change occurs not only as a result of internal metabolism and product partitioning but also as a response to variations in the osmotic potential of the surrounding cytosol which is also subjected to perturbations in the water dynamics of the associated organelles and the water potential of the external apoplast (Britz, 1979; Gupta & Berkowitz, 1988; McCain & Markley, 1992; McCain, 1995; Nobel, 1968; Robinson, 1985; Tyerman *et al.*, 1999; Weiss, 1996). The bulk of the water is contained in three major areas within bryophytes: within the cell walls (apoplast water); in the cytoplasm (symplast water); and within the cell vacuole (symplast water) (Dilks & Procter, 1979). The apoplast of *M. pellucidus* is highly saturated because of its wet habitat (Chapters 2 and 4). The central vacuole can occupy more than 80% of a mature plant cell volume, thus forming a major portion of the liquid phase (Roland & Vian, 1991).

Because of the abundant rainwater supply, *M. pellucidus* is generally unlikely to experience water deficit. However, the significant changes in the chloroplast volume ($P < 0.001$, Figure 5.8) imply that water moves in and out of the chloroplast, as it does in higher plants (McCain & Markley, 1992; McCain, 1995). Both the plasmalemma and the tonoplast have aquaporins (Maurel, 1997; Maurel &

Chrispeels, 2001) that are water selective, operate bi-directionally and can achieve rapid bulk water transport (Tyerman *et al.*, 1999). However, there do not appear to be any reports of aquaporins or homologues of them in the chloroplast envelope. McCain and Markley (1985) estimated that the diffusive permeability of *Liriodendron tulipifera* chloroplast envelope to be $9 \pm 2 \times 10^{-4}$ cm s^{-1} from NMR measurements using whole leaves. While these measurements raise some issues relating to boundary layers within the leaf, the value is less than 5% of the largest values reported for the tonoplast and the plasmalemma (Maurel, 1997; Tyerman *et al.*, 1999), and is similar to the permeability reported for lipid vesicles (Tyerman *et al.*, 1999). Furthermore, while diffusive permeability is less than the osmotic permeability for membranes containing aquaporins, it seems likely that these data are consistent with the absence of aquaporins (or their homologues) from the chloroplast envelope.

The chloroplasts of *M. pellucidus* tissue incubated with a range of concentrations of PEG (section 5.6) shrank at a rate only slightly faster than that observed during blue light illumination (Figures 5.10, 5.12 and 5.13). A comparison of the rate constants estimated for these processes prompts the suggestion that ratio of the osmotic and diffusive permeabilities was about 1.5-2, which is small compared to the values for aquaporin-containing membranes (Tyerman *et al.*, 1999). Furthermore, using the permeability estimated by McCain and Markley (1985) and reasonable estimates for the chloroplast surface:volume ratio, it is possible to estimate rate constants for the PEG induced volume change that are similar to those measured (section 5.5). This is consistent with the absence of aquaporins from the chloroplast envelope and implies that the flux of water in and out of the chloroplast is essentially diffusive.

In the dark or in red light (662 nm, 130 μmoles photons m^{-2} s^{-1}) the apparent rate constant for re-expansion of a shrunken chloroplast was about 0.008 min^{-1} (Figure 5.14), which was about half of the rate constant for blue light-induced shrinkage (about 0.02 min^{-1}, Figure 5.13). Exposure of the tissue to 1.5% (*w/v*) PEG in the dark caused chloroplast shrinkage with an apparent rate constant of 0.032 min^{-1} (Figure 5.15). However, subsequent illumination of PEG incubated tissue with red light (662 nm, 130 μmoles photons m^{-2} s^{-1}) caused chloroplast re-expansion with a maximum rate constant of about 0.046 min^{-1} (Figure 5.17). This might imply that

the partial dehydration induced by PEG increased the permeability of the chloroplast envelope (and perhaps other membranes) and when the tissue was exposed to red light solute accumulation in the chloroplast drove water flow into the chloroplast at a relatively rapid rate due to the enhanced permeability.

In addition to playing roles in phototropism (Ahmad *et al.*, 1998; Sakai *et al.*, 2001), photomorphogenesis (Gautier & Varlet-Grancher, 1996), gene expression (Anderson *et al.*, 1999; Thum *et al.*, 2001), cytoplasmic streaming (Takagi, 1997), chloroplast movement (Gorton *et al.*, 1999; Jarillo *et al.*, 2001; Kadota *et al.*, 2000; Kagawa & Wadal, 2002; Kagawa & Wada, 1996; Kagawa & Wada, 1999; Sakai *et al.*, 2001; Tlalka & Gabrys, 1993; Tlalka & M.., 1999; Yatsuhashi, 1996), it is well established that blue light can affect both the function of ion channels (Lewis *et al.*, 1997; Mawson, 1993; Takashi *et al.*, 2001) and the volume of higher plant protoplasts (Long & Iino, 2001; Wang & Iino, 1998). Therefore, one might speculate that blue light could alter the activity of ion channels in the chloroplast envelope (Packer *et al.*, 1970) which might promote changes in the stromal osmotic potential, which would drive the flux of water out of the chloroplast. It is possible that this is related to the well established light-dependent flux of ions across the chloroplast envelope (Krause, 1973; Krause, 1974; Nobel, 1968) and the thylakoid membrane (Hind *et al.*, 1974). Alternatively, if there are water channels in the chloroplast envelope, blue light could activate them with similar effect.

Any reduction in water in the cytoplasm would increase the osmotic potential and create a water loss from the chloroplast. The shrinkage of the *M. pellucidus* chloroplast was reversed when irradiated by red light of 662 nm (130 μmoles photons m^{-2} s^{-1}), and caused the chloroplasts to increase in volume (Figure 5.17) in contrast to the volume reduction that both blue light induced and a PEG solution of 0.37 MPa could maintain.

6.12 Ultrastructural characterisation of the *M. pellucidus* chloroplast

Very little work has been carried out on the ultrastructure of the Anthocerophyte chloroplast (Vaughn *et al.*, 1992). Burr (1970; 1968) described the general structure of the chloroplast, including the channel thylakoids, the open-endedness of the thylakoid membranes and observed pyrenoid bodies in a range of Anthocerophyta.

Subsequently, Valentine (1984; Valentine & Campbell, 1986) observed that pyrenoid bodies were absent from *M. pellucidus*.

While Burr (1968), Valentine (1984) and Vaughn *et al.* (1992) commented on the light-induced change in chloroplast volume, they did not examine the effects of light quality or PFD on chloroplast ultrastructure. The light-induced difference in chloroplast volume was apparent in the electron micrographs (Figures 5.18 and 5.19), which also showed changes in the size and appearance of the starch granules (section 5.7). Chloroplasts from dark-adapted tissue had proportionally more stroma and thylakoid grana (Figure 5.21) than those from light-exposed tissue (Figures 5.19 and 5.20).

Considering the low tensile strength of biological membranes, some of which have been recorded as rupturing with stresses of only 0.2 to 1.0 MPa (Wolfe & Steponkus, 1981), and the rate at which the chloroplast volume changes occur, the chloroplast envelope must undergo a profound change in the transition between light and dark. There is insufficient time for large areas of chloroplast envelope to be synthesised. In spite of rapid light-induced changes in chloroplast volume, there is no obvious invagination of the chloroplast envelope in any of the micrographs. However, there were some structures that might have been membrane vesicles in chloroplasts from light-adapted tissue (Figures 5.19 and 5.26), which might account for the conservation of chloroplast envelope membrane.

In chloroplasts from blue light-exposed tissue, the thylakoid membranes were even more compact (Figure 5.20) than in high light-exposed samples (Figure 5.19). There appeared to be much less stroma, the thylakoids were highly appressed, the starch granules appeared to be much reduced and the pyrenoglobuli were more apparent (Figure 5.20) compared with chloroplasts from tissue maintained in all other conditions (Figures 5.18, 5.19 and 5.21).

The arrangement of the thylakoid membranes within the chloroplast in different light regimes could be explained by space optimisation. As the chloroplast contracts, the thylakoids condense, and as the chloroplast expands, the thylakoids become more separate and the stroma becomes evident.

In all of the micrographs, there is a close association between the chloroplast and the plasmalemma. In many instances it appeared as though the chloroplast was trapped between the tonoplast and the plasmalemma (Figures 5.19, 5.21, 5.24 and 5.26). If this is the case, then chloroplast movement might be explained by changes in the volume or turgor of the vacuole. For example, as the vacuole expands, the chloroplast could be compressed and forced into a different orientation by the shearing effect of the tonoplast. On relaxation, the pressure might be released, allowing the chloroplast to expand and return to its normal position. The current model of chloroplast movement is based on cytoskeletal control (Kadota & Wada, 1992; Mineyuki *et al.*, 1995; Yoshikatsu *et al.*, 2001), which is consistent with the influence of blue light on the cytoskeleton (Kagawa & Wada1, 2002; Kagawa & Wada, 1996; Mineyuki *et al.*, 1995).

In the habitat in which *M. pellucidus* can be found, there is very little light (chapter 4) and, presumably, minimal blue light. Consequently, the chloroplasts might be expected to be in the expanded conformation much of the time. Presumably, this would maximise the light harvesting capability of the plant.

6.13 Summary

The phrase, "the whole is far greater than the sum of the parts ...", could be well applied to the success of *M. pellucidus* in its adaptation to the very low light, wet environment in which it has an established niche. The plant has limited light available to it and so it is important that it captures as much of it as possible. The work described here provides support for the hypothesis that the extreme shade tolerant plant has a number of coordinated, anatomical and physiological characteristics that enable it to survive in the extreme low light situations in which it is found. Without these adaptations *M. pellucidus* would be unable to survive in its habitat.

6.14 Suggestions for further work

The following work is prompted by the questions arising from the experiments described in the forgoing chapters.

1. Further TEM of chloroplast envelope membrane to investigate vacuolation or exocytosis or invagination. How this membrane accommodates the large expansion that is presumably required to accommodate the observed volume change, considering that membrane area expansion rarely exceeds 2% (Wolfe & Steponkus, 1981), is unclear. The rate of change makes *de novo* synthesis unlikely although rapid lysis could occur to explain shrinkage.

2. Investigative comparison of the tonoplast and chloroplast envelope membrane when subject to high and low PFD. This might involve a consideration of whether chloroplast movement might occur as a result of a mechanical compression or shear from the tonoplast as its turgor varies.

3. Comparative measurements of the rate of photosynthesis when the plant is subjected to high and low light regimes. Neither the light compensation point, nor the amount of light required to saturate the activity of photosynthesis are known for *M. pellucidus*.

4. Temperature measurements at the various habitat sites and an application of these temperatures as parameters in all experiments.

5. Light pigment analysis and identification. The possibility of a new pigment should be investigated and any such pigment identified.

6. Immunoassay of water channel homologues in the plasmalemma, tonoplast and chloroplast envelope of the Anthocerophyta.

7. Measurement of water flux within and between the chloroplast, cytosol, vacuole and apoplast and the associated differences in water potential and its

components in these compartments. It would be useful to investigate whether this changes with wavelength and PFD.

8. Determine whether all Anthocerophytes posses a cuticle. Considering the wet environment in which this division exist a waxy cuticle could be advantageous, but ~~the~~ this might affect light absorption given the very low levels of light that are available.

9. Ion fluxes in the chloroplast in different light regimes. In particular, Ca^{2+} appears to be a trigger in many physical and biochemical signalling situations, such as guard cell response to blue light.

10. A comparison of wavelengths other than red and blue. In particular, the effect of far-red, green and ultraviolet wavelengths could be of interest.

11. Volume measurements of *M. pellucidus* cells and their organelles when subjected to selected PFDs and wavelengths.

REFERENCES

Ahmad, M., Jarillo, J. A., Smirnova, O. & Cashmore, A. R. (1998). Cryptochrome blue light photoreceptors of *Arabidopsis* implicated in phototropism. *Nature* **392,** 720 - 723.

Anderson, J. M. & Aro, E. M. (1994). Grana stacking and protection of PSII in thylakoid membranes of higher plant leaves under sustained high irrradiance: an hypothesis. *Photosynthesis Research* **41,** 315-326.

Anderson, J. M., Chow, W. S. & Goodchild, D. J. (1988). *Thylakoid Membrane Organisation in Sun / Shade Acclimation.* CSIRO Australia, Melbourne.

Anderson, J. M., Goodchild, D. J. & Boardman, N. K. (1973). Composition of the photosystems and chloroplast structure in extreme shade plants. *Biochimica et Biophysica Acta* **325,** 573-585.

Anderson, M. B., Folta, K., Warpeha , K. M., Gibbons, J., Gao, J. & Kaufman, L. S. (1999). Blue light directed destabilization of the Pea Lhc b1*4 transcript depends on sequences within the 5' untranslated region. *The Plant Cell* **11,** 1579-1589.

Aro, E. M. (1982). A comparison of the chlorophyll-protein composition and chloroplast ultrastructure in 2-bryophytes and 2 higher plants. *Zeitschrift fuer Pflanzenphysiologie* **108,** 97-106.

Augustynowicz, J. & Gabrys, H. (1999). Chloroplast movements in fern leaves: correlation of movement dynamics and environmental flexibility of the species. *Plant, Cell and Environment* **22,** 1239-1248.

Barbour, M. G., Burk, J. H., Pitts, W. D., Gilliam, F. S. & Schwartz, M. W. (2000). *Terrestrial Plant Ecology*, Addison Wesley, New York.

Becker, H. (1994). Secondary metabolites from bryophytes in vitro cultures. *Journal of the Hattori Botanical Laboratory* **76,** 283-291.

Benson-Evans, K. (1963). Some aspects of the physiology of reproduction in bryophytes. In *British Bryological Society*, Bristol, Autumn, 27-28 September.

Berecki, G., Varga, Z., Van Iren, F. & Van Duijn, B. (1999). Anion channels in *Chara corallina* tonoplast membrane: Calcium dependence and rectification. *Journal of Membrane Biology* **172,** 159-168.

Bischof, K., Hanelt, D. & Wienck, C. (1999). Acclimation of maximal quantum yield of photosynthesis in the Brown Alga, *Alaria esclenta*, under high light and UV radiation. *Plant Biology* **1,** 435-444.

Bjorkman, O. (1968). Carboxydismutase activity in shade-adapted and sun adapted species of higher plants. *Plant Physiology* **21,** 1-10.

Bjorkman, O. (1981). *Responses to Different Quantum Flux Densities.* Springer-Verlag, New York.

Bjorkman, O., Boardman, N. K., Anderson, J. M., Thorne, S. W., Goodchild, D. J. & Pylliotis, N. A. (1972). Effect of light intensity during growth of *Atriplex patula* on the capacity of photosynthetic reactions, chloroplast components and structure. *Carnegie Institute Washington Year Book* **71,** 115-135.

Bjorkman, O. & Holmgren, P. (1963). Adaptability of the photosynthetic apparatus to light intensity in ecotypes from exposed and shade habitats. *Physiologia Plantarum* **16,** 889-914.

Bjorn, L. A. (1994). Modelling the light environment. In *Photomorphogenesis in Plants* (ed. R. E. Kendrick and G. H. M. Kronenberg), Kluwer Academic Publishers, Dordrecht.

Black, M. & Pritchard, H. W. (2002). *Life After Desiccation. Dessication and Survival in Plants Drying Without Dying*, CABI Publishing, New York.

Boardman, N. K. (1977). Comparative photosynthesis of sun and shade plants. *Annual Review of Plant Physiology* **28,** 355 - 377.

Böhning, R. H. & Burnside, C. A. (1956). The effect of light intensity on rate of apparent photosynthesis in leaves of sun and shade plants. *American Journal of Botany* **43,** 557-561.

Bold, H. C., Alexopoulos, C. J. & Delevoryas, T. (1987). *Morphology of Plants and Fungi*, Harper and Row, Publishers, Inc., New York.

Bopp, M. (2000). 50 Years of the Moss story. *Progress in Botany* **61,** 1-34.

Bozzola, J. J. & Russell, L. D. (1992). *Electron Microscopy, Principles and Techniques for Biologists*. Jones & Bartlett Publishers, London.

Brewer, C. A., Smith, W. K. & Vogelmann, T. C. (1991). Functional interaction between leaf trichomes, leaf wettability, and the optical properties of water droplets. *Plant, Cell and Environment* **14,** 955-62.

Britz, S. J. (1979). Chloroplast and Nuclear migration. In *Encyclopedia of Plant Physiology*, vol. New Series 7 (ed. A. Pirson and M. H. Zimmermann), pp. 170 - 205. Springer, New York.

Brown, M. J. & Parker, G. G. (1994). Canopy light transmittance in a chronosequence of mixed species deciduous forest. *Canadian Journal of Forest Research* **24,** 1694-1703.

Brownlee, C., Goddard, H., Hetherington, A. M. & Peake, L.-A. (1999). Specificity and integration of responses: Ca^{2+} as a signal in polarity and osmotic regulation. *Journal of Experimental Botany* **50,** 1001-1011.

Burr, F. A. (1970). Phylogenetic transitions in the chloroplasts of the Anthocerotales. I. The number and ultrastructure of the mature plastid. *American Journal of Botany* **57,** 97-110.

Burr, F. M. (1968). Chloroplast structure and division in *Megaceros* species. PhD thesis, University of California.

Campbell, E. O. (1995). Name changes in Australasian *Megaceros* (Anthocerotae). *New Zealand Journal of Botany* **33,** 279-283.

Chapman, V. J. & Chapman, D. J. (1973). *The Algae*, The MacMillan Press Ltd., Hong Kong.

Chazdon, R. L., Pearcy, R. W., Lee, D. W. & Fetcher, N. (1996). *Photosynthetic Responses of Tropical Forest Plants to Contrasting Light Environments.* Chapman and Hall, USA.

Chow, W. S. (1999). Grana formation: Entropy-assisted local order in chloroplasts? *Australian Journal of Plant Physiology* **26,** 641-647.

Chow, W. S., Melis, A. & Anderson, J. M. (1990). Adjustments of photosystem stoichiometry in chloroplasts improve the quantum efficiency of

photosynthesis. *Proceedings of the National Academy of Sciences of the United States of America* **87,** 7502-7506.

Chow, W. S., Thorne, S. W., Duniec, J. T., Sculley, M. J. & Boardmann, N. K. (1982). The stacking of chloroplasts, evidence for segregation of charged groups into non stacked regions. *Archives of Biochemistry & Biophysics* **216,** 247-254.

Cockell, C. S. & Knowland, J. (1999). Ultraviolet radiation screening compounds. *Biological Reviews* **74,** 311-345.

Cook, M. E. & Graham, L. E. (1998). Structural similarities between surface layers of selected charophycean algae and bryophytes and the cuticles of vascular plants. *International Journal of Plant Sciences* **159,** 780-787.

Cook, M. E., Graham, L. E., Botha, C. E. J. & Lavin, C. A. (1977). Comparative ultrastructure of plasmodesmata of Chara and selected bryopytes: toward an elucidation of the evolutionary origin of plasmodesmata. *American Journal of Botany* **84,** 1169.

Corle, T. R. & Kino, G. S. (1996). *Confocal Scanning Optical Microscopy and Related Imaging Systems*. Academic Press, Inc., San Diego.

Cosgrove, D. J. (1993). Water uptake by growing cells: an assessment of the controlling roles of wall relaxation, solute uptake, and hydraulic conductance. *International Journal of Plant Sciences.* **154,** 10-21.

Dilks, T. J. K. & Procter, M. C. F. (1979). Photosynthesis, respiration and water content in Bryophytes. *The New Phytologist* **82,** 97-114.

Dodds, W. K., Gudder, D. A. & Mollenhauer, D. (1995). The ecology of *Nostoc*. *Journal of Phycology* **31,** 2-18.

Dong, X. J., Nagai, R. & Takagi, S. (1998). Microfilaments anchor chloroplasts along the outer periclinal wall in *Vallisneria* epidermal cells through co-operation of P-FR and photosynthesis. *Plant & Cell Physiology* **39,** 1299-1306.

Duckett, J. G., Prasad, A. K. S. K., Davies, D. A. & Walker, S. (1977). A cytological analyses of the *Nostoc* - Bryophyte relationship. *New Phytologist* **79,** 349-362.

Duckett, J. G. & Renzaglia, K. S. (1988). Ultrastructure and development of plastids in the bryophytes. *Advances in Bryology* **3,** 33-93.

Eckert, M., Biela, A., Siefritz, F. & Kaldenhoff, R. (1999). New aspects of plant aquaporin regulation and specificity. *Journal of Experimental Botany* **50,** 1541-1545.

Esau, K. (1953). *Plant Anatomy*. John Wiley & Sons, Inc., New York.

Etherington, J. R. (1982). *Environment and Plant Ecology*, 2nd edition. John Wiley & Sons, New York.

Fahn, A. (1997). *Plant Anatomy*, Butterworth-Heinmann, Oxford.

Fisher, T., Berner, T., Iluz, D. & Dubinsky, Z. (1998). The kinetics of the photoacclimation response of *Nannochloropsis sp.* (Eustigmatophyceae): A study of changes in ultrastructure and PSU density. *Journal of Phycology* **34,** 818-824.

Gabrys-Mizera, H. (1976). Model considerations of the light conditions in noncylindrical plant cells. *Photochemistry and Photobiology* **24,** 453-461.

Gabrys-Mizera, H., Walczac, T. & Malec, P. (1997). Interaction between phytochrome and the blue light photoreceptor system in *Mougeotia:* Temperature dependence. *Journal of Photochemistry & Photobiology.* **38,** 35-39.

Gamalei, Y. V., Fromm, J., Krabel, D. & Eschrich, W. (1994). Chloroplast movement as a response to wounding in *Elodea canadensis. Journal of Plant Physiology* **144,** 518 - 524.

Garbary DJ and Renzaglia KS. (1998). *Bryophyte Phylogeny and the Evolution of Land Plants. Evidence from Development and Ultrastructure.* W. S. Manct and Sons Ltd, Leeds.

Garjeanne, A. J. M. (1932). Bryological Physiology. In *Manual of Bryology* (ed. F. e. a. Verdoorn), pp. 207-232. Martinus Nijhoff, The Hague.

Gates, D. M. (1980). *Biophysical Ecology*. Springer-Verlag, New York.

Gautier, H. & Varlet-Grancher, C. (1996). Regulation of leaf growth of grass by blue light. *Physiologia Plantarum* **98,** 424 - 430.

Ghoshroy, S. & Fagerberg, W. R. (1998). Light detection system in mature sunflower (*Helianthus annuus* L.) chloroplasts: wavelength dependent or total photon flux density related. *International Journal of Plant Sciences* **159,** 110-115.

Gilbert, A. & Baggott, J. (1991). *Essentials of Molecular Photochemistry,*. Blackwell Scientific Publications, Oxford.

Glenny, D. (1998). A revised checklist of New Zealand Liverworts and Hornworts. *Tuhinga (Te Papa Museum of N.Z)* **10,** 119-149.

Gorton, H. L., Williams, W. E. & Vogelmann, T. C. (1999). Chloroplast movement in *Alocasia macrorrhiza*. *Physiologia Plantarum.* **106,** 421-428.

Gray, J. D., Kolesik, P., Hoj, P. B. & Coombe, B. G. (1999). Confocal measurement of the three-dimensional size and shape of plant parenchyma cells in a developing fruit tissue. *The Plant Journal* **19,** 229-236.

Grignon, C. (1999). Recent advances on proteins of plant terminal membranes. *Biochimie* **81,** 577-596.

Grime, J. P. (1981). *Plant Strategies in Shade.* Academic Press, London.

Gupta, A. S. & Berkowitz, G. A. (1988). Chloroplast osmotic adjustment and water stress effects on photosythesis. *Plant Physiology* **88,** 200 - 206.

Hader, D.-P. (1987). *Photomovement*, CRC Press, Inc., Boca Raton.

Hanson, D., John Andrews, A. T. & Badger, M. R. (2002). Variability of the pyrenoid-based CO_2 concentrating mechanism in hornworts (Anthocerotophyta). *Functional Plant Biology* **29,** 407-416.

Hasegawa, J. (1988). A proposal for a new system of the Anthocerote, with a revision of the genera. *Journal of the Hattori Botanical Laboratory* **64,** 87-95.

Hasegawa, J. (1994). A new classification of the Anthocerotae. *Journal of the Hattori Botanical Laboratory* **76,** 21-34.

Haupt, W. (1982). Light-mediated movement of chloroplasts. *Annual Review of Plant Physiology* **33,** 205 - 233.

Haupt, W. (1999). Chloroplast movement: from phenomenology to molecular biology. *Progress in Botany.* **60,** 3 - 35.

Haupt, W. & Hader, D.-P. (1994). *Photomovement*, Kluwer Academic Publishers, Dordrecht.

Hay, R. F. (1967). *Geological Map of New Zealand.* D.S.I.R, Wellington.

Hicklenton, P. R. & Oechel, W. C. (1976). Physiological aspects of the ecology of *Dicranum fuscescens* in the sub arctic. *Canadian Journal of Botany* **54,** 1104-1119.

Hind, G., Nakatani, H. & Izawa, S. (1974). Light-dependent redistribution of ions in suspensions of chloroplast thylakoid membranes. *Proceedings of the National Academy of Sciences of the USA* **71,** 1484-1488.

Hodgson, J. G., Wilson, P. J., Hunt, R., Grime, J. P. & Thompson, K. (1999). Allocating C-S-R plant functional types: A soft approach to a hard problem. *Oikos* **85,** 282-294.

Horvath, G. (1995). Reflection-polarization patterns at flat water surfaces and their relevance for insect polarization vision. *Journal of Theoretical Biology* **175,** 27-37.

Huner, N. P. A., Öquist, G., Hurry, V. M., Krol, M., Falk, S. & Griffith, M. (1993). Photosynthesis, photoinhibition and low temperature acclimation in cold-tolerant plants. *Photosynthesis Research* **37,** 19-39.

Hutner, S. H., Provosli, L., Schatz, A. & Haskins, C. P. (1950). *Proceedings of the American Philosophical Society* **94,** 152.

Ishikawa, T., Takeda, T., Shigeoka, S., Hirayama, O. & Mitsunaga, T. (1993). Hydrogen peroxide generation in organelles of *Euglena gracilis*. *Phytochemistry* **33,** 1297-1299.

Ivanchenko, V. M., Marshakova, M. I., Izbavitelev, S. P. & Kruchinina, S. S. (1980). Characteristics of light-induced changes in volume of isolated chloroplasts in connection with conditions of their incubation. *Fiziologiya Rastenii* **27,** 696-703.

Jarillo, J. A., Gabrys, J. C., Alonso, M. A., Ecker, J. R. & Cashmore, A. R. (2001). Phototropin-related NPL1 controls chloroplast relocation induced by blue light. *Nature* **410,** 952-954.

Kadota, A., Sato, Y. & Wada, M. (2000). Intracellular chloroplast photorelocation in the moss *Physcomitrella patens* is mediated by phytochrome as well as by a blue-light receptor. *Planta* **210,** 932-937.

Kadota, A. & Wada, M. (1992). Photoinduction of formation of circular structures by microfilaments on chloroplasts during intracellular orientation in protonemal cells of the fern *Adiantum capillus veneris*. *Protoplasma* **167,** 97-107.

Kadota, A. & Wada, M. (1999). Red light-aphototrophic (rap) mutants lack red light induced chloroplast re-location movement in the fern *Adiantum capillus-veneris*. *Plant and Cell Physiology* **40,** 238 - 247. 30 ref.

Kagawa, T. & Wada, M. (2002). Blue light-induced chloroplast relocation. *Plant and Cell Physiology* **43,** 367-371.

Kagawa, T. & Wada, M. (1996). Phytochrome and blue light absorbing pigment mediated directional movement of chloroplasts in dark adapted prothallial cells of fern *Adiantum* as analyzed by microbeam irradiation. *Planta* **198,** 488 - 493.

Kagawa, T. & Wada, M. (1999). Chloroplast avoidance response induced by high fluence blue light in prothallial cells of the fern *Adiantum capillus-veneris* as analyzed by microbeam irradiation. *Plant Physiology* **119,** 917 - 923.

Kaja, H. (1954). Untersuchungen uber die Chromatophoren und Pyrenoid der Anthocerotales. *Protoplasma* **44,** 136-153.

Karabourniotis, G., Bornman, J. F. & Liakoura, V. (1999). Different leaf surface characteristics of three grape cultivars affect leaf optical properties as measured with fibre optics: possible implication in stress tolerance. *Australian Journal of Plant Physiology* **26,** 47 - 53.

Kendrick, R. E. & Kronenberg, G. H. M. (1994). *Photomorphogenesis in Plants*. Kluwer Academic Publishers, Dordrecht.

Khurana, J. P. (1998). Photosensory perception and signal transduction in higher plants - Molecular genetic analysis. *Critical Reviews in Plant Sciences.* **17,** 465-539.

Kjellbom, P., Larsson, C., Johansson, I., Karlsson, M. & Johanson, U. (1999). Aquaporins and water homeostasis in plants. *Trends in Plant Science* **4,** 308-314.

Knapp, A. K. & Carter, G. A. (1998). Variability in leaf optical properties among 26 species from a broad range of habitats. *American Journal of Botany* **85,** 940-946.

Koller, D. (2000). Plants in search of sunlight. *Advances in Botanical Research* **33,** 35-131.

Können, G. P. (1985). *Polarized Light in Nature.* Cambridge University Press, Cambridge.

Kraml, M. (1994). *Light Direction and Polarization*, Kluwer Academic Publishers, Dordrecht.

Krause, G. H. (1973). The high-energy state of the thylakoid system as indicated by chlorophyll fluorescence and chloroplast shrinkage. *Biochimica et Biophysica Acta* **292,** 715-728.

Krause, G. H. (1974). Light-induced movement of metal cations in chloroplasts. Evidence from chlorophyll fluorescence and light scattering. In *Proceedings of the Third International Congress on Photosynthesis* (ed. M. Avron), pp. 1021-1030. Elsevier Scientific Publishing Company, Amsterdam.

Krupa, J. (1978). Photosynthesis rate in moss leaves of various anatomical structure. *Acta Societatis Botanicorum Poloniae* **47,** 391-402.

Lao, W. (1998). *Using LRWhite for Electron Microscopy.* Agar Scientific Ltd., London.

Larcher, W. (1995). *Physiological Plant Ecology*, Springer, New York.

Lawlor, D. W. (1993). *Photosynthesis: Molecular, Physiological and Environmental Processes.* Longman Scientific & Technical, Harlow.

Lee, J. A. & Stewart, G. R. (1971). Dessication injury in mosses. Intra-specific differences in the effect of moisture stress on photosynthesis. *New Phytologist* **70,** 1061-1068.

Leigh, R. A. (1997). The solute composition of plant vacuoles. *Advances in Botanical Research* **25,** 171-194.

Lembi, C. A. & Lang, N. J. (1965). Electronmicroscopy of *Carteria* and *Chlamydomonas*. *American Journal of Botany* **52,** 464-477.

Lewis, B. D., Karlin-Neumann, G., Davis, R. W. & Spalding, E. P. (1997). Ca^{2+} activated anion channels and membrane depolarizations induced by blue light and cold in *Arabidopsis* seedlings. *Plant Physiology* **114,** 1327 - 1334.

Lewis, F. T. (1943). The geometry of growth and cell division in epithelial mosaics. *American Journal of Botany* **30,** 766-776.

Lichtenthaler, H. K., Kuhn, G., Prenzel, U., Buschmann, C. & Meier, D. (1982). Adaptation of chloroplast-ultrastructure and of chlorophyll-protein levels to high-light and low-light growth conditions. *Zeitschrift fuer Naturforschung Section C Biosciences 3* **37,** 464-475.

Lin, S. & Carpenter, E. J. (1997). Rubisco of *Dunaliella tertiolecta* is redistributed between the pyrenoid and the stroma as a light/shade response. *Marine Biology* **127,** 521-529.

Lloyd, C. W. (1991). How does the cytoskeleton read the laws of geometry in aligning the division plane of plant cells? *Development* **Suppl. 1,** 55-65.

Long, C. & Iino, M. (2001). Light-dependent osmoregulation in pea stem protoplasts. Photoreceptors, tissue specificity, ion relationships, and physiological implications. *Plant Physiology* **125,** 1854-1869.

Loomis, R. S. and Connor, D. J. (1992). *Crop Ecology: Productivity and Management in Agricultural Systems*. Cambridge University Press, Melksham.

Mache, R. & Loiseaux, S. (1973). Light saturation of growth and photosynthesis of the shade plant *Marchantia polymorpha*. *Journal of Cell Science* **12,** 391-401.

Manton, I. (1962). Observations on plastid development in the meristem of *Anthoceros*. *Journal of Experimental Botany.* **13,** 325-333.

Maurel, C. (1997). Aquaporins and water permeability of plant membranes. *Annual Review of Plant Physiology & Molecular Biology* **48,** 399 - 429.

Maurel, C. & Chrispeels, M. J. (2001). Aquaporins. A molecular entry into plant water relations. *Plant Physiology* **125,** 135-138.

Mawson, B. T. (1993). Regulation of blue-light-induced proton pumping by *Vicia faba* L. guard-cell protoplasts: Energetic contributions by chloroplastic and mitochondrial activities. *Planta* **191,** 293-301.

McCain, D. & Markley, J. L. (1992). In vivo study of chloroplast volume regulation. *Biophysical Journal* **61,** 1207 - 1212.

McCain, D. C. (1995). Combined effects of light and water stress on chloroplast volume regulation. *Biophysical Journal* **69,** 1105 - 1110.

McCain, D. C. (2000). NMR Study of chloroplast water in *Acer platanoides*: Water exchange at membrane-bound sites and across the chloroplast envelope membrane. *Plant Biology* **2,** 204-207.

McCain, D. C. & Markley, J. L. (1985). Water permeability of chloroplast envelope membranes. *FEBS Letters* **183,** 353-358.

McKay, R. M. & Gibbs, S. P. (1989). Immunocytochemical localization of ribulose 1,5-bisphosphate carboxylase / oxygenase in light limted and light saturated cells of *Chlorella pyrenoidosa*. *Protoplasma* **129,** 31-37.

Mckay, R. M. L., Gibbs, S. P. & Vaughn, K. C. (1991). Rubisco activase is present in the pyrenoid of green algae. *Protoplasma.* **162,** 38.45.

Miller, R. B. (1968). *Soils of New Zealand; Part 2.* New Zealand Soil Bureau Bulletin, Wellington.

Mineyuki, Y., Kataoka, H., Masuda, Y. & Nagai, R. (1995). Dynamic changes in the actin cytoskeleton during high-fluence rate response of the *Mougeotia* chloroplast. *Protoplasma* **185,** 222-229.

Mishler, B. D. & Churchill, S. P. (1985). Transition to a land flora. Phylogenetic relationships of the green algae and bryophytes. *Cladistics* **1,** 305-328.

Murakami, S. (1992). Structural and functional organization of the thylakoid membrane system in photosynthetic apparatus. *Journal of Electron Microscopy* **41,** 424-433.

Myneni, R. B. & Ross, J. (1991). *Photon-Vegetation Interactions*. Springer-Verlag, Berlin.

Neinhuis, C. & Barthlott, W. (1997). Characterisation and distribution of water-repellent, self-cleaning plant surfaces. *Annals of Botany* **79,** 667-677.

Neinhuis, C., Koch, K. & Barthlott, W. (2001). Movement and regeneration of epicuticular waxes through plant cuticles. *Planta* **213,** 427-434.

Niinemets, U., Kull, O. & Tenhunent, J. D. (1999). Variability in leaf morphology and chemical composition as a function of canopy light environment in coexisting deciduous trees. *International Journal of Plant Science* **160,** 837-848.

Nobel, P. S. (1968). Energetic basis of the light induced chloroplast shrinkage in vivo. *Plant and Cell Physiology* **9,** 499 - 509.

Nobel, P. S. (1991). *Physiochemical and Environmental Plant Physiology,* Academic Press, Inc, New York

Nobel, P. S. (1999). *Biophysical Plant Physiology*, Freeman, San Francisco.

Olesen, T. (1992). Daylight spectra (400-740 nm) beneath sunny, blue skies in Tasmania, and the effect of a forest canopy. *Australian Journal of Ecology* **17,** 451-461.

Osmond, C. B., Austin, M. P., Berry, J. A., Billings, J. S., Boyer, J., Dacey, P. S., Nobel, S. D., Smith, S. D. & Winner, W. E. (1987). Stress physiology and the distribution of plants. *BioScience* **37,** 38-48.

Paau, A. S., Uro, J. & Cowles, J. R. (1978). Applications of flow cytometry to the study of algal cells and isolated chloroplasts. *Journal of Experimental Botany* **29,** 1011-1022.

Packer, L., Murakami, S. & Mehard, C. W. (1970). Ion transport in chloroplasts and plant mitochondria. *Annual Review of Plant Physiology* **1970,** 271-304.

Pandey, S., Tiwari, S. B., Upadhyaya, K. C. & Sudhir, K. (2000). Calcium signaling: Linking environmental signals to cellular functions. *Critical Reviews in Plant Sciences* **19,** 291-318.

Parsegian, V. A., Rand, R. P., Fuller, N. L. & Rau, D. C. (1986). Osmotic stress for the direct measurement of intermolecular forces. *Methods in Enzymology* **127,** 400-416.

Pawley, J. B. (1995). *Handbook of Biological Confocal Microscopy*, Plenum Press, New York.

Pearcy, R. W. (1989). *Radiation and Light Measurements*. Chapman and Hall, New York.

Pearcy, R. W. & Calkin, H. W. (1983). The light environment and growth of C_3 and C_4 tree species in the understory of an Hawaiian forest. *Oecologia* **58,** 19-25.

Raemaekers, G. & Longwith, J. E. (1987). The use of dimethyl sulfoxide (DMSO) as a solvent to extract chlorophyll from mosses. *Symposia Biologica Hungarica* **35,** 151-164.

Ramus, J. (1978). Seaweed anatomy and photosynthetic performance: the ecological significance of light guides, heterogenous absorption and multiple scatter. *Journal of Phycology* **14,** 352-362.

Renzaglia, K. S. (1978). A comparative morphology and developmental anatomy of the Anthocerophyta. *Journal of the Hattori Botanical Laboratory* **44,** 31-90.

Renzaglia, K. S. & Carothers, Z. B. (1986). Ultrastructural studies of spermatogenesis in the Anthocerotales. 4. The blepharoplast and mid-stage spermatid of *Notothylas*. *Journal of the Hattori Botanical Laboratory* **60,** 97-104.

Resnick, R. & Halliday, D. (1966). *Physics - Combined Edition 1 & 2*. John Wiley & Sons. Inc., Tokyo.

Reynolds, E. S. (1963). The use of lead citrate at high pH as an electron-opaque stain in electron microscopy. *Journal of Cell Biology* **17,** 208-12.

Richards, P. W. (1932). *The Ecology of Bryophytes*. Martinus Nijhoff, The Hague,.

Richards, P. W. (1984). *The Ecology of Tropical Forest Bryophytes*. The Hattori Botanical Laboratory, Tokyo.

Rincon, E. & Grime, J. P. (1989). Plasticity and light interception by six bryophytes of contrasted ecology. *Journal of Ecology* **77,** 439-446.

Robinson, S. P. (1985). Osmotic adjustment by intact isolated chloroplasts in response to osmotic stress and its effect on photosynthesis and chloroplast volume. *Plant Physiology* **79,** 996 - 1002.

Roland, J. C. & Vian, B. (1991). *Electron Microscopy of Plant Cells*. Academic Press, Cambridge.

Ross, J. (1981). *The Radiation Regime and Architecture of Plant Stands*. Dr. W. Junk Publishers, The Hague.

Sakai, T., Kagawa, T., Kasahara, M., Swartz, T. E., Christie, J. M., Briggs, W. R., Wada, M. & Okada, K. (2001). Arabidopsis nph1 and npl1: Blue light receptors that mediate both phototropism and chloroplast relocation. *Proceedings of the National Academy of Sciences of the United States of America* **98,** 6969-6974.

Salisbury, J. L. & Floyd, G. L. (1978). Molecular, enzymatic and ultrastructure characterization of the pyrenoid of the scaly green monad *Micromonas squamata*. *Journal of Phycology* **14,** 362-368.

Sauer, K. (1975). Primary events and the trapping of energy. In *Bioenergetics of Photosynthesis*, vol. 1 (ed. Govindjee), pp. 115-181. Academic Press, Inc., New York.

Schreiber, L., Skrabs, M., Hartmann, K. D., Diamantopoulus, P., Simanova, E. & Santrucck, J. (2001). Effect of humidity on cuticular water permeability of isolated cuticular membranes and leaf disks. *Planta* **214,** 274-282.

Schuster, R. M. (1984). *Morphology, Phylogeny and Classification of the Anthocerotae*. Columbia University Press, New York.

Senger, H. (1984). *Blue Light Effects in Biological Systems*. Springer-Verlag, Berlin.

Smith, E. C. & Griffiths, H. (1996). A pyrenoid based carbon concentrating mechanism is present in terrestrial bryophytes of the class Anthocerotae. *Planta* **200,** 203-212.

Smith, H. (1986). The perception of light quality. In *Photomorphogenesis in Plants* (ed. R. E. Kendrick and G. H. M. Kronenberg), pp. 187-217. Martinus Nijhoff Publishers, Dordrecht.

Smith, H. & Morgan, D. C. (1981). The spectral characteristics of the visible radiation incident upon the surface of the earth. In *Plants and the Daylight Spectrum* (ed. H. Smith). Academic Press (London) Ltd.., London.

Stevens, J. K., Mills, L. R. & Trogadis, J. E. (1994). *Three-Dimensional Confocal Microscopy: Volume Investigation of Biological Systems*. Academic Press, Inc., San Diego.

Stotler, R. & Crandall-Stotler, B. (1977). A checklist of the liverworts and hornworts of North America. *Bryologist* **80,** 405-428.

Takagi, S. (1997). Photoregulation of cytoplasmic streaming: cell biological dissection of signal transduction pathway. *Journal of Plant Research* **110,** 299 - 303.

Takashi Emi, Toshinori Kinoshita & Shimazaki, K. -I. (2001). Specific binding of vf14-3-3a isoform to the plasma membrane H^+-ATPase in response to blue light and fusicoccin in guard cells of broad bean. *Plant Physiology* **125,** 1115-1125.

Tanaka, A. & Melis, A. (1997). Irradiance-dependent changes in the size and composition of the chlorophyll *a-b* light-harvesting complex in the green alga *Dunaliella salina. Plant & Cell Physiology* **38,** 17-24.

Tang, Y. (1997). Light. In *Plant Ecophysiology* (ed. M. N. V. Prasad). John Wiley & Sons, Inc., New York.

Tazawa, M., Shimada, K. & Kikuyama, M. (1995). Cytoplasmic hydration triggers a transient increase in cytoplasmic Ca^{2+} concentration in *Nitella flexilis. Plant & Cell Physiology* **36,** 335-340.

Thompson, C. S. (1981). The climate and weather of the Taranaki region. New Zealand Meterological Service, Wellington.

Thum, K. E., Kim, M., Christopherb, D. A. & Mullet, J. E. (2001). Cryptochrome 1, cryptochrome 2, and phytochrome A co-activate the chloroplast psbD blue light–responsive promoter. *The Plant Cell* **13,** 2747-2760.

Tlalka, M. & Gabrys, H. (1993). Influence of Ca on blue light induced chloroplast movement in *Lemna trisulca* L. *Planta* **189,** 491 - 498.

Tlalka, M., Runquist, M. & Fricker, M. (1999). The role of calcium in blue-light-dependent chloroplast movement in *Lemna trisulca* L. *Plant Journal* **20,** 461-473.

Toyama, S. (1974). Electron microscope studies on the morphogenesis of plastids; The phylogeny of photosynthetic apparatus with special reference to lamellar structure. *Japanese Journal of Botany* **20,** 413-438.

Tyerman, S. D., Bohnert, H. J., Maurel, C., Steudle, E. & Smith, J. A. C. (1999). Plant aquaporins: their molecular biology, biophysics and significance for plant water relations. *Journal of Experimental Botany* **50,** 1055-1071.

Valanne, N. (1984). Photosynthesis and photosynthetic products in mosses. In *The Experimental Biology of Bryophytes* (ed. A. F. Dyer and J. G. Duckett), pp. 257-273. Academic Press, London.

Valentine, L. J. (1984). A comparison of selected New Zealand species of *Megaceros* and *Dendroceros* (Anthocerophyta) with special reference to chloroplast gross morphology and ultrastructure. BSc (hons) thesis, Massey University, Palmerston North.

Valentine, L. J. & Campbell, E. O. (1986). A study of chloroplast structure in 3 *Megaceros* species and 3 *Denroceros* species (Anthocerotae) indigenous to New Zealand. *New Zealand Journal of Botany* **24,** 1-8.

Vaughn, K. C., Campbell, E. O., Hasegawa, J., Owen, H. A. & Renzaglia, K. S. (1990). The pyrenoid is the site of ribulose 1,5-bisphosphate carboxylase / oxygenase accumulation in the hornwort (Bryophyta: Anthocerotae) chloroplast. *Protoplasma* **156,** 117-129.

Vaughn, K. C., Ligrone, R., Owen, H. A., Hasegawa, J., Campbell, E. O., Renzaglia, K. S. & Monge-Najera, J. (1992). The anthocerote chloroplast: a review. *New Phytologist* **120,** 169-190.

Vogelmann, T. C. (1993). Plant tissue optics. *Annual Review of Plant Physiology & Molecular Biology* **44,** 231 - 251.

Vogelmann, T. C. (1994). Light within the plant. In *Photomorphogenesis in Plants* (ed. R. E. Kendrick and G. H. M. Kronenberg). Kluwer Academic Publishers, Dordrecht.

Vogelmann, T. C. & Bjorn, L. O. (1986). Plants as light traps. *Physiologia Plantarum* **68,** 704-708.

Vogelmann, T. C., Bornman, J. F. & Yates, D. J. (1996.). Focusing of light by leaf epidermal cells. *Physiologia Plantarum* **98,** 43 - 56.

Vogelmann, T. C., Nishio, J. N. & Smith, W. K. (1996). Leaves and light capture: light propagation and gradients of carbon fixation within leaves. *Trends in Plant Science* **1,** 65-70.

Wada, K., Hirabayashi, Y. & Saito, W. (1984). Light germination of *Anthoceros miyabeanus* spores. *The Botanical Magazine* **97,** 369-379.

Wang, X. & Iino, M. (1998). Interaction of cryptochrome 1, phytochrome and Ion fluxes in blue light induced shrinking of *Arabidopsis* hypocotyl protoplasts. *Plant Physiology* **117,** 1265-1279.

Weiss, T. F. (1996). *Cellular Biophysics*. Massachusetts Institute of Technology, Cambridge.

Wheeler, W. S. & Fagerberg, W. R. (2000). Exposure to low levels of photosynthetically active radiation induces rapid increases in palisade cell chloroplast volume and thylakoid surface area in sunflower (*Helianthus annuus* L.). *Protoplasma* **212,** 38-45.

Witham, F. H., Bladyes, D. F. & Devlin, R. M. (1986). *Exercises in Plant Physiology*. Prindle, Weber & Schmidt., Boston.

Wolfe, J. & Steponkus, P. L. (1981). The stress-strain relation of the plasma membrane of isolated plant protoplasts. *Biochimica et Biophysica Acta* **643,** 663-668.

Yatsuhashi, H. (1996). Photoregulation systems for light-oriented chloroplast movement. *Journal of Plant Research* **109,** 139-146.

Yoda, K. (1974). Three dimensional distribution of light intensity in a tropical rainforest of West Malaysia. *Japanese Journal of Ecology* **24,** 247-254.

Yoshikatsu, S., Wada, M. & Kadota, A. (2001). Choice of tracks, microtubules and/or actin filaments for chloroplast photo-movement is differentially controlled by phytochrome and a blue light receptor. *Journal of Cell Science* **114,** 269-279.

Yoshinaga, K., Kakehi, T., Shima, Y., Iinuma, H., Masuzawa, T. & Ueno, M. (1997). Extensive RNA editing and possible double-stranded structures determining editing sites in the atpB transcripts of hornwort chloroplasts. *Nucleic Acids Research* **25,** 4830-4834.

APPENDIX A.

Stock Solutions (Hutner, et al , 1950)

Hutner's Base Solution (Stock)

Ingredient	grams / L
Na Citrate·$2H_2O$	100 g
$FeCl_3 \cdot 6H_2O$	10 g
$CaCl_2 \cdot 6H_2O$	53 g
$MgSO_4 \cdot 7H_2O$	100 g
NH_4NO_3	100 g
KH_2PO_4	100 g
K_2HPO_4	100 g

Hutners trace element Solution (Stock)

BO_3H_3	11.4 g
$ZnSO_4 .7H_2O$	22.0 g
$MnCl_2 . 4H_2O$	5.06 g
$FeSO_4 . 7H_2O$	4.99 g
$CoCl_2 . 6H_2O$	1.61 g
$CuSO_4 . 5H_2O$	1.57 g
$Mo_7O_{24}(NH_4)_6 . 4H_20$	1.1 g

Preparation of trace element solution

1. Dissolve 50g of acid free EDTA in 250 ml of ddH_2O. Heat to dissolve.
2. Dissolve the trace elements, one by one, in order, heating to approximately100° in 550 ml ddH_2O.

3. Mix the two solutions (1 and 2) together. The resulting solution should be blue-green.

4. Heat to 100°. Cool slightly, but don't let the temperature drop below 80°-90°.

5. Adjust pH to 6.5 to 6.8 with 20% KOH (approximately 83 ml). Don't let the temperature drop below 70 ° until after the pH is adjusted.

6. Make up to 1L and let stand in a 2L Erlenmeyer flask, stoppered loosly. The colour should change from green to purple.

7. Remove the rust-coloured precipitate by filtering, with suction, through 3 layers of Whatman #1 filter paper in a Buckner funnel. Repeat until no more precipitate is seen on the filter paper.

8. Store in a brown bottle at 4°.

Phosphate buffer II

$K2HPO_4$	10.8 g / 100 mL mille-Q
KH_2PO_4	5.6 g / 100 mL mille-Q

Solution A

NH_4Cl	20.0 g / 500 mL mille-Q
$MgSO_4 . 7H_2O$	5.0 g / 500 mL mille-Q
$CaCl_2 . 2H_2O$	2.5 g / 500 mL mille-Q

Dilution (add to 1L mille-Q)

Base Stock sol	30 ml
Phosphate Buffer II	1 ml
Hutner's Trace stock solution	1 ml
Hutners Base Solution A	10 ml
CH_3COOH (glacial) Adjust pH to 7.0)	1 ml